Parkinson's Disease Model in vitro and in C. elegans

Abdurrahman Mubayyid

A thesis submitted to fulfil requirements for the degree of Master of Philosophy

The University of Sydney
Faculty of Medicine

Contents

Acknowledgements

Haydn Allbutt PhD – Planning, protocols, writing and mentoring.

Courtney Wright – Experimentation/mentoring

Rayaan Mubayyid Editor – Juris Doctor/Graduate Candidate in Legal Practice

Matthew Hoe PhD – *C. elegans* experimental troubleshooting

Abstract

Current treatments of Parkinson's Disease (PD), a neurodegenerative disease affecting voluntary movement, do not target the underlying pathology, focussing on the symptoms instead. The focus of this study was the usage of a protein involved in the earliest known pathology of PD, α-synuclein (α-syn), to conduct preliminary experiments that could determine potential treatments that affect aggregation of α-syn. First, aggregation of α-syn was measured using a commonly used assay for detecting protein aggregation, thioflavin T (ThT) fluorescence assay. Second, Caenorhabditis elegans (C. elegans), nematodes more recently used as a low-cost model for diseases, were treated with α-syn (transgenic species were used overexpressing α-syn in muscle cells and C. elegans were also exogenously exposed to α-syn) and observed for any behavioural changes in movement and bend speed. Treating α-syn with hops, an ingredient used in brewing beer, showed a 53-fold reduction in fluorescence in the ThT assays performed. The mechanism in which hops was affecting ThT fluorescence was unclear but the effect, regardless, demonstrates its potential use as a treatment and warrants further study on its effects on α-syn aggregation. C. elegans overexpressing α-syn and exogenously exposed to α-syn showed changes in movement speed compared to untreated populations and this study found that exposure to hops reversed the changes in speed possibly caused by α-syn.

Abbreviations

PD, Parkinson's disease; ThT, thioflavin T; α-syn, α-synuclein; *C. elegans*, *Caenorhabditis elegans*; DDP1 (uonEx1 [unc-54::alpha-synuclein::CFP + unc-54::alpha-synuclein::YFP(Venus)]; DDP2 (uonEx2 [unc-54::CFP::YFP(Venus)];

1 Introduction

1.1 Parkinson's Disease

Parkinson's Disease (PD) is a neurodegenerative disease with cases developing in 1 in 50 people over the age of 65 (Schapira, 2009). The average duration of PD from diagnosis to death is 15 years with an increasing severity of motor and non-motor symptoms developing over the course of the disease (Lees et al., 2009). The severity of PD and its increasing occurrence call for more effective treatments than the standards used.

PD is typically diagnosed when a patient demonstrates four cardinal motor symptoms 1) bradykinesia (slow movement), 2) rigid joint movement, 3) resting tremors, and 4) postural instability (Postuma et al., 2015). Resting tremors are classified as a 3- to 6-Hz distal resting tremor (Gelb et al., 2008). PD is usually diagnosed by the four symptoms listed, but also includes gait freezing (freezing while walking) or festination (a random increase in walking speed), blink rate and speech abnormalities (Lees et al., 2009). PD also includes several nonmotor symptoms described next.

Nonmotor symptoms include autonomic dysfunction and cognitive dysfunction (Zesiewicz et al., 2006). The most common autonomic symptom in PD is orthostatic hypotension, a drop in blood pressure within 3 minutes of standing; PD patients can also develop abnormal thermoregulation, gastrointestinal or urinary tract dysfunction, or impotence (Gelb et al., 2008). Examples of cognitive dysfunction in PD are dementia, depression and hallucinations. These symptoms are less prevalent in all PD patients, but still impair quality of life and occur in 25-40% of PD cases (Gelb et al., 2008). The motor and non-motor symptoms become more severe as PD progresses and treatments currently do not target the pathophysiology allowing disease symptoms to worsen over time. The pathophysiology is outlined next with a brief history in PD research to provide insight into more effective treatments that can halt progression.

1.2 *Venus* Principle pathology in PD

The earliest recorded characterisation of PD was a description of symptoms by James Parkinson in 1817 (Parkinson, 1817). Nearly a century later in 1912, Fritz Jakob Heinrich Lewy described inclusions in cell bodies found in several brain regions of subjects with PD (Brundin and Melki, 2017). Over 200 years after the first description of PD symptoms, the initial cause of PD is still unknown, however, research points to two major pathophysiological characteristics in PD, degeneration of the nigrostriatal pathway and cytoplasmic inclusions.

The first major pathology discussed is the degeneration of the nigrostriatal pathway in the basal ganglia. Nerve cell loss was found in post mortem PD patients in the ventrolateral nerve cell group of the substantia nigra, and less neuronal loss in the dorsomedial group (Goedert et al., 2017). The regions containing the most lesions were part of the dopaminergic network of neurons in the nigro-striatal pathway (dopamine neurotransmitter acting at the synapse) (Beyer et al., 2009). PD pathology was linked to the dopaminergic projections mentioned and the first clue to a possible cause was the cytoplasmic inclusions found at the sites of neuron death.

1.2.1 Lewy Bodies

The cytoplasmic inclusions would come to be known as Lewy bodies, the other defining characteristic of PD pathology (Pollanen et al., 1993). Several years after the first description of Lewy bodies by Heinrich, in 1919, researcher Tretiakoff described the presence of Lewy bodies in the pars compacta of the substantia nigra (see Figure 1.1 A) (Tretiakoff, 1919). Later, researchers also found inclusions in the dorsal motor nucleus of the vagus nerve, the nucleus basalis of Meynert and some thalamic nuclei of PD patients (Goedert et al., 2017). The Lewy bodies were localised to these regions as opposed to being widespread in all brain regions. The brain regions containing Lewy bodies are identified and the physical characteristics of Lewy bodies are described next.

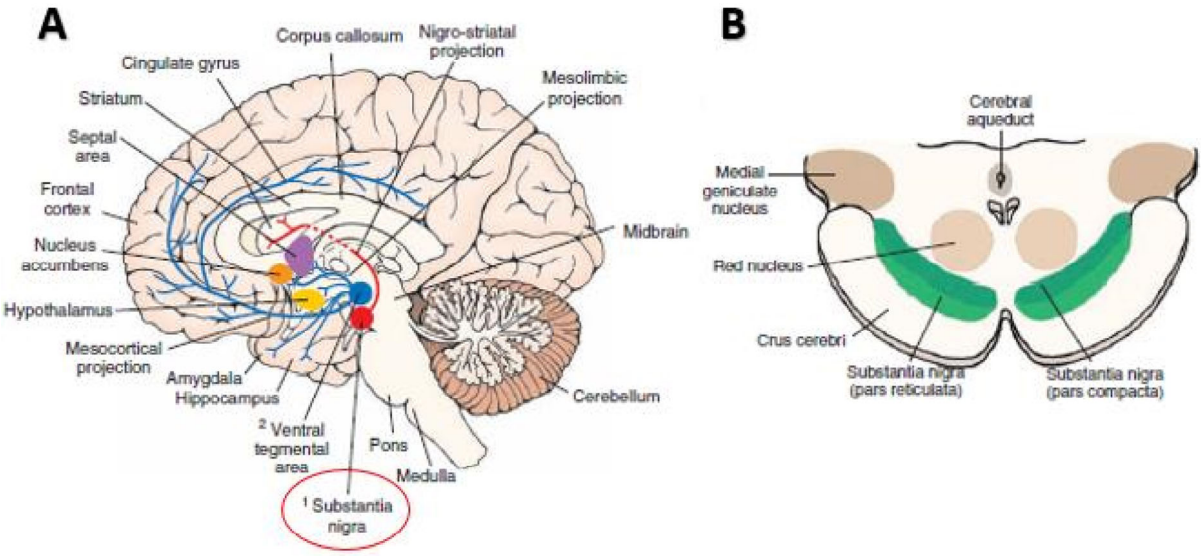

Figure 1.1 (A) Sagittal cross-section illustration of human brain, (B) coronal cross-section illustration of human brain highlighting the position of the pars compacta region of the substantia nigra shown in panel A. Pg. 118, 345; Siegel, A., & Sapru, H. N. (2011). Essential neuroscience (2nd;2; ed.). Philadelphia: Wolters Kluwer/Lippincott Williams & Wilkins Health.

Lewy bodies are 8–30 µm wide spherical structures that are eosinophilic (eosin stain left of the black arrow with a darker pink stain in panel A of Figure 1.2) (Olanow et al., 2004). Lewy bodies in neurons of the substantia nigra observed with an electron micrograph in panel B Figure 1.2 have a darker stained central core (dense granular material indicated by the white arrow) and a ring of filaments stained around the core (radiating filaments of 7–20 nm in diameter; black arrow in Figure 1.2 B) (Olanow et al., 2004; Beyer et al., 2009).

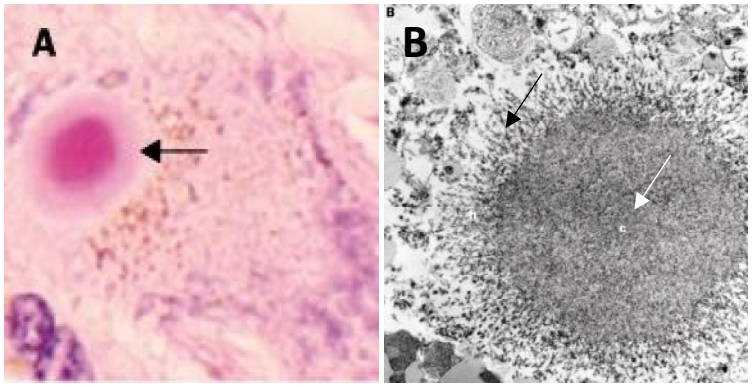

Figure 1.2 Images of Lewy bodies (A) in dopamine neurons of the substantia nigra with eosin stain, (B) electron micrograph showing the dense core and filaments. Page 497 (Olanow et al., 2004)

The second important PD pathology involves one of the key components of Lewy bodies. Lewy bodies were found to be made of more than 76 components, which belong to 10 different protein

classes such as structural elements, proteins involved in cellular responses, phosphorylation, signal transduction, cell cycle, cytoskeletal and cytosolic proteins (Beyer et al., 2009). The main component of Lewy bodies was the protein α-synuclein and the previously mentioned components were thought to be captured after the initial structure comprising α-synuclein is formed (Beyer et al., 2009). Although, Lewy bodies are a pathological marker of PD, researchers found that Lewy bodies are not cytotoxic because there was no correlation between neuronal loss and the formation of Lewy bodies (Hill and Tompkins, 1997; Tanaka et al., 2004) and instead, may be cytoprotective aggresomes, inclusions that degrade excessive amounts of, or dysfunctional proteins (Taylor et al., 2003; Olanow et al., 2004; Tanaka et al., 2004). Lewy bodies also share similar development processes with aggresomes, making them less likely to be responsible for the spreading degeneration in PD (McNaught et al., 2002). Alpha-synuclein being the main component of Lewy bodies became a new research priority because of its possible link to the origin of PD pathology.

1.3 Alpha-synuclein

Alpha-synuclein (α-syn) is a protein found near presynaptic terminals, encoded by the SNCA gene, with the highest levels found in the neocortex, hippocampus, substantia nigra, thalamus and cerebellum (Kim et al., 2014). Human α-syn contains 140 amino acids with a molecular mass of approximately 14 kDa (Ghosh et al., 2017). While the function of α-syn is unknown there is some evidence to indicate that α -syn may regulate neurotransmitter synthesis, release and vesicular storage (Cheng et al., 2011). In PD, Lewy bodies comprising of α-syn are an identifying factor of the disease. Alpha-syn could play an important role either initiation or progression of PD, hence, what researchers currently know about where α-syn is found and its functions are explored next.

In 1988, Maroteaux et al., (2018) identified α-syn in neuronal cell soma and found that it mostly localised at the synaptic nerve terminal. The localisation of α-syn was determined using light and electron microscopy; cross sections were stained with synuclein fusion protein antibody and fluorescein-conjugated wheat germ lectin, fluorescence was greatest near the nerve terminals. Later research involving immunostaining of rat brain tissue revealed α-syn was in abundant in the

neocortex, hippocampus, olfactory bulb, striatum, thalamus, and cerebellum and less abundant in the brain stem (Iwai et al., 1995). These are also the areas that contain Lewy bodies or neurodegeneration.

After identifying where α-syn localises in the body, researchers investigated the possible function of α-syn. Researchers showed α-syn may inhibit dopamine synthesis by influencing enzyme activity of tyrosine hydroxylase (TH) (Cheng et al., 2011). TH is an enzyme that catalyses the hydroxylation of tyrosine to L-dopa, which is converted to dopamine by an aromatic amino acid decarboxylase, making TH a rate-limiting enzyme in dopamine synthesis (Daubner et al., 2011). Alpha-syn is thought to most likely reduce the phosphorylation of TH, bind with TH in a dephosphorylated state, and maintain TH in an inactive form, all of which result in reduced dopamine synthesis (Cheng et al., 2011).

Alpha-syn may also affect vesicular storage and release of dopamine. Entry of dopamine into vesicles is controlled by vesicular monoamine transporter 2 (VMAT2) (Daubner et al., 2011). Overexpression of α-syn caused down-regulation of VMAT2 and increased dopamine release into cytosol, whereas knockdown of α-syn increased dopamine vesicular storage (Cheng et al., 2011). Any effect on α-syn was shown to directly affect dopamine activity demonstrating the protein's role in regulating neurotransmitter synthesis and release.

Although the exact mechanisms of α-syn function are yet to be determined, this protein plays a positive role in neurotransmitter activity and some factor or incident causes the protein to aggregate in PD. Alpha-syn is an intrinsically disordered protein that can bend into different shapes and is susceptible to aggregation because of its flexible structure, unlike ordered proteins that exist in stable 3-dimensional structures (Frimpong et al., 2010; Breydo et al., 2012). As an amyloid protein, α-syn is prone to aggregation, however very little aggregation is observed in normal individuals. Since greater than 90% of PD cases are idiopathic in nature with no known genetic cause (Rocca et al., 2004; Deleidi and Gasser, 2013; Ghosh et al., 2017). The challenge faced then is to

identify what causes idiopathic PD. If not a genetic mutation, what pathology is first induced which then spreads throughout the brain leading to the syndrome referred to as PD. Aggregation of α-syn appears to be one of the earliest pathologies associated with the disease, and so it is likely that any potential initiating trigger may be associated with disruption to or aggregation of this protein (Braak et al., 2003; Danzer et al., 2007). In the next section we will examine evidence presented in the literature that suggest α-syn is involved in the earliest stages of the disease and therefore how disruption of α-syn aggregation may therefore represent a promising avenue of investigation as a potential mechanism for treating the disease.

1.3.1 Alpha-syn pathology

The aggregation pathway of α-syn is still unclear but outlined next are some possible aggregation pathways based on recent research (Ghosh et al., 2017). The original consensus was that α-syn proteins existed in the cytoplasm as single molecules referred to as monomers in this study. After being examined in non-denaturing conditions, researchers discovered that endogenous α-syn exist as stable folded tetramers that do not easily aggregate (~58kDa) (Ahmad and Lapidus, 2012; Kim et al., 2014). According to this evidence, an extra step in the aggregation process might occur, destabilising the tetramers and allowing monomeric α-syn to aggregate. The initial molecular structures thought to be formed were dimers, two α-syn molecules bound together (~29 kDa) (Kim et al., 2014).

After dimer formation, different α-syn oligomer species were shown to form in vitro (Cremades et al., 2017). The mechanism in which the different oligomer species form is unknown, however, the physical characteristics of these species were described in vitro (Danzer et al., 2007). Two unique archetypes of oligomers were observed, spherical and ring shaped (Ghosh et al., 2017). The two species of oligomer are an intermediate between monomeric α-syn and the fibrillar Lewy Bodies; they are functionally different to each other.

Of the two species, the spherical oligomers showed no cytotoxic effect (Danzer et al., 2007), but nonetheless, showed a characteristic that could be important in PD. SH-SY5Y human

dopaminergic neuroblastoma cells exposed to spherical oligomers caused intracellular aggregation of α-syn (Danzer et al., 2009). The seeding effect of these oligomers falls in line with the understanding that PD is progressive. Further studies showed the possible means in which oligomers spread from neuron to neuron (Luk et al., 2009, 2012).

Originally, researchers thought oligomers spread to other neurons by membrane leakage from dying cells, but this was overlooked because α-syn released from dying cells did not propagate to other neurons (Ottolini et al., 2017). In vitro, extracellular oligomers were up taken by human H4 neuroglioma cells via exosomes (small vesicles with sizes between 60–100 nm) (Danzer et al., 2012). The oligomers were both inside the vesicular space of exosomes and bound to the outside surface of exosomes. Exosome bound oligomers were more likely to be taken up by neighbouring neurons than unbound oligomers and were also more likely to be cytotoxic (Danzer et al., 2012). Exosomal uptake of oligomers explains the first part of α-syn propagation linked to the spreading neurodegeneration found in PD.

The second part of propagation involves axonal transport. Once inside the neuron, oligomers still need to travel along the axon to reach other neurons. The method in which axonal transport occurs is under debate because the anterograde axonal pathway becomes degraded over time (Li et al., 2010; Tang et al., 2012; Ottolini et al., 2017). The oligomers are thought to hinder microtubules and kinesin motors responsible for anterograde transport (from cell body to synapse) without affecting dynein mediated retrograde transport (synapse to cell body) (Ottolini et al., 2017). Oligomers are thought to travel along the axon from synapse to the cell body, after fibrillar a-syn was monitored using live-cell imaging and immunofluorescence to characterize the transport of fluorescent a-synuclein fibrils and their transfer to second-order neurons (Freundt et al., 2012). Although more research is required to ascertain the exact mechanism of α-syn propagation, growing evidence indicates exosomal uptake and retrograde transport are the probable means of propagation.

Continued research showed the transmission of α-syn from the stomach to the brain along the vagus nerve using female Sprague-Dawley rats (Ulusoy et al., 2017), further supporting the uptake and transfer of α-syn. Although these results did not specify exosomal uptake or axonal transport, these findings also demonstrate that α-syn is being transmitted from to neuron to neuron, highlighting the need to stop the spread of α-syn oligomers.

The final mechanism of PD pathology involving oligomers to be discussed is neuronal death, mostly but not limited to dopaminergic neurons (Paleologou et al., 2009; Agosta et al., 2013; Daviaud et al., 2014). Originally, the Lewy body deposits found in post mortem PD brains were thought to be cytotoxic, however, researchers later discovered that ring-shaped α-syn oligomers were actually the species causing apoptosis (Chen et al., 2015). In vitro, ring-shaped α-syn oligomers bound to the cell membrane disrupting the lipid bilayer (Cremades et al., 2017), forming pore-like channels (Breydo et al., 2012). Oligomers caused cytotoxicity in cell cultures by triggering an influx of calcium into cells through the newly formed channels, affecting mitochondrial function (Danzer et al., 2007), causing cell death through caspase-3 activation (Dehay et al., 2015); caspase-3 is a protease that mediates apoptosis in neurons (D'Amelio et al., 2010).

Most research points to α-syn oligomers as the main cause of progression in PD severity and continual degeneration of neurons (Hashimoto et al., 1997; Irizarry et al., 1998; Danzer et al., 2007, 2009; Saito et al., 2016) rather than the Lewy bodies, which are thought to be cytoprotective and not cytotoxic (Olanow et al., 2004; Tanaka et al., 2004). Current PD treatments, however, do not target oligomers or any mechanisms linked to their spreading toxicity and allow PD symptoms to worsen overtime. One of the aims in this study is to target the aggregation process of α-syn in vitro to prevent oligomer formation, which would prevent uptake, seeding and cytotoxicity.

1.4 Treating PD

The primary therapeutic treatments of PD treat symptoms by targeting the deficiency of dopamine in the dopaminergic neurons; the treatments most commonly used are levodopa, mono amine

oxidase inhibitors (MAO), and dopamine agonists (Lees et al., 2009). The mechanism of these treatments is to increase the reduced dopamine levels in PD. The loss of dopamine is likely due to the loss of dopaminergic neurons (Daviaud et al., 2014) thought to be caused by toxic α-syn oligomers (Danzer et al., 2007), however, based on the research of α-syn function and its control of dopamine release (Yavich et al., 2004), less dopamine could be available at the synapse due to the loss of functional α-syn. None of the treatments stop the underlying disease process of neurodegeneration, and only help alleviate some of the motor symptoms caused by neurodegeneration. The mechanisms and disadvantages of current treatments will be described to demonstrate why there is a need for a new treatment that targets the earliest known origin of PD pathology, α-syn aggregates.

1.4.1 Levodopa

The standard and most prescribed treatment for PD is dopamine replacement with levodopa (Lees et al., 2015). Levodopa is used instead of dopamine because it can cross the blood brain barrier whereas dopamine cannot. It is an amino acid that is converted to dopamine by dopaminergic neurons after it bypasses the blood brain barrier (Haddad et al., 2018). Levodopa treats PD by replacing lost dopamine at dopaminergic synapses in the brain and is currently the most effective treatment in PD (Bereznicki, 2010).

The first issue that was resolved with levodopa treatments was the low bioavailability because of decarboxylation by the enzyme amino acid decarboxylase (Freitas et al., 2016). This was resolved by administration of a decarboxylase inhibitor with treatments. Even after levodopa bioavailability is increased, continued use causes dyskinesia and involuntary movement from response fluctuations (Lees et al., 2009). After long term use, PD patients require increased doses due to diminishing therapeutic action (Freitas et al., 2016). A solution to the dramatic fluctuation in dopamine levels and the reduced effectiveness occurring with levodopa usage was to administer dopamine agonists with longer half-lives such as ropinirole as a first line treatment (Lees et al., 2009; Rascol et al., 2015). Using dopamine agonists, would provide a more continuous administration of

dopamine to dopaminergic neurons, reduce dopamine fluctuation and delay the required use of levodopa (Schapira, 2009).

1.4.2 Dopamine agonists

Dopamine agonists such as ropinirole are also effective in treating PD and their longer half-life provides continuous dopaminergic stimulation compared to levodopa (Schapira, 2009). Dopamine agonists do not cause dyskinesia, but they are not as effective as levodopa (Kulisevsky and Pagonabarraga, 2010), making them useful in delaying the use of levodopa.

1.4.3 MAO inhibitors

Another treatment used in PD is MAO inhibitors, which work by inhibiting enzymes that break down dopamine thereby increasing dopamine availability at the synapse (Schapira, 2009). MAO inhibitors are not as potent as levodopa when treating the motor symptoms because when the dopaminergic neurons die, the rate of metabolism becomes greater than the rate of dopamine preserved by MAO inhibitors (Lees et al., 2009). However, using MAO inhibitors in the early stages of PD may delay disease progression (Lees et al., 2009). The combined therapy of levodopa and MAO inhibitors both reintroduce lost dopamine and prolong its availability (Schapira, 2009).

Although more effective methods of replacing dopamine are now used, they still do not treat postural instability and cognitive symptoms like dementia. The symptoms that develop in the later stages of PD as a result of disease progression put patients at risk of injury making the need for a treatment that targets the original pathology of PD (Schapira, 2009).

To find better treatments for PD, researchers used different models to further elucidate the underlying pathology of PD and investigate possible therapies. This study aims to add a preliminary model that requires less time to undertake, allowing careful refinement of therapies before using larger animal models. The commonality between all the current treatments used to treat PD is that they do not treat the earliest known pathology of PD. They do not treat the cytotoxicity caused by α-syn oligomers. Hence, the first aim of this study was to optimise a protocol for an assay that examines the rate of α-syn aggregation that can be used to test treatments that target α-syn

aggregation and prevent oligomer formation. The following section discusses how treatments should be chosen for testing using the assay and what was the first treatment tested in this study.

1.5 Approaches to discovering PD treatments

This section will go through the general drug discovery process and the current process used in PD. There are several approaches and pathways to discovering new treatments for diseases. The first phase is usually identifying the treatment of the target (Hughes et al., 2011). Target identification is followed by assay development that examines the effects of the treatment on the target. The next phase is the screening process for different compounds that will be used in the assays. The final phases involve hit identification and lead optimisation of compounds, in which compounds are selected based on characteristics based on potency and bioavailability (Waring, 2010). The final phases are not discussed in detail because they are not the focus of this study.

1.5.1 PD treatment target

The first phase in finding a potential treatment is identifying the treatment of the target (Hughes et al., 2011). The target can be proteins, genes or RNA involved with the disease or its progression. In PD, the earliest known pathology is the development of oligomeric α-syn species as mentioned earlier, making α-syn aggregates a target for treatments. The origin of PD is unknown and cannot be targeted, however, a treatment that targets the earliest pathology that is known to cause neuronal degeneration can delay or prevent the progression of PD. Targets other than the α-syn pathology will be described to illustrate some of their benefits and why targeting the earliest pathology is the most promising.

1.5.1.1 Dopamine depletion

Reducing dopamine levels was one of the early models of PD because of the onset of PD like symptoms reproduced by this model. Altering dopamine levels was one of the first models that led to the discovery of the gold standard of PD treatment, levodopa (Lees et al., 2015). The administration of reserpine depleted dopamine levels and caused PD like symptoms by inhibiting the vesicular transporter of monoamines (VMAT2) (Leão et al., 2015). Levodopa was used to reverse the

reduced levels of dopamine caused by reserpine administration, thereby, reversing the symptoms induced (Lees et al., 2015). As impactful as the reserpine model of PD was, reserpine did not mimic the pathology found in PD. Most current research is focused on neurotoxic and transgenic models of PD because those models better emulate the neuronal loss seen in PD (Leão et al., 2015). Since reserpine works by reducing dopamine levels, this model does not allow researchers to understand the documented loss of neurons.

1.5.1.2 Dopaminergic neurotoxins

The models discussed next are those that mimic the neurodegeneration found in the nigrostriatal dopaminergic pathways. 6-hydroxydopamine (6-OHDA) is a neurotoxin that causes lesions at the site of injection (Stott and Barker, 2014). 6-OHDA selectively targets catecholaminergic transporters, but requires correct dosing, injection technique, injection site and other factors to ensure the brain region being studied is targeted (Sachs and Jonsson, 1975). Treating rats with 6-OHDA allowed researchers to test possible PD therapies such as curcumin, which showed a neuroprotective effect against 6-OHDA exposure (Zbarsky et al., 2005). The 6-OHDA model does not involve α-syn or result in inclusions at the sites of degeneration (Duty and Jenner, 2011; Stott and Barker, 2014). Instead, the 6-OHDA model relies on the remaining presence of tyrosine hydroxylase-stained cells to determine a therapy's effects. This model can still be used to discover new treatments for PD, but not specifically those that target α-syn pathology.

Another neurotoxin used to model neurodegeneration in PD is 1-methyl-4-phenyl-1,2,3,6-tetrahydropyridine (MPTP) (Müller and Bohnen, 2013). MPTP is a toxin with an affinity to dopaminergic neurons (Muñoz-Manchado et al., 2016). MPTP PD models helped identify possible mechanisms of neuron death in PD and similar to 6-OHDA administration, MPTP was injected directly into the brain regions being studied (Noelker et al., 2013). Using MPTP in this way, however, resulted in rapid cell death as opposed to the progressive degeneration found in PD. Unlike 6-OHDA, researchers later showed that consistent low doses of MPTP can better model progressive

degeneration of PD (Muñoz-Manchado et al., 2016), but the remaining disadvantage of an MPTP model is the lack of α-syn pathology.

Rotenone is a more recent neurotoxin used to model PD that inhibits mitochondrial complex I (Tanner et al., 2011). Rotenone causes neuron death at exposure sites like MPTP and 6-OHDA, and can also cause most of the movement disorders found in PD along with Lewy body formation (Panov et al., 2005; Maturana et al., 2015). The main limitation of the rotenone model is in the variability of subjects that develop nigrostriatal lesions, but new research shows that intraperitoneal administration increases reproducibility (Cannon et al., 2009). Of the three models described, rotenone shows the most similarity to PD pathological manifestations and could be the model of choice when working with larger subjects such as rodents.

1.5.1.3 Transgenic

The final class of PD models discussed here is the use of transgenic species, consisting of either knockout or overexpression of genes associated with PD. Knockout models proved to be pertinent to PD because knockout mice with targeted deletion of α-syn showed reduced impulsivity (Peña-Oliver et al., 2012) and some impairment with dopamine and glutamate release (Gureviciene et al., 2007), however, these models demonstrate the long term effect of the loss of α-syn function (Greten-Harrison et al., 2010) rather than the cytotoxicity and the reason why α-syn is losing its function (Rieker et al., 2011). Transgenic models can be used to mimic the α-syn pathology involved in PD depending on the genes that are overexpressed, and the animal species used (Blesa and Przedborski, 2014).

Some of the different transgenic animal models used in previous PD research are mice, Drosophila, C. elegans and zebrafish (Duty and Jenner, 2011). Mice overexpressing human α-syn demonstrated substantial atrophy and reduced brain volume (Haggerty et al., 2011). Other studies looking at the overexpression of wildtype mouse ortholog (m α-syn) also showed pathological changes resembling those found in post-mortem human PD because of the strong α-syn staining in the brainstem and cerebellum (Rieker et al., 2011).

Drosophila expressing human α-syn showed a reduction in climbing ability, which was reversed when treated with L-DOPA (Pendleton et al., 2002). Haywood and Staveley (2004) also showed a reversal in α-syn-induced premature loss of climbing ability of Drosophila using conditional expression of parkin, a gene that encodes for ubiquitin protein ligases. Ubiquitin protein ligases act to identify damaged or misfolded proteins to facilitate the attachment of a number of ubiquitin monomers of these proteins and are targeted to the proteasome (Haywood and Staveley, 2004).

Transgenic C. elegans expressing A30P or A53T mutant α-syn failed to control locomotory rate in response to food and showed a reduction in neuronal dopamine content (Kuwahara et al., 2006). Transgenic Zebrafish, 3-4 cm long vertebrates, were modified with the deletion of leucine-rich repeat kinase 2 (LRRK2) (Prabhudesai et al., 2016). LRRK2 mutations are one of the most common causes of genetic PD and knocking out LRRK2 in zebrafish, caused a loss of dopaminergic neurons and reduced swimming distance (Duty and Jenner, 2011; Prabhudesai et al., 2016). The different transgenic models discussed all demonstrated some form of α-syn pathology and in many cases are proving useful in treatment discovery. The study described in this thesis also attempted to add a novel means of administering α-syn to c elegans to try and induce α-syn pathology, without the need to generate genetically modified organisms. The method proposed, to induce α-syn pathology by feeding exogenous α-syn is non-invasive, and technically very easy to do using existing standard lab equipment. This model will be discussed below.

1.5.1.4 Alpha-syn aggregation

More research is being done to target the aggregation of α-syn to screen for PD treatments. Several studies tested treatments targeting α-syn aggregation because of the toxicity of oligomers and because this is the earliest known pathology in PD (Giehm et al., 2011; Daturpalli et al., 2013; Macchi et al., 2016). The studies used different assays and techniques to measure the effects of a treatment on aggregation. Some of these assays and techniques are discussed next.

Exogenous exposure to α-syn was considered a valid means of treatment administration in this study because of research showing prion presence in blood via nasal and oral exposure in

hamster and deer (Elder et al., 2015). Research pertaining to PD also showed that α-syn can travel through the vagus nerve in rats from the gut to the brain (Holmqvist et al., 2014) and from the brain to the gut (Ulusoy et al., 2017). Both findings are important because the gut-brain transfer represents a means of contracting α-syn pathology and possibly PD through feeding. The brain-gut transfer shows that α-syn pathology could be infectious. Since C. elegans have a much more simplified digestive tract consisting of only 100 cells that serve as the pharynx, intestine and rectum (Kormish et al., 2010), they should be more susceptible to α-syn pathology through feeding. The simplicity of the digestive tract and the high concentrations of α-syn used in this study increase the likelihood of α-syn uptake. Past studies also showed that transgenic *C. elegans* exposed to *E. coli* producing the extracellular bacterial amyloid protein curli exhibited enhanced α-syn aggregation (Chen et al., 2016).

1.5.2 PD assay development

Target identification is followed by assay development that examines the effects of a treatment on the target. Assays can be in vitro or in vivo with examples of each found in the literature. In vitro assays typically include the use of colorimetric or fluorescence assays to measure a response or an affinity to the selected target (Hughes et al., 2011). One of the most commonly used in vitro assays in measuring α-syn aggregation is the thioflavin T assay (Lee and Lee, 2002; Voropai and Samtsov, 2003; Niidome et al., 2007; Giehm et al., 2011; Ono et al., 2012; Daturpalli et al., 2013; Wördehoff et al., 2015). Thioflavin T (ThT) is a yellow dye that was shown to fluoresce in the presence of amyloid β-sheets (Wördehoff et al., 2015). The ThT assay is one among many different techniques used to visualise the aggregation of α-syn.

1.5.2.1 In vitro

Other in vitro assays include light scattering, dynamic light scattering (DLS), small angle X-ray scattering, transmission electron microscopy (TEM), atomic force microscopy (AFM), far-UV circular dichroism, Fourier transform infrared spectroscopy (FTIR) and fibre X-ray diffraction (Giehm et al., 2011). Light scattering is one of the least sensitive to detection of aggregates of the techniques

listed. Although optimisations of this technique exist for DNA (Feng et al., 2011), other techniques require fewer optimisations. Dynamic light scattering, unlike light scattering, is highly sensitive to aggregates, but this is both useful for detecting low concentrations of aggregates and impractical because of the necessity to have highly pure samples (Giehm et al., 2011). X-ray scattering, TEM, AFM, far-UV circular dichroism, FTIR and fibre X-ray diffraction allow a greater level of visualisation compared to using a fluorescence assay. The limitation for these techniques is the inability to conduct high throughput testing of treatments (Giehm et al., 2011). The use of the ThT assay to detect α-syn in vitro is prevalent in research because it balances sensitivity and high throughput screening (Lee and Lee, 2002; Voropai and Samtsov, 2003; Niidome et al., 2007; Giehm et al., 2011; Ono et al., 2012; Daturpalli et al., 2013; Wördehoff et al., 2015).

1.5.2.2 In vivo and ex vivo assays

In vivo or ex vivo assays can also be used to measure the effects of a treatment. Ex vivo assays encompass cell culture, using distinct cell lines and in vivo, animal models using different species. Cell cultures and animal models each provide a different insight to the effects a treatment has on the target. (Anders and Vielhauer, 2007)

Cell cultures provide a model that leaves out the complexity of a full organism and they allow researchers to observe the effects of a treatment on individual cells and interactions between cells without the need for ethics committee approval. The ability to monitor interactions between cells was used to observe the spread of oligomeric proteins from cell to cell using the SH-SY5Y neuron cell line (Freundt et al., 2012; Krauss and Vorberg, 2013). Studies also observed the cytotoxicity of oligomers using SH-SY5Y (Danzer et al., 2007; Schlachetzki et al., 2013). Using cell cultures to test treatments and study disease will remain a powerful research tool, but one of the main drawbacks considered by this study is the susceptibility to contamination.

Before mentioning the species used in this study other species will be examined to address the reasons they were not selected. There are many species used in vivo models for studying diseases. Some of the mammalian species include: monkeys, pigs, rat, mouse, rabbit (Ribeiro et al.,

2013; Vaquer et al., 2013). Miniature pigs are usually used in research because of anatomical, physiological, and genetic similarities to humans; they have a fully gyrencephalic brain and as adults have an equal ratio of cerebral white and grey matter, comparable to that in humans (Conrad et al., 2014; Ryan et al., 2018). From mammals, rodents are the main animal order used for developing disease models (Anders and Vielhauer, 2007). Rodents are used because of their high reproduction rate (Lohmiller and Swing, 2006) and their handling ease (Koch, 2006), however there are species that have an even greater reproduction rate at a smaller cost.

The use of mammals involves a greater maintenance cost and requires ethics committee approval whereas smaller non-mammalian models such as drosophila or *C. elegans* require no approval and little maintenance costs (Lim, 2010). *C. elegans* is a species gaining research interest in neurodegenerative disease because of documented neuronal loss and behavioural changes with the overexpression of α-syn (Raslan and Kee, 2013). *C. elegans* allow the study of cell interactions like cell cultures and behavioural analysis like other animal models (Harrington et al., 2010; Risley et al., 2016). *C. elegans* do not require any ethics committee approval like other animal models and have shorter life spans with a high reproduction rate. A population with high statistical power can be achieved within a few weeks of breeding and multiple studies can be conducted within this same time frame (Harrington et al., 2010).

Compared to other invertebrate species like drosophila, another commonly used invertebrate in modelling disease (Whitworth et al., 2006), *C. elegans* is also advantageous because of the limited movement on a 2-D plane allowing easier video analysis. Both drosophila and *C. elegans* allow high throughput screening, but the ease in handling *C. elegans* made its use more feasible for behavioural analysis in this study.

C. elegans as subjects allow a high throughput level of testing treatments because of their short life span and high reproduction rate allow greater statistical power than mammal models. This leads to another aim, which was to develop an α-syn pathology in *C. elegans* that can be used to test

the effects of different treatments that can reverse any behavioural changes. This would be done by exogenous exposure to α-syn and then measuring movement speed of the nematodes.

1.5.3 Treatment screening

After developing assays to screen treatments, a method of selecting treatments needs to be considered. There are several screening strategies which include: high throughput, focused screen, fragment screen, structural aided drug design, virtual screening, physiological and nuclear magnetic resonance (Hughes et al., 2011). The most time-consuming method of screening would be high throughput screening, which is screening the whole library of compounds (Hughes et al., 2011). The other methods involve a categorization of compounds that are more likely to bind or affect the target.

The goal of focused, structure based, and virtual screening is to reduce the number of compounds to be tested. Compounds found in online databases are selected based on their structures by either virtual high throughput testing or selection according to specific structures (Sliwoski et al., 2014). To further reduce the number of compounds to test, other studies used automated datamining to determine which herbs and constituents from the literature could treat neurodegenerative disease (Harvey, 2008; Ke et al., 2016).

The treatment chosen in this study was hops because of its polyphenol content (Liu et al., 2014). Polyphenols are thought to be neuroprotective because of the inhibition of amyloid formation (Porat et al., 2006; Pandey et al., 2008; Singh et al., 2013; Magalingam et al., 2015). Polyphenols such as curcumin were shown to inhibit the aggregation of α-syn both in vitro using a colorimetric assay and in vivo using catecholaminergic SH-SY5Y cell lines with red fluorescent protein (DsRed2) fused with an A53T mutant of α-syn (Pandey et al., 2008). The polyphenol present in hops is the flavonoid xanthohumol, which was shown to reversibly inhibit α-Glucosidase enzyme in vitro (Franco et al., 2013; Liu et al., 2014). Even though xanthohumol was the constituent that was shown to inhibit an enzyme, homogenous unfiltered hops was used as a treatment in this study rather than isolating xanthohumol, in case there were other active constituents. The use of hops to affect α-syn

aggregation is a novel part of this investigation and the lab. The final aim was to study the effects of hops on the aggregation of α-syn using an optimised protocol developed in the lab.

1.6 Aims and Hypotheses

Two major aims were chosen in this study. The first was developing an in vitro ThT assay that could observe the formation of α-syn aggregates and to use this assay to test treatments that would prevent aggregate formation. The ThT assay alone will not resolve whether a treatment is preventing the formation of aggregates, but any changes in fluorescence will represent a possible interaction with protein aggregation. The assay would be a preliminary step in discovering treatments that target the formation of α-syn oligomers in PD. Any treatments that reduce fluorescence could be studied and the mechanism of fluorescence reduction could be determined with confocal microscopy. The treatment used first was hops because research showed flavonoids affect the aggregation of α-syn and it was expected to have an inhibitory effect on fluorescence in the ThT assays (Stevens and Page, 2004; Liu et al., 2014). The second major aim was to develop a preliminary behaviour assay using *C. elegans* and exposing them to α-syn. This study looked at behavioural changes to be able to test a greater number of subjects in a shorter period. Observing a decrease or increase in movement and bend speed was expected in *C. elegans* treated with α-syn oligomers because of studies showing the uptake of α-syn protein from the vagus nerve (Ulusoy et al., 2017).

2 Methods

2.1 Producing α-synuclein

The pET28a plasmid containing human α-syn sequence was used to express α-syn in the *Escherichia coli* strain BL21*(DE3). BL21 is a protease deficient strain of *E. coli* which results in fewer problems with protease activity when purifying proteins grown in them (Ratelade et al., 2009). The engineered *E. coli* was a kind donation from Dr Agata Rekas (https://archive.ansto.gov.au/ResearchHub/OurPeople/StaffProfiles/REKAS-AGATA), a protein chemist at the Australian Nuclear Science and Technology Organisation (ANSTO). Dr Rekas examined the α-syn by small angle x-ray

crystallography (Rekas et al., 2010) and determined the purity of the protein to be above 95% by SDS-PAGE and Mass spectrometry (Rekas et al., 2010; Pham et al., 2014).

The α-syn expressing *E. coli* was shaken overnight at 37°C in LB 5052 containing 50 µg/mL of kanamycin until solution turbidity reached an optical density range of 0.6 – 1.02. IPTG was not used to induce protein expression of α-syn as the protocol utilizes autoinduction (IPTG is commonly used to induce protein expression where genes are regulated by the lac operator). The whole LB solution was spun for 20 minutes at 6000g. The supernatant was discarded, and the pellet was frozen at 20°C until the next step.

The pellet was resuspended in osmotic shock buffer (40% w/v sucrose in 30 mM Tris-HCl 2 mM EDTA pH 7.2) and centrifuged at 6500g for 30 minutes. The supernatant containing the proteins was collected and vortexed with 7.7 mM $MgCl_2 \bullet (H_2O)_6$ in a final concentration of 20 mM Tris-HCl pH 7.0. The new suspension was centrifuged for 20 minutes at 27000g at 4°C. The supernatant was collected, and the pH was adjusted to 3.5, which caused other cellular proteins to precipitate, leaving α-syn soluble. This suspension was centrifuged for 30 minutes at 27000g at 4°C and the supernatant was collected, and pH adjusted to 7.

Finally, the α-syn was purified using an FPLC anion exchange column (Nuvia Q, Cat No. 156-0415, BioRad). Alpha-syn was then dialysed against reverse osmosis (RO) H_2O. After dialysis the concentration of α-syn was determined using Fourier Transform Infrared (FTIR) spectroscopy (Direct Detect, Millipore). The samples were portioned into 1 mg of protein, freeze dried and stored at -80°C until use. The lyophilization of α-syn was used in previous studies in which α-syn oligomers were produced (Kostka et al., 2008). In these studies, it was noted that lyophilised α-syn was reconstituted prior to use and that no protein was used more than once, thereby avoiding problems associated with repeated freeze thaw cycles. The purity of the α-syn was determined using SDS-PAGE and western blot and was found to be greater than 98% pure. Western blots were performed in the lab prior to this study and all bands appearing on the blot were identified by two different

commercially available antibodies against human alpha-synuclein (Mouse anti-alpha Synuclein antibody (abcam; ab27766); Rabbit anti-α-Synuclein antibody (Sigma; S3062-.2ML)). Mouse anti-alpha Synuclein antibody (abcam; ab27766) reacts with an epitope located in the region encoded by amino acids 115-122 of α-syn. The rabbit polyclonal anti-α-Synuclein antibody was described as recognizing human and rat α-syn in the specification sheet provided by the manufacturer and the positive staining of α-syn in immunoblot experiments was specifically inhibited by an immunizing peptide. Samples were thawed and dissolved before use and no protein samples were used more than once.

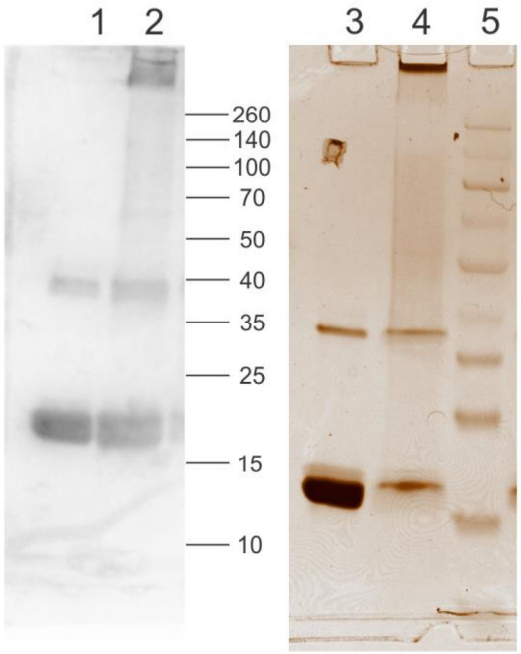

Figure 2.1 The western blot above was run in 2019. 15µg of protein was loaded into wells 2 and 4. 10µg of protein was loaded into wells 1 and 3. The lanes contained the following: Lane 1) α-syn aggregated and prepared in 2019, lane 2) 2016 α-syn (from 20190208 HP5 Sample 6), lane 3) 2019 α-syn, lane 4) α-syn aggregated and produced in 2016 (from 20190208 HP5 Sample 6) and lane 5) 20µL Pre-stained Rainbow Mw Markers (Spectra Multicolour Broad Range Protein Ladder (Thermofisher; #26634)).

Protein purity was calculated using densitometry using BioRad Image Lab software (version 5.2). The background density of a suitably matched empty space on the gel was subtracted from each lane to normalise each lane. The background-corrected density of the protein band by the background-corrected density of the whole lane was divided and multiplied by 100 to get % purity (Stessl et al., 2009; 2017). The majority of papers that use recombinant proteins use SDS-PAGE as a

measure of the purity of the protein after the purification steps, typically describing the purification steps as achieving a greater than 95% level of purity (e.g. Yanamandra et al., 2011; Magdeldin et al., 2014; Wu et al., 2019). The method used to establish the purity of the protein is standard across the literature and the level of purity reached is consistent with that reported by other papers (Huang et al., 2005; Manne et al., 2019; Wu et al., 2019). Silver stain is an extremely sensitive method of protein detection on an SDS-PAGE gel, detecting protein content as little as 0.07 ng/mm2 (Oakley et al., 1980). If all the bands detected by silver stain were shown to be α-syn, then it is reasonable to conclude that the purity of the α-syn produced is high.

2.2 Thioflavin T assays

The thioflavin T (ThT) assay was performed in a 96-well plate. Assay was performed in triplicate using 150 µL of sample in each well. Each well contained a 3-mm glass bead to assist with mixing the sample during the incubation unless otherwise noted. The plate was incubated at 37°C for 169 hours and fluorescence was read each hour using a FLUOstar Omega plate reader (BMG Labtech) with excitation of 440 nm and emission of 480 nm. The plate was shaken at 500 rpm for two minutes immediately prior to each reading. Each treatment contained a final concentration of 1 mg/mL α-syn (concentration was chosen to keep aggregation time within 1 week; lower concentrations increase aggregation time (Kostka et al., 2008; Daturpalli et al., 2013)) in the ThT buffer (40 µM ThT in 0.1M PBS with 0.05% w/v thimerosal), with a 10% v/v of the treatment solution. The solution was filtered with a 0.2-µm filter prior to adding the treatment and loading onto the plate.

Hops treatments were prepared in four different ways. Firstly, raw cold hops extract was prepared by homogenizing 10 mg/mL of compressed hops pellets from a commercially available supplier (Ella Hops Pellets; craftbrewer.com.au) for two minutes in the ThT buffer at room temperature (~21°C) using a stick blender. The unfiltered homogenate was then used as a treatment in the ThT assay. A second treatment was prepared by filtering the raw cold hops extract used in treatment 1 through a 0.2-µm filter. A third treatment was hops boiled at 10 mg/mL of the

same compressed hops pellets in ThT buffer for 10 minutes. Any volume that was lost during boiling was replaced using RO water. The raw homogenate from this process was referred to as Hot Hops and was used as Treatment 3. Lastly the active components from hops for use in brewing can be extracted from the plant material using liquid CO_2. A 1 mg/mL of the liquid CO_2 extract purchased from a commercial source (CO_2 Hops extract; Yakima Valley Hops) was used as Treatment 4. Once the plate was loaded, the plate was sealed using Micro-seal 'B' PCR Plate Sealing Film (BioRad) to prevent evaporation of sample during incubation.

2.2.1 Analysis of ThT assays

The data from the plate reader was arbitrary fluorescence units over time. Data was normalised in excel by setting the lowest value to zero. The normalised data was exported to GraphPad Prism for analysis. Four key features of the α-syn aggregation graphs were determined: maximal fluorescence, time to half maximal fluorescence, maximum reaction rate and the lag phase (time until the fluorescence became 5% greater than the blank sample). Nonlinear regression was used to fit a curve to the data. The maximal fluorescence was automatically calculated (the highest point of the curve). The time to half maximal fluorescence and the lag phase were interpolated from the curve (finding the value of time for 0.5*max and 0.05*max). The maximal reaction rate was determined by calculating the derivative of the curve and finding the peak value. These four characteristics of the α-syn aggregation curve were used to compare the effects of different treatments on aggregation.

2.2.2 PAGE analysis of the ThT assays

After the ThT assays were completed, the well samples were stored at 4°C overnight. The ThT assay samples were analysed using gel electrophoresis to observe the size of the aggregates. PAGE gels (BioRad Mini-PROTEAN TGX Stain-Free Gels #456-8123) were run at 200 V for 45 min, stained using the Silver Stain Plus silver staining kit (Bio-Rad; -#161-0449). Samples were prepared using a loading buffer (250 mM Tris pH 6.8; 0.12% bromophenol blue; 40% v/v glycerol; 8% w/v SDS; 20% v/v β-mercaptoethanol) and ran in a Tris glycine running buffer (25 mM Tris; 192 mM glycine; 0.1% w/v

SDS). The gels were imaged using Bio-Rad ChemiDoc MP System with Image Lab using similar steps described in section 2.1.

2.3 *C. elegans*

C. elegans strains were provided by the CGC, which is funded by NIH Office of Research Infrastructure Programs (P40 OD010440). *C. elegans* were grown on nematode growth medium (see below for complete description) on 5.5 cm ventilated plates. Unused plates (plates without worms) were sealed and stored at 4°C. Plates containing *C. elegans* were stored at ambient room temperature. To reduce rapid temperature fluctuation, plates were stored in a larger container with ventilation holes. Naphthalene (moth ball) was placed in a 50-mL beaker and stored at the centre of the NGM plates at room temperature. The naphthalene was used to prevent the infestation of mites, which was a common occurrence in the lab setting because of the ability of mites to crawl into plates. *C. elegans* treated with gaseous naphthalene increased the number of extra cells during exposure from the L4 larval state to adulthood, but when exposed only as adults, no significant difference was found (Kokel et al., 2006). This study found that any effects of naphthalene were warranted to avoid mite infestation and all subjects would be exposed so any differences in behaviour should be caused by the unique treatments rather than naphthalene.

2.3.1 *C. elegans* growth media

Nematode growth media (NGM) is an agar formulation optimised to allow movement and development of *C. elegans*. The final composition of NGM was 1.7% (w/v) agar, 50 mM NaCl, 0.25% (w/v) tryptone, 1 mM $CaCl_2$, 5 µg/mL cholesterol (dissolved in EtOH), 25 mM KH_2PO_4 and 1 mM $MgSO_4$. Sodium chloride, agar and tryptone (in distilled H_2O) were autoclaved before the cholesterol, magnesium sulphate, calcium chloride and phosphate buffer were added. The NGM solution was cooled until ~60°C before being poured into 5.5 cm ventilated plates. Plates were filled with 8 mL of NGM solution.

The plates were left to dry at room temperature overnight and checked for fungal contamination the following day. Sterile NGM plates were sealed and stored after an extra day of drying at 4°C (until the agar can easily be sliced).

M9 buffer (a buffer safe for *C. elegans*) was used as a solvent for all treatments added to *C. elegans* media. The final composition of M9 buffer was 22 mM KH_2PO_4, 42 mM Na_2HPO_4 and 86 mM NaCl, which was autoclaved. All solutions that would contact *C. elegans* were autoclaved or aseptically prepared using 0.2-µm filters. All solutions and treatments were prepared before or during *C. elegans* breeding.

2.3.2 *C. elegans* nutrition

Two strains of bacteria (OP50-1 and α-syn overexpressing *E. coli*) were used to feed the *C. elegans*. Both strains of bacteria were grown using the same Lysogeny Broth, but with the addition of streptomycin (100 µg/mL) for OP50-1 and kanamycin (50 µg/mL) for the α-syn overexpressing *E. coli*. A small culture was prepared using bacteria from stock that had been stored at -80°C. The mini culture was grown on a shaking incubator overnight at 37°C and was used the following day to inoculate a larger preparation of 300 mL, which was shaken for 12 hours at 37°C.

After the incubation period, the resulting bacterial broth was stored at 4°C. When the bacteria settled to the bottom of the flask, the excess LB was removed, and the bacteria was transferred into falcon tubes. The falcon tubes were spun for 10 minutes at 2200 x g followed by the removal of remaining LB supernatant. The bacterial pellet was resuspended in M9 buffer at a concentration of 100 mg/mL.

2.3.3 Preparing α-syn

Before beginning the *C. elegans* age synchronisation, freeze-dried α-syn (stored at -80°C) was dissolved in M9 buffer to a concentration of 4 mg/mL. The α-syn in M9 buffer was added to the wells of a 96-well plate in volumes of 150 µL together with a 3-mm glass bead. In addition to making up α-syn in M9 buffer a sample of monomeric α-syn at the same concentration was made up in the ThT buffer and was run on the plate in triplicate to monitor the aggregation reaction. As previously

the plates were then run at 37°C for 169 hours. Fluorescence was measured each hour using a FLUOstar Omega plate reader at 440-nm excitation and 480-nm emission. The plates were shaken at 500 rpm for two minutes immediately prior to each reading. After the plate run, the microplate was removed from the reader and stored at 4°C until use.

2.3.4 *C. elegans* breeding

Egg-laying adults of *C. elegans* were prepared by first plating the *C. elegans* in breeding plates and allowing them to multiply. Worms were given 5-6 days to breed and were starved by not adding any more bacteria. Chunks of agar from the starved breeding plates were then inverted onto fresh plates and grown for an additional 48 hours.

Different strains required different times of incubation to ensure all strains contained a maximal number of egg laying adults at the same time; some strains were prepared earlier than others. Three different strains were used in this study. The first was the wild type N2 (*C. elegans* wild isolate var Bristol provided by the CGC, which is funded by NIH Office of Research Infrastructure Programs (P40 OD010440)). The second strain was DDP1 (uonEx1 [unc-54::alpha-synuclein::CFP + unc-54::alpha-synuclein::YFP(Venus)]; also acquired from the CGC), a *C. elegans* strain overexpressing a-synuclein in its muscle cells, and DDP2 (uonEx2 [unc-54::CFP::YFP(Venus)]; acquired from the CGC), a strain containing the same plasmid without the overexpression. DDP1 strains were grown 12 hours prior to the N2 and DDP2 strains for a total of 60 hours because of their observed developmental delay. Breeding the worms twice worked to partially synchronise the growth of egg-laying adult *C. elegans* to maximise the number of eggs produced for the hatch synchronisation steps that follow.

An important aspect of *C. elegans* growth is temperature regulation and maintaining even ambient temperature. *C. elegans* were incubated in an insulated container stored in a temperature-controlled room with a digital thermometer to track temperature change. The ideal temperature range for *C. elegans* is between 16°C and 24°C. The *C. elegans* grow and reproduce more slowly on

the cooler side of this range and much more rapidly on the warmer side of this range. In this study, the average temperature was 23°C.

Once the *C. elegans* reached the egg laying stage, their eggs were harvested using the following steps. The *C. elegans* were rinsed off their plates, spun down and washed with water. Bleach (hypochlorite) was used to lyse all the worms, a process that leaves their eggs intact. After several washes in M9 buffer to neutralise the bleach, the eggs were spun down a final time and resuspended in M9 buffer. They were rocked overnight in 50 mL centrifuge tubes with at least 50% empty space in the incubation tube to allow sufficient aeration.

Overnight, the eggs hatched at different times according to the developmental stage of the eggs, however subsequent growth of the worms were halted by the absence of food resulting in an age synchronised batch of worms. The worms were counted and diluted to 90 worms/mL before adding the treatments. A total of 200 µL was added to each plate bringing the total plate population to 10-20 worms.

2.3.5 Treating the *C. elegans*

The age synchronised *C. elegans* hatchling plates were treated with four different treatments and grown with two different types of *E. coli* as food. The two bacterial strains (OP50-1 and α-syn expressing *E. coli*) were added to separate diluted hatchling solutions then the inoculated hatchling solutions were added to pre-treated NGM plates with one of the four treatments described below. The *C. elegans* were incubated for 24 hours before adding FUDR to sterilise the worms and prevent new eggs from hatching. All the worms at this point should be approximately the same size and age with little variation.

The control treatment was M9 buffer, the second treatment was aggregated α-syn dissolved in M9 buffer to see if the worms could take in the protein. The third treatment was aggregated α-syn with hops in M9 buffer to see if hops reduced any effects of aggregated α-syn. The final treatment was hops dissolved in M9 buffer to see if the hops had any effects on the worms. The

OP50-1 worms were denoted normal worms and the treatment was indicated with an O, e.g. worms fed OP50-1 bacteria in M9 buffer were N2 OMM, worms fed OP50-1 bacteria in M9 buffer to which had been added aggregated α-syn were denoted Treatment N2 OAM etc. Worms that were fed α-syn expressing *E. coli* were indicated with an α symbol, so worms fed α-syn expressing *E. coli* in M9 buffer were denoted N2 EMM. Worms that were fed α-syn expressing *E. coli* in M9 buffer that contained 4 mg/mL aggregated α-syn were denoted N2 EAM, etc (See Table 1 for full list of *C. elegans* treatment groups). The worm plates were incubated at an ambient room temperature in an insulated container for 48 hours before recording.

Table 1 Behavioural treatments used on worm plates

Strain	Food	Amount of food (mg in 50 µL)	a-synuclein aggregated over time	Amount of a-synuclein (µg in 50 µL)	Counter treatment	Amount of hops (µg in 11.11 µL)	Number of plates
N2	OP50-1	5	M9	0	M9	0	2
					Hops	5.55	2
			a-synuclein aggregated over time	200	M9	0	2
					Hops	5.55	2
	E. coli a-syn	5	M9	0	M9	0	2
					Hops	5.55	2
			a-synuclein aggregated over time	200	M9	0	2
					Hops	5.55	2
DDP1	OP50-1	5	M9	0	M9	0	2
					Hops	5.55	2
			a-synuclein aggregated over time	200	M9	0	2
					Hops	5.55	2
DDP2	OP50-1	5	M9	0	M9	0	2
					Hops	5.55	2
			a-synuclein aggregated over time	200	M9	0	2
					Hops	5.55	2

2.4 Behaviour analysis

2.4.1 Recording

After the worms were treated, and adults were moving around on the NGM plates, the NGM plates were recorded. Before recording the plates, the plates were removed from the insulated container and were allowed 10 minutes to acclimate to the new temperature and lighting. The plates were

recorded 48 hours after treatment. Plates were recorded one at a time with the field of view of the microscope focused on different regions of the plate for each recording. Worms were recorded with an eyepiece camera. Recordings were made through the 4x objective of a benchtop microscope. The videos recorded were set to a manual exposure of 112, 30 ms exposure time and 1.00 gain. The videos were 872 x 654 px, RGB format and set to grayscale. Videos were recorded for 60 seconds.

2.4.2 Video Analysis

ImageJ Fiji with the wrmtrck plugin was used with a macro to complete analysis in batch. For the wrmtrck plugin to work, the following steps were done to make videos compatible. Videos were uploaded in an uncompressed AVI format. The videos were then converted to 8-bit grayscale. The grayscale footage was then converted to binary black and white images using a threshold (MaxEntropy setting under AutoThreshold) where a certain level of grey colour was converted to white and darker shades of grey were converted to black, making any moving objects black with the background white. ImageJ was used to get an average background image, which was subtracted from all the images in the video, leaving behind objects in motion. Once the video was prepared, the wrmtrck plugin was used.

The plugin requires specific settings to be able to detect moving objects. The first setting is the estimated size of the moving object (*C. elegans*) in pixels with a minimum (300 px) and maximum (20000 px) range. The next field was the estimated maximum velocity of the worm (10 px/s). The last important field was the bend threshold (setting 2, explained in the next paragraph), which is a method of bend calculation. The other fields do not affect the analysis of the video, they only affect the presentation of analysis.

The data collected from the video was length, distance, #frames, time, maximum speed, average speed, body lengths per second (calculated by dividing the Length of the track by Perimeter/2 and the time in seconds). Not all this data was used to compare behaviour between treatments but were used instead to remove artefacts from the data. For example, any objects

detected for less than 5 frames per second were removed from the data. This data was imported in to excel for processing.

As previously mentioned, the data from all the *C. elegans* videos were screened for artefacts by removing objects tracked for less than 5 frames per second. The data was organised for statistical analysis. The data was also tested for normal distribution using box plots to determine the statistical test that would be used. A high percentage of the data did not follow normal distribution.

2.4.3 Statistical Analysis of video data

Since the data did not show normal distribution, the non-parametric Kruskal–Wallis one-way analysis of variance test was used to compare multiple sets of data together with Bonferroni correction. After determining any significance between multiple sets of data, the data was compared individually using the non-parametric t-test equivalent, the Mann Whitney U test.

2.5 Life span assay

2.5.1 Assay preparation

A life span assay was repeated multiple times using a 96-well plate (Solis and Petrascheck, 2011). After age synchronising the worms, an average of 10 worms were added to each well of a microplate (the bottom of the microplate was marked into four equal quadrants for future counting). The same treatments used in the behavioural analysis were used in the life span assay. Instead of NGM, the worms were kept in S-complete because of the small size of the wells.

The final media, S-complete is a liquid media that allows *C. elegans* to move and develop. S-media is useful when growing *C. elegans* in 96-well plates because it is easier to dispense and maintain in small volumes. S-complete was prepared by first making a solution called S-basal medium (50 mM potassium phosphate, pH 6.0, 100 mM NaCl with 1 mL of 5 mg/mL cholesterol added after autoclaving). A trace metal solution, another ingredient in S-complete, was prepared by adding 1.86 g Na_2EDTA, 0.69 g $FeSO_4 \cdot 7H_2O$, 0.20 g $MnCl_2 \cdot 4H_2O$, 0.29 g $ZnSO_4 \cdot 7H2O$ and 0.016 g $CuSO_4$ to a final volume of 1 L in deionised water; the solution was autoclaved and stored in the dark. Potassium citrate was also necessary for the preparation of S-complete; 268.8 g tripotassium

citrate, 26.3 citric acid monohydrate, pH 6.0 and a final volume of 1 L deionised water. All the solutions prepared were autoclaved before being combined. The final composition of S-complete was 977 mL S-basal, 10 mL 1M potassium citrate, 10 mL Trace metals solution, 3 mL 1M $CaCl_2$ and 3 mL 1M $MgSO_4$ (Solis and Petrascheck, 2011).

2.5.2 Assay observation

The wells were counted both daily and intermittently using a microscope for living and dead worms. Wells were counted in quadrants to minimise double counting. Worms that did not move when the plate was tapped were counted as dead. Moving worms were counted as alive.

3 Results – In Vitro

The work described in this thesis was performed in two parts, part one was performed in vitro and part two was performed in vivo. The principal aim of this study was to develop a screening system to investigate potential therapeutic agents for their ability to modify α-syn aggregation, one of the principle pathologies thought to underlie the development and progression of PD. The in vitro experiments allow rapid screening of agents to determine which can alter the rate of α-syn aggregation. Having identified these potential therapeutics, the second part of this study was to develop an invertebrate in vivo model which would allow rapid testing of any identified agent in a living organism.

3.1 Effects of Hops on α-syn aggregation

3.1.1 A-syn aggregation fluorescence curves

The goal in this experiment was to determine whether hops has any effect on α-syn aggregation. These experiments were performed in vitro. The first step was to observe α-syn aggregation without hops.

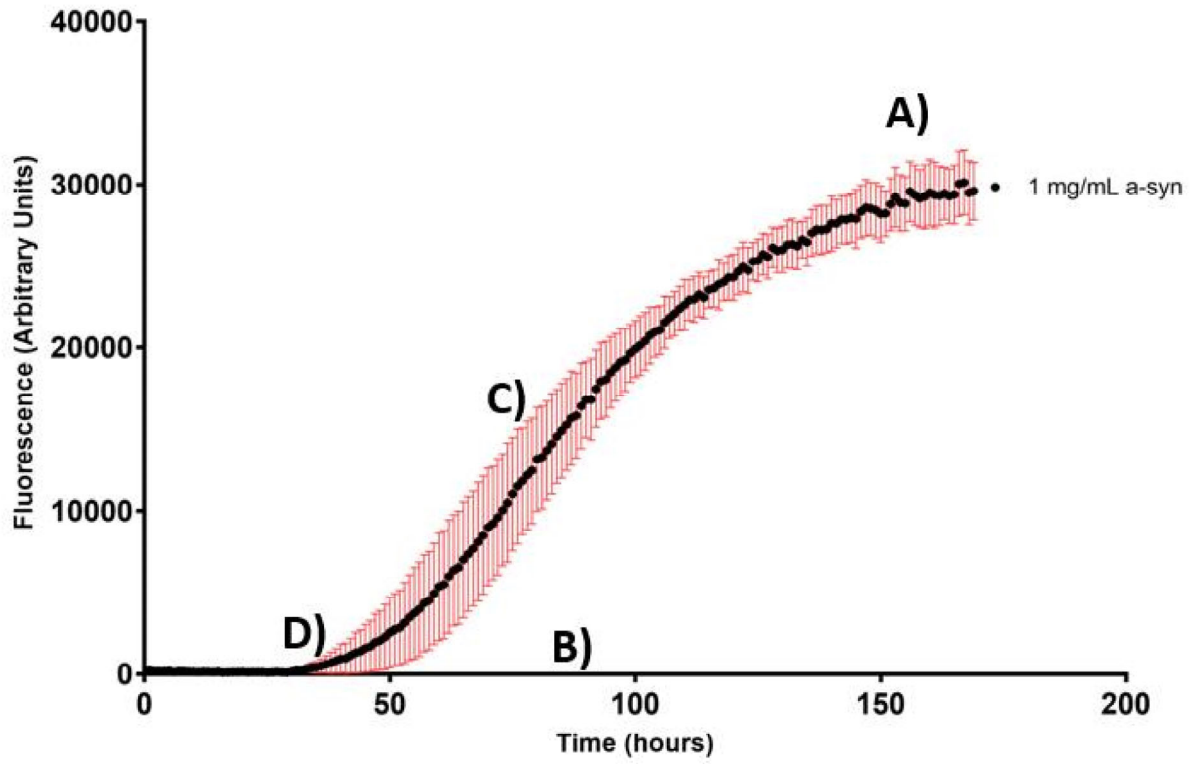

Figure 3.1 The graph above is an average of three independent experiments (n=3) in which aggregation of 1 mg/mL α-syn was monitored over 169 hours at 37°C. Each experiment was performed in triplicate. Error bars are standard error of mean

(SEM). Measurements were taken every hour after being shaken at 500 rpm for two minutes with an excitation of 440 nm and an emission of 480 nm. The data for each run was normalised before analysis.

After completing a ThT assay, four key points were analysed in all treatments. Key points to note on this graph are A) the maximum fluorescence, B) the time when fluorescence is half of max, C) the peak rate and D) the lag phase, which was the time when fluorescence was 5% of maximum fluorescence. The lag phase represents the time when β-sheets initially form and fluorescence can be detected. The peak rate is when β-sheets should be forming at the fastest rate and the maximum fluorescence represents the plateau of β-sheet formation.

The maximum fluorescence for α-syn at a concentration of 1 mg/mL was 30794, which occurred at 169 hours. The fluorescence was half of maximum (15397 at 86.8 hours. The peak rate (fastest increase in fluorescence) was at 76.5 hours which happened before half max. Finally, the lag phase was at 44.4 hours. These four values were compared to the values in ThT assays containing α-syn aggregated with hops.

3.1.2 Effects of hops prepared at room temperature on α-synuclein aggregation

ThT assays were performed using unfiltered hops prepared at room temperature to detect any constituents that may cause changes in fluorescence. The following graphs present fluorescence data using hops homogenate prepared at room temperature.

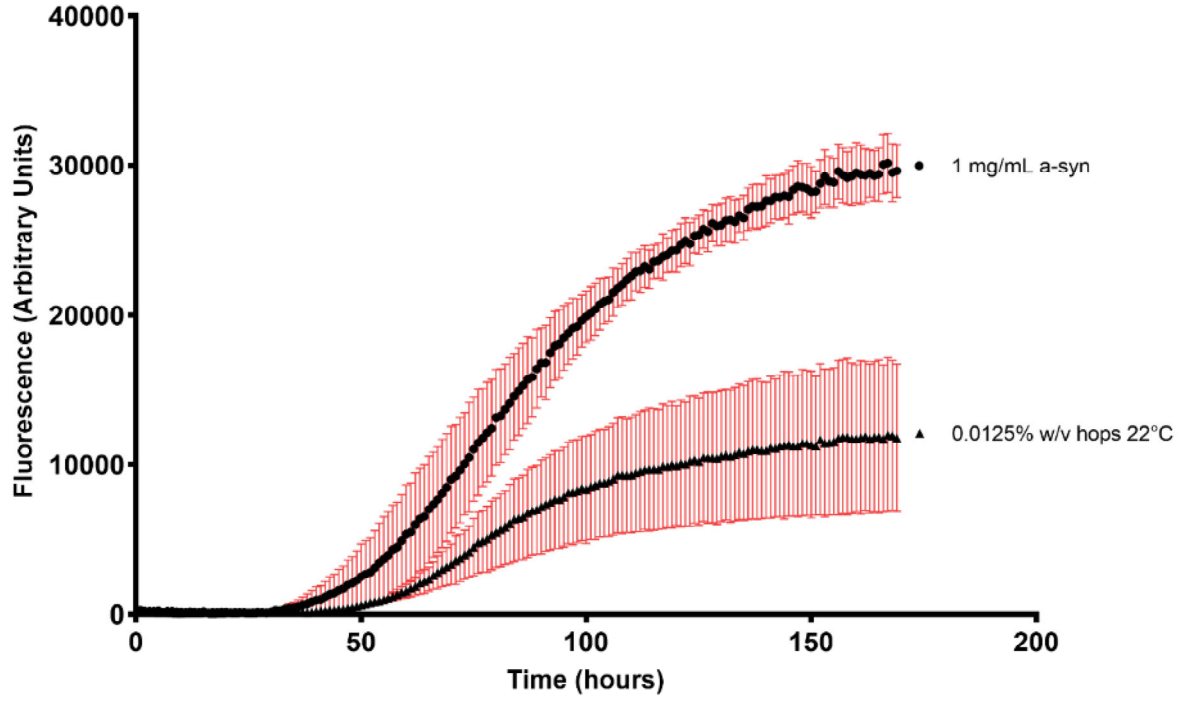

Figure 3.2 The graph above contains the same α-syn curve in Figure 3.1 compared with the addition of 1 mg/mL α-syn aggregated with a final concentration of 0.0125% w/v hops prepared at 22°C (n=3). The error bars are SEM. Microplates were incubated at 37°C for 169 hours, with measurements taken every hour after being shaken at 500 rpm for two minutes with an excitation of 440 nm and an emission of 480 nm.

The first treatment added to α-syn in the ThT assay was 0.0125% w/v. Adding hops to the α-syn samples to a final concentration of 0.0125% w/v, resulted in a greater than 2.6-fold decrease in maximal fluorescence compared to the maximum fluorescence of α-syn. The half-max and the lag phase fluorescence were also 2.6-fold greater. The α-syn solution's half-max was 3.22 hours earlier than the 0.0125% w/v hops sample, 3.7% earlier than the α-syn. The hops solution's lag phase was 4.73 hours after the α-syn solution. The time to hit peak rate was 1 hour earlier in the α-syn solution.

The standard error of mean for the hops curve was close to 50% of the fluorescence value. There was a greater amount of variance in the hops solution, whereas the SEM for α-syn was close to 6-10% of the fluorescence value and fluorescence across different assay runs were consistently the same. The concentration of hops was increased to observe the impact on fluorescence or aggregation.

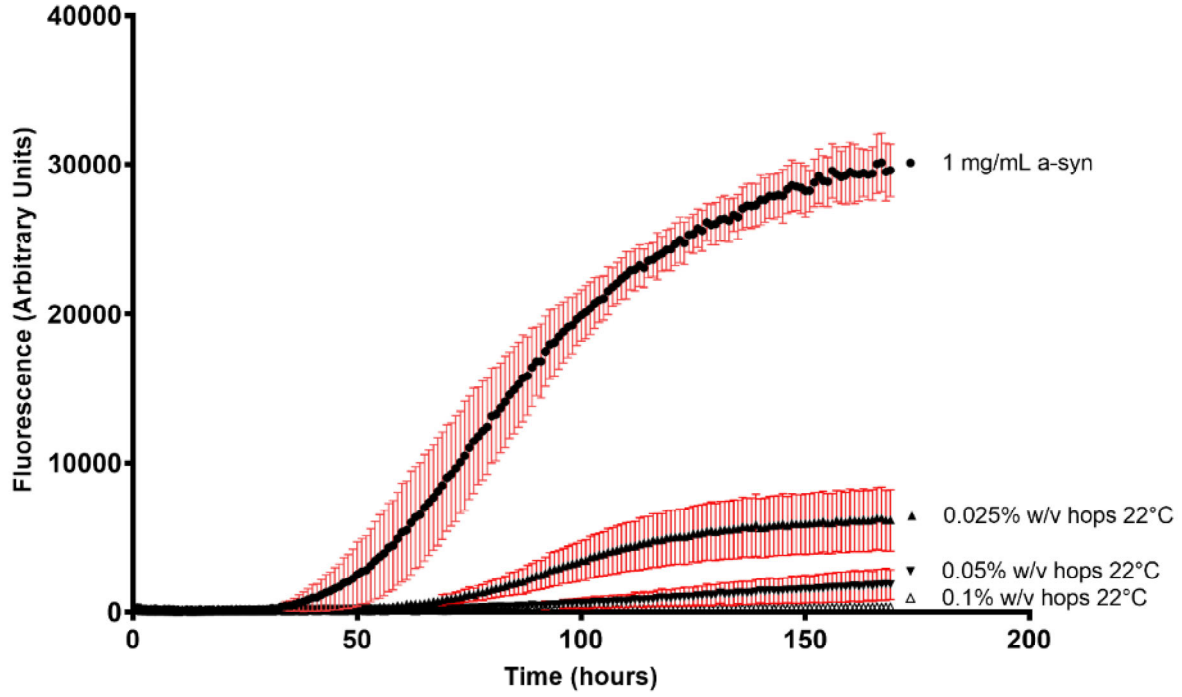

Figure 3.3 The graph above shows aggregated α-syn and 3 different concentrations of hops prepared at room temperature (0.025-0.1% w/v hops in α-syn solution n=3). The error bars are SEM. The error bars are SEM. Microplates were incubated at 37°C for 169 hours, with measurements taken every hour after being shaken at 500 rpm for two minutes with an excitation of 440 nm and an emission of 480 nm.

Increasing the concentration of hops prepared at room temperature further decreased the fluorescence readings compared to the α-syn sample. A concentration of 0.1% w/v hops was enough to reduce maximum fluorescence to less than 1.5% of the α-syn sample. The standard error of mean also decreased for every increase in hops concentration because there was less variance in fluorescence for the 0.05-0.1% w/v hops between assay runs. To highlight the fold difference between the key phases, the maximum fluorescence of all dilutions was presented in Figure 3.4.

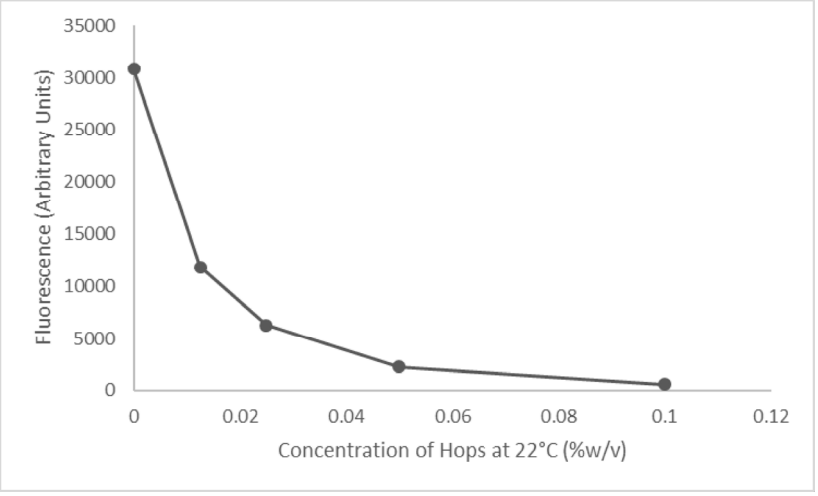

Figure 3.4 This graph shows the maximum fluorescence of α-syn aggregation with different concentrations of hops prepared at room temperature from the samples graphed in Figure 3.2 and Figure 3.3.

Each time the concentration of hops was doubled the maximum fluorescence decreased. From 0% w/v to 0.0125% w/v hops, the fluorescence decreased 2.60-fold. From the 0.0125% w/v to 0.025% w/v, the fluorescence decreased 1.89-fold. From 0.025% w/v to 0.05% w/v, the fluorescence decreased by 2.80-fold. From 0.05% w/v of hops to 0.1% w/v, the fluorescence decreased by 3.89-fold. Adding 0.1% w/v hops caused a 53-fold decrease in maximum fluorescence compared to α-syn alone.

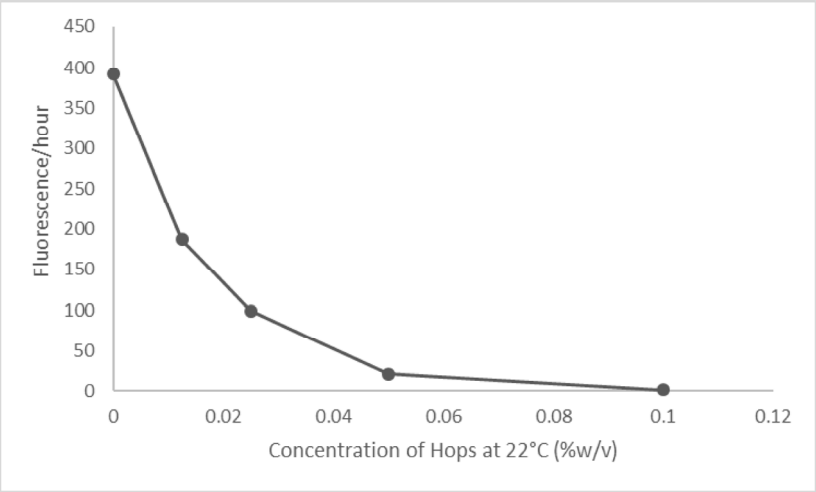

Figure 3.5 The peak rate of fluorescence growth (the point of inflection) of the curves in Figure 3.1 and Figure 3.2.

The peak rate of aggregation in Figure 3.5, the point of inflection on the curve had a similar fold difference between each concentration as the maximum fluorescence. From 0% w/v to 0.0125% w/v hops, the peak rate decreased 2.10-fold. From the 0.0125% w/v to 0.025% w/v, the peak rate

decreased 1.89-fold. From 0.025% w/v to 0.05% w/v, the fluorescence decreased by 4.72-fold. From 0.05% w/v of hops to 0.1% w/v, the fluorescence decreased by 14.73-fold. This means the fluorescence curves were proportionally smaller than each other due to the higher concentrations of hops. The difference in time for each fluorescence key phase was graphed below to determine if the curves were not only proportionally smaller, but also had an earlier lag phase.

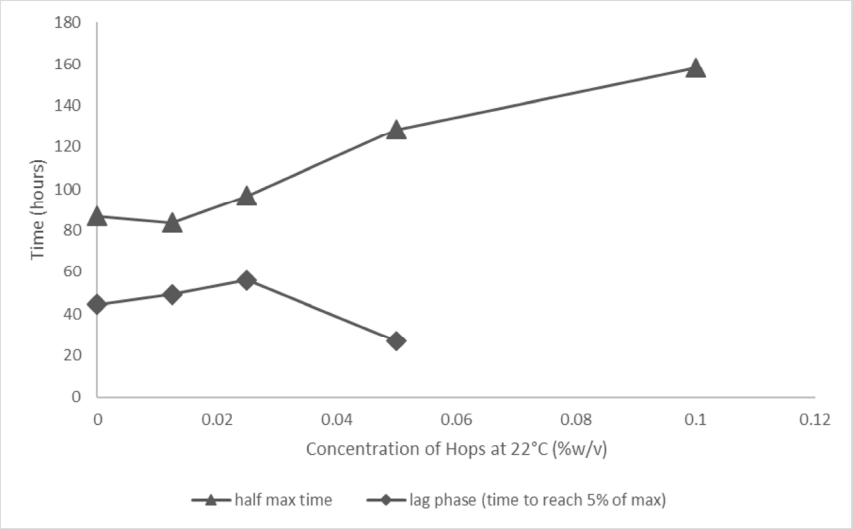

Figure 3.6 The time of each phase: half max time and lag phase (time to reach 5% of max) for the different concentrations of hops prepared at room temperature were compared.

The time to reach each phase increased as the concentration of hops increased, meaning the curves shifted to the right. The curves are proportional in shape, but the size and position on the timeline is different depending on the concentration. Hops could either be competitively binding to ThT, binding to α-syn monomers preventing aggregates from forming or even changing the shape of aggregates to no longer contain β-sheets. To see how the hops influenced fluorescence in the assays, the samples were run on polyacrylamide gels.

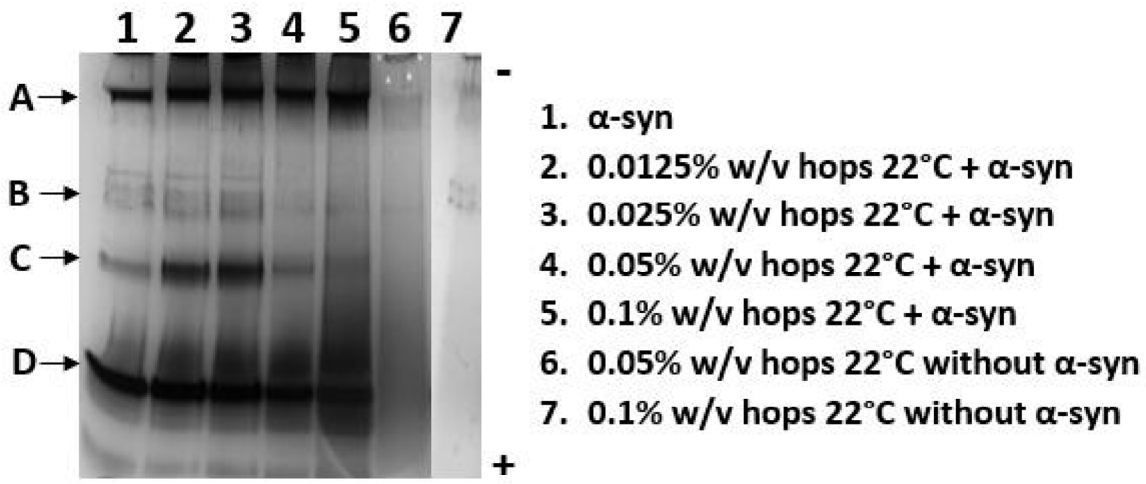

Figure 3.7 The samples used in the ThT assays in Figure 3.2 and Figure 3.3 were analysed using gel electrophoresis. The concentrations of hops were the final concentrations in the assay and not in the gel. The gel (BioRad Mini-PROTEAN TGX Stain-Free Gels #456-8123) above was run at 200 V for 30 min, stained using Bio-Rad Silver Stain Plus #161-0449 and were imaged using Bio-Rad ChemiDoc MP System with Image Lab. Total exposure time to white epi illumination was 0.113 s. Samples were taken after a microplate run, prepared using 4X loading buffer to 1 µL sample and were diluted using Tris glycine running buffer. All gel samples contained ~1 µg of α-syn protein dissolved in ThT buffer. Molecular weights were calculated using Bio-Rad Precision Plus and Linear (semi-log) regression. Three independent replicates of this gel were performed.

SDS PAGE were run to determine the presence of α-syn after exposure to hops and after a week of being incubated at 37°C. Although SDS PAGE is not as conclusive as a western blot when checking for specific protein presence, previous western blots were run by the lab to determine the presence of α-syn, thereafter, any bands in the 14-16 kDa region were determined to be α-syn in SDS PAGE. Previous research demonstrated that some α-syn aggregates were SDS-resistant when exposed to dopamine, which could be possible with hops as well (Cappai et al., 2005). The gels were also run to see if any protein aggregates were preserved even after exposure to SDS, a detergent used to break bonds and denature proteins to allow size separation and β-mercaptoethanol, used to break disulphide bonds.

There were four notable band regions in Figure 3.7, A-D. The average molecular weights of these four bands were 164.76 kDa (A), 66.97 kDa (B), 40.92 kDa (C) and 14.72 kDa (D). Increased concentrations of hops caused more smearing and increased staining intensity in the higher molecular weights. Running hops without α-syn protein in lane 6 resulted in light smearing in line with arrow A and D. The light bands found in lane 7 and 6 (hops only) are also found in lane 1 with greater intensity, meaning there may have been some lane leakage from the lanes containing α-syn

into the hops only lanes. The different adjusted volume of band intensity (arbitrary unit of measurement) was compared for the 4 molecular weights.

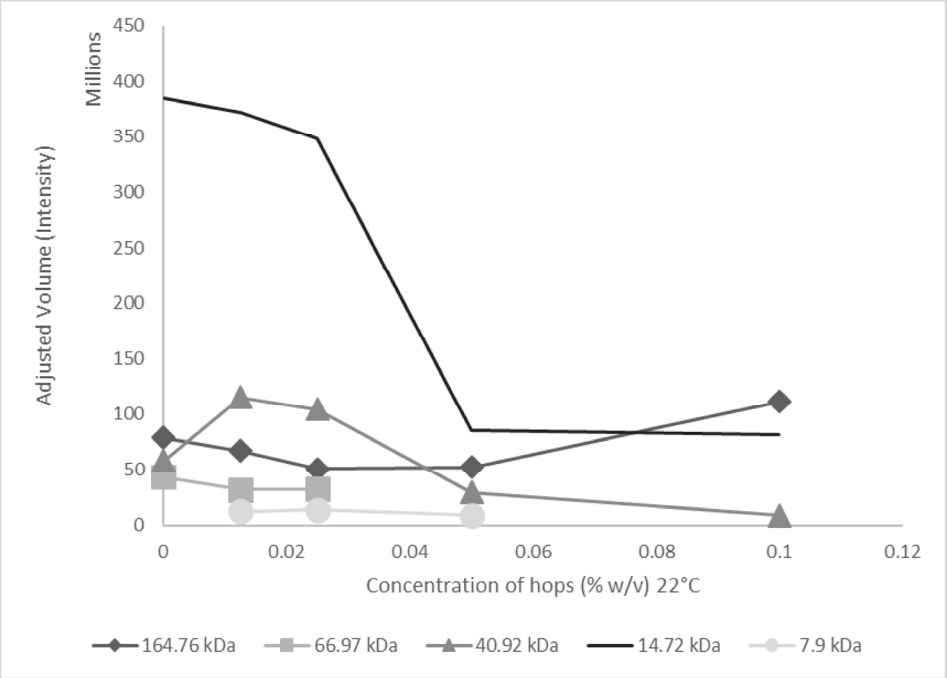

Figure 3.8 Intensity of bands with molecular weights 164.76 kDa (A), 66.97 kDa (B), 40.92 kDa (C) and 14.72 kDa (D) of 1 µg α-syn and different concentrations of hops. These bands can be seen Figure 3.7 to the right of the arrows.

The intensity of the 164.76 kDa band decreased from 0% w/v hops to 0.025% w/v hops and then increased again after 0.05% w/v to 0.1% w/v. The intensity of the 66.97 kDa band decreased from 0% w/v hops to 0.025% w/v hops. Bands were undetected with molecular weight 66.97 kDa in solutions with 0.05 and 0.1% w/v. The intensity of the 40.92 kDa band increased from 0% w/v hops and peaked at 0.0125% w/v hops. From 0.025 to 0.1% w/v band intensity dropped. The intensity of the 14.72 kDa band decreased from 0% w/v hops to 0.0125% w/v hops. From 0.025 to 0.1% w/v band intensity dropped by 4-fold. The 0.05% w/v hops sample bands showed similar results with the darkest stain occurring in the highest molecular weight with lesser intensity in the lower molecular weights. The lower concentrations of hops resulted in the darkest bands being in the monomeric region of 14.72 kDa and 40.92 kDa and lighter staining in 66.97 kDa.

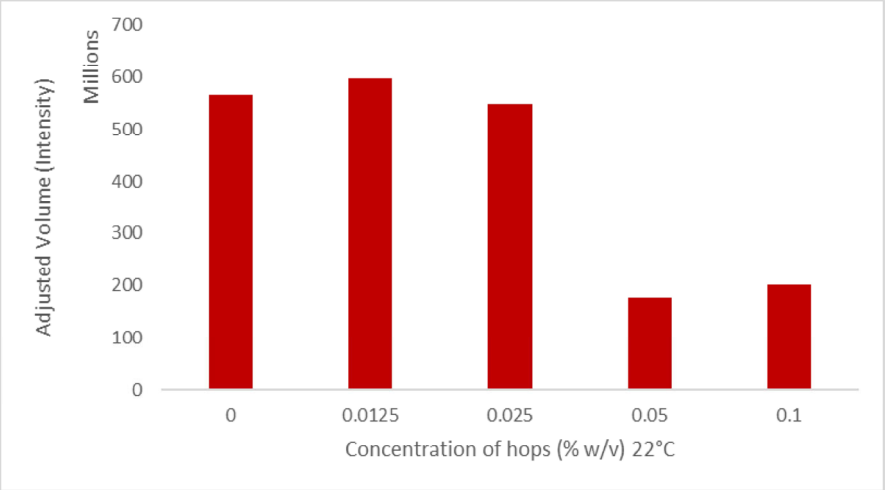

Figure 3.9 Total adjusted volume of band intensity for lanes 1-5 in Figure 3.7.

Since all samples have ~1 µg of α-syn, the protein content or band intensities in each lane should add up to a similar total. Total adjusted volume of band intensity for concentrations 0-0.025% w/v were an average of 3-fold greater than 0.05 and 0.1% w/v, meaning that there may be some protein loss in the lanes containing 0.05 and 0.1% w/v.

3.1.3 Effects of boiled hops on aggregation

In the results above, hops was prepared at room temperature without filtration. Different methods of extraction were tested to find the best method of preparing hops to reduce α-syn aggregation. CO_2 extracted hops could not be analysed because of the high turbidity of the solution upon preparation and during the 169 hour incubation in the plate reader. The ThT assay results of the hops prepared by boiling are presented next. Hops was boiled for 10 minutes and evaporated water was replaced and cooled before being added as a treatment in the ThT assay.

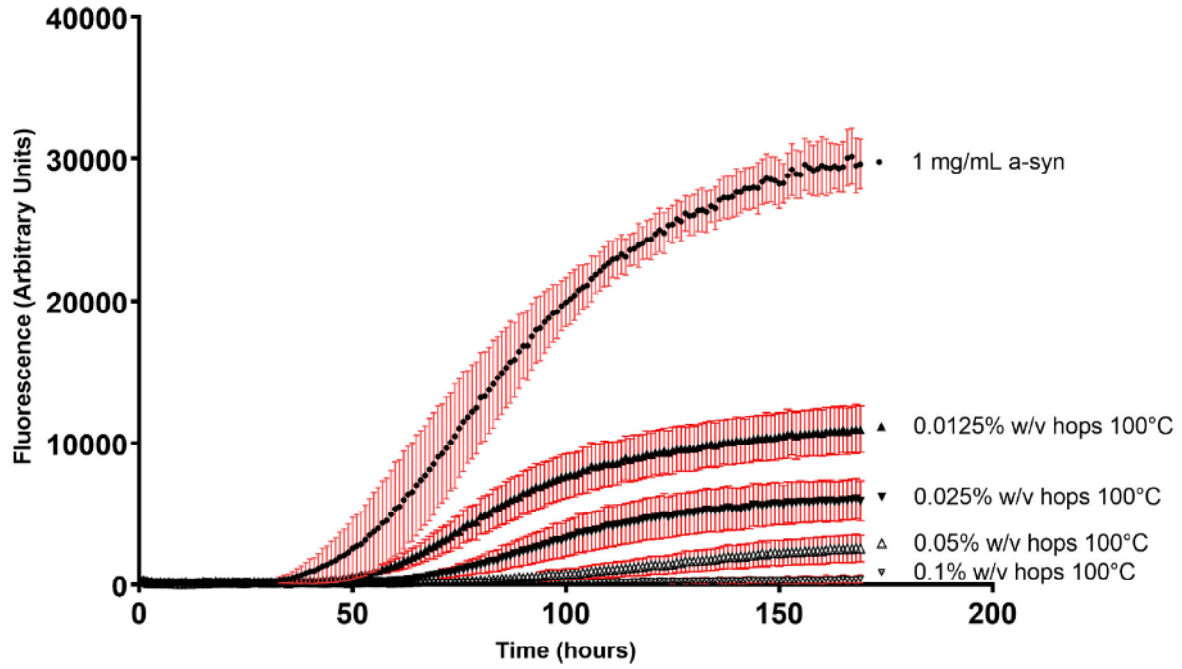

Figure 3.10 The graph above shows aggregated α-syn and 4 dilutions of hops prepared by boiling at 100°C for 10 minutes (0.0125-0.1% w/v hops in α-syn solution n=3). The error bars are SEM. Microplates were incubated at 37°C for 169 hours, with measurements taken every hour after being shaken at 500 rpm for two minutes with an excitation of 440 nm and an emission of 480 nm.

The error bars for each concentration of hops were less than 10% of fluorescence and represent minimal variance of fluorescence across assay repetitions. The 4 phases of the different concentrations of boiled hops treatments were analysed below starting with maximum fluorescence.

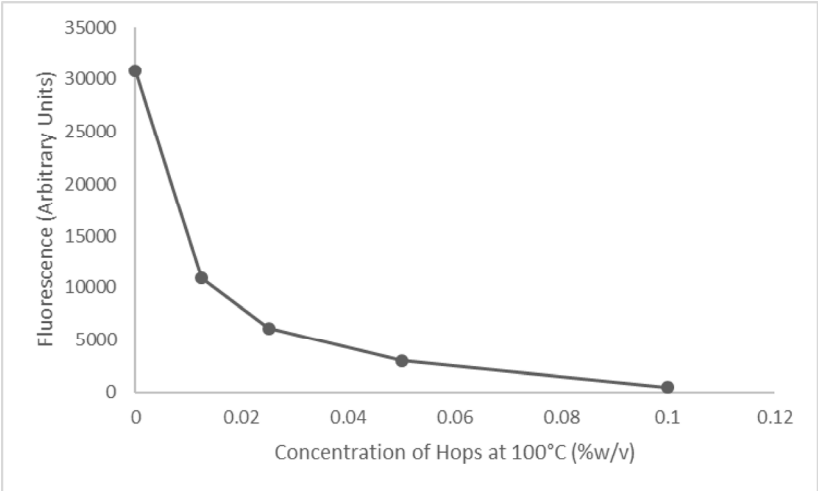

Figure 3.11 The maximum fluorescence for each dilution of hops prepared by boiling at 100°C for 10 minutes from the samples graphed in Figure 3.10.

The maximum fluorescence change between the dilutions at 100°C have a similar change to the hops prepared at room temperature. The change in maximum fluorescence was increasingly smaller with

each increase in hops concentration. The maximum fluorescence of 1 mg/mL α-syn was 2.8-fold greater than 0.0125% w/v hops, 5-fold greater than 0.025% w/v hops, 10-fold greater than 0.05% w/v hops and 71-fold greater than 0.1% w/v hops. The peak rate of fluorescence of the different hops dilutions was compared next.

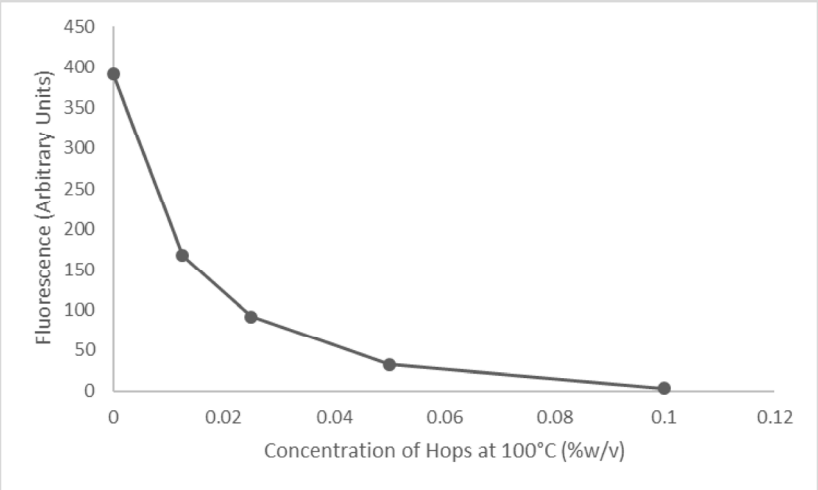

Figure 3.12 The peak rate of fluorescence for each dilution of hops prepared by boiling at 100°C for 10 minutes from the samples graphed in Figure 3.10.

The peak rate of fluorescence for 1 mg/mL of α-syn in Figure 3.12 was 2.3-fold greater than 0.0125% w/v hops, 4.2-fold greater than 0.025% w/v hops, 12-fold greater than 0.05% w/v hops and 119-fold greater than 0.1% w/v hops. Time to reach half max and lag phase were also compared.

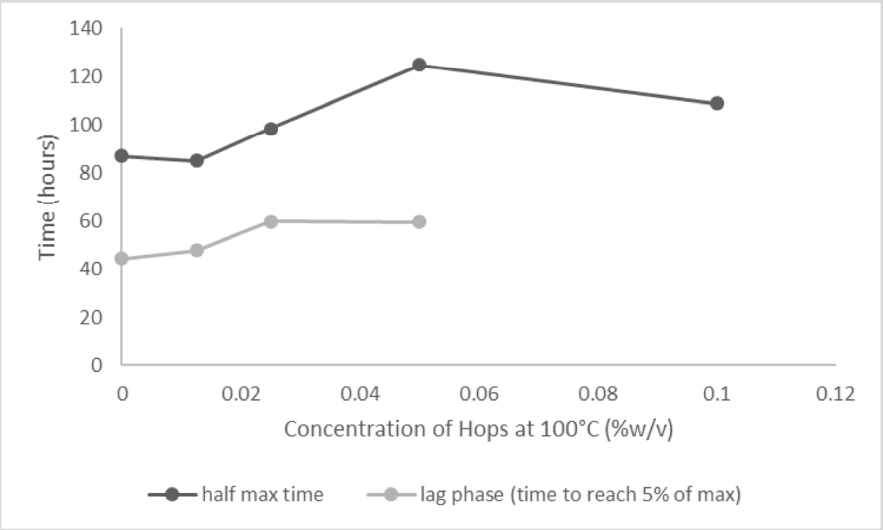

Figure 3.13 The time of each phase: half max time and lag phase (time to reach 5% of max) for the different concentrations of hops prepared by boiling were compared.

Similar to the hops prepared at room temperature, every increase in hops concentration led to an increased delay to reach a phase in Figure 3.13. The lag phase could not be calculated in 0.1% w/v hops when prepared at room temperature or by boiling. To see the effect of hops on aggregate size, samples were analysed using gel electrophoresis.

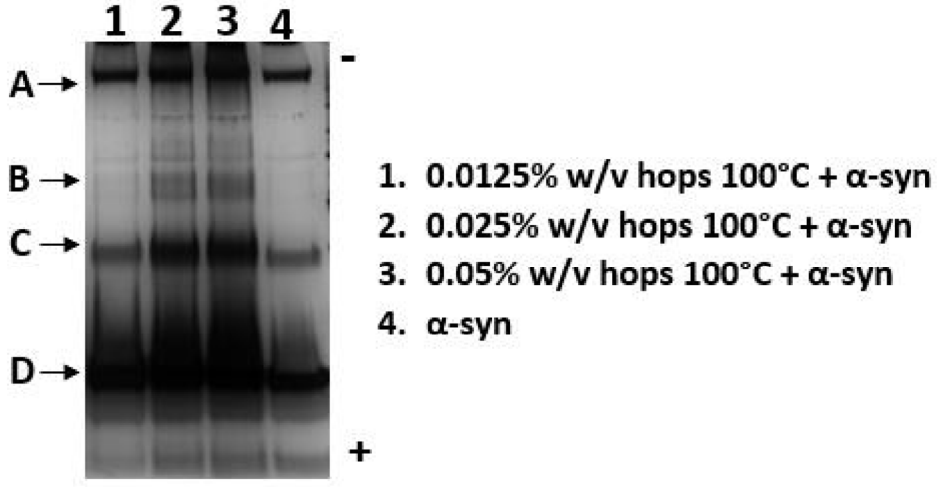

Figure 3.14 The samples used in the ThT assays in Figure 3.10 were analysed using gel electrophoresis. The concentrations of hops were the final concentrations in the assay and not in the gel. The gel (BioRad Mini-PROTEAN TGX Stain-Free Gels #456-8123) above was run at 200 V for 30 min, stained using Bio-Rad Silver Stain Plus #161-0449 and were imaged using Bio-Rad ChemiDoc MP System with Image Lab. Total exposure time to white epi illumination was 0.116 s. Samples were taken after a microplate run, prepared using 4X loading buffer to sample and were diluted using Tris glycine running buffer. All gel samples contained ~1 µg of α-syn protein dissolved in ThT buffer. Lane 5 in the figure above was originally lane 1 in the gel; other lanes were removed because the treatments were not analysed in this study. Molecular weights were calculated using Bio-Rad Precision Plus and Linear (semi-log) regression.

The samples from the ThT assays were analysed to show the effect of hops on aggregation. There were four notable band regions stained in the gel in Figure 3.14, A-D. The average molecular weights of these four bands were 164.76 kDa (A), 66.97 kDa (B), 40.92 kDa (C) and 14.72 kDa (D). Increased concentrations of hops caused more smearing.

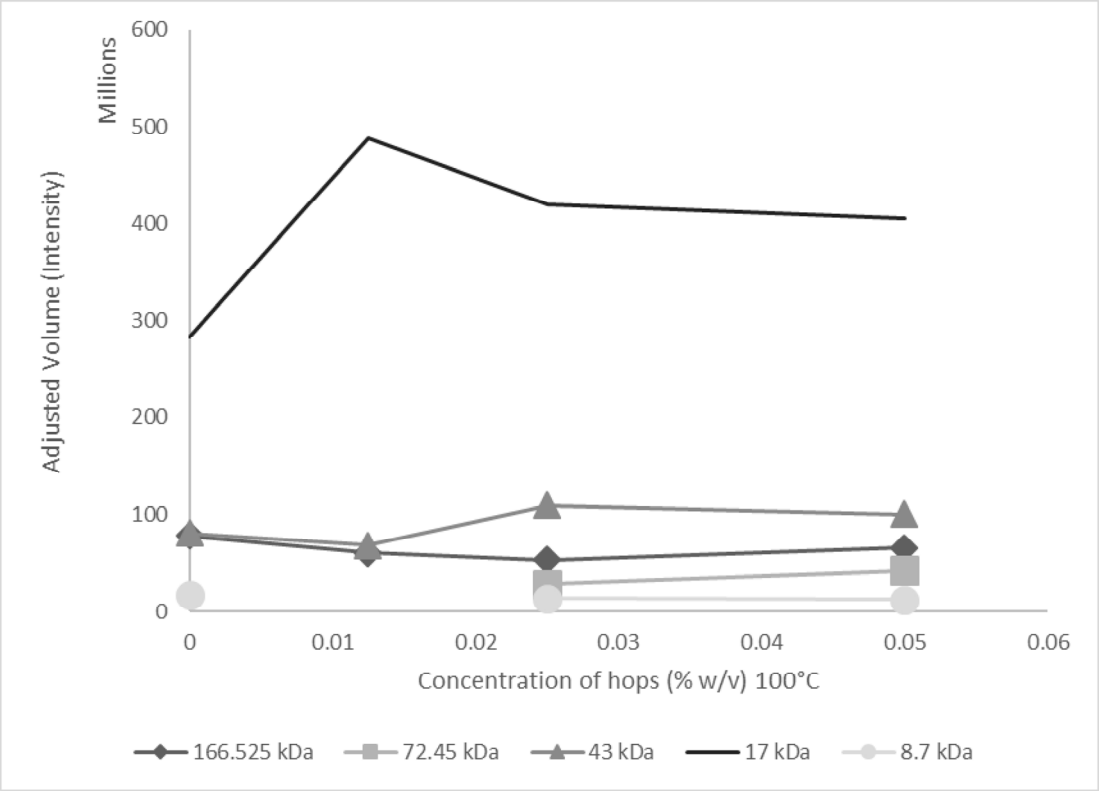

Figure 3.15 Intensity of bands with molecular weights 166.525 kDa (A), 72.45 kDa (B), 43.0 kDa (C) and 17.0 kDa (D) of 1 µg α-syn and different concentrations of hops. These bands can be seen Figure 3.14 to the right of the arrows.

The intensity of the 166.525 kDa band decreased from 0% w/v hops to 0.025% w/v hops and then increased again after 0.025% w/v to 0.05% w/v. The intensity of the 66.97 kDa band decreased from 0% w/v hops to 0.025% w/v hops. Bands were undetected with molecular weight 72.45 kDa in solutions with 0.0125 and 0% w/v. The intensity of the 43 kDa band increased from 0% w/v hops and peaked at 0.0125% w/v hops. From 0.025 to 0.05% w/v band intensity dropped. The intensity of the 17 kDa band decreased from 0% w/v hops to 0.0125% w/v hops. From 0.025 to 0.05% w/v band intensity dropped by 20%. In the 0.05% w/v hops sample, the darkest bands were in the 166.525 and 17 kDa regions and lightest in the 40.92 and 66.97 kDa regions. The 0.05% w/v hops sample bands showed similar results with the darkest stain occurring in the highest molecular weight with lesser intensity in the lower molecular weights. The lower concentrations of hops resulted in the darkest bands being in the monomeric region of 17 kDa and 43 kDa and lighter staining in 72.45 kDa.

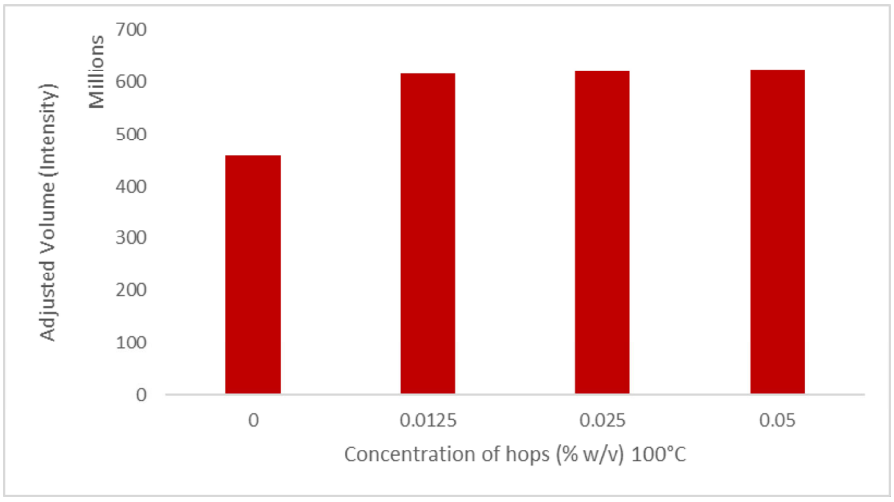

Figure 3.16 Total adjusted volume of band intensity for lanes 1-5 in Figure 3.14.

In Figure 3.16, all bands were totalled in each lane to calculate the total protein content collected from the 1 µL ThT assay sample. Total adjusted volume of band intensity for concentrations 0.025-0.05% w/v were an average of 35% greater than 0% w/v intensity.

3.1.4 Comparing the effects hops prepared at different temperature on aggregation

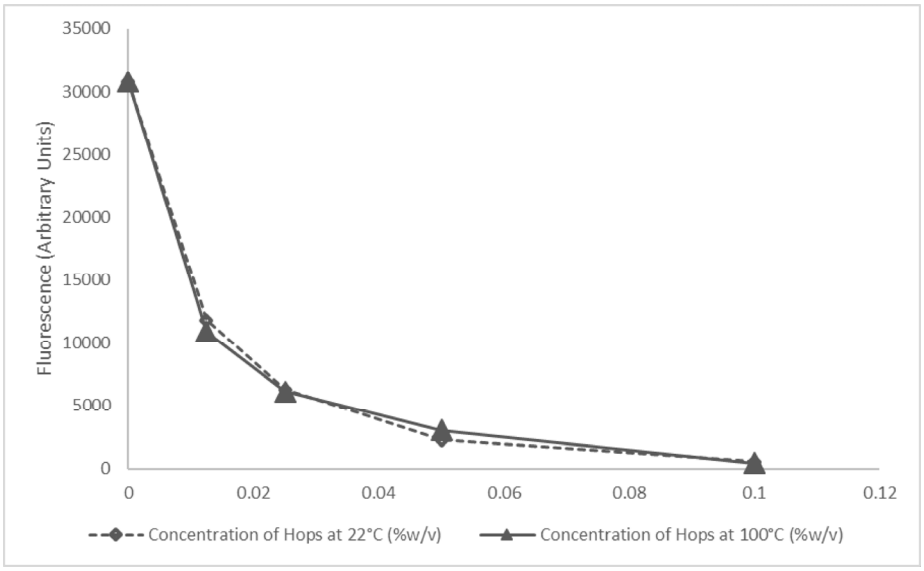

Figure 3.17 The maximum fluorescence for different concentrations of hops prepared at different temperatures.

The effect on aggregation of the two different methods of preparing hops were compared. The maximum fluorescence was nearly identical for hops prepared at different temperatures. The difference between preparation temperatures occurred at 0.0125 and 0.05% w/v of hops. The difference occurring at 0.0125% w/v of hops might be due to the higher variance in the sample prepared at room temperature.

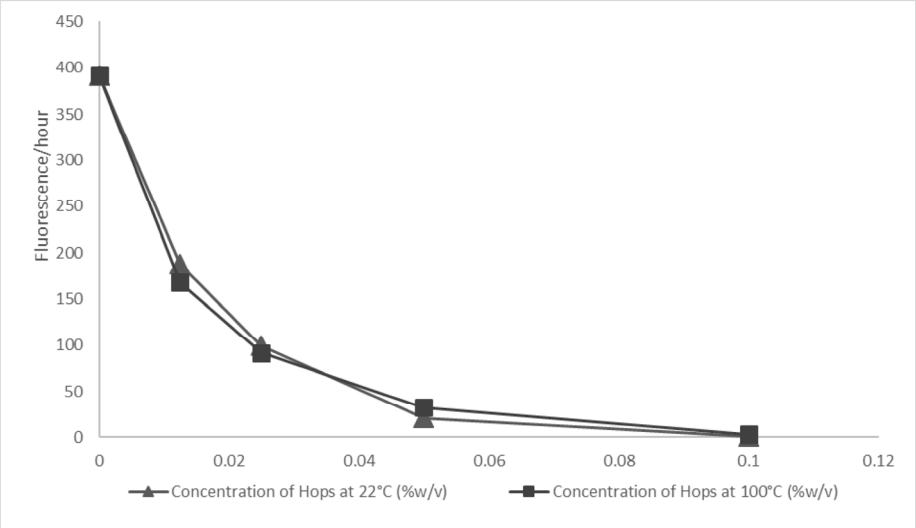

Figure 3.18 The peak rate of fluorescence for different concentrations of hops prepared at different temperatures.

The peak rate of fluorescence between hops preparations was also similar. The final comparison of the time to reach is presented next.

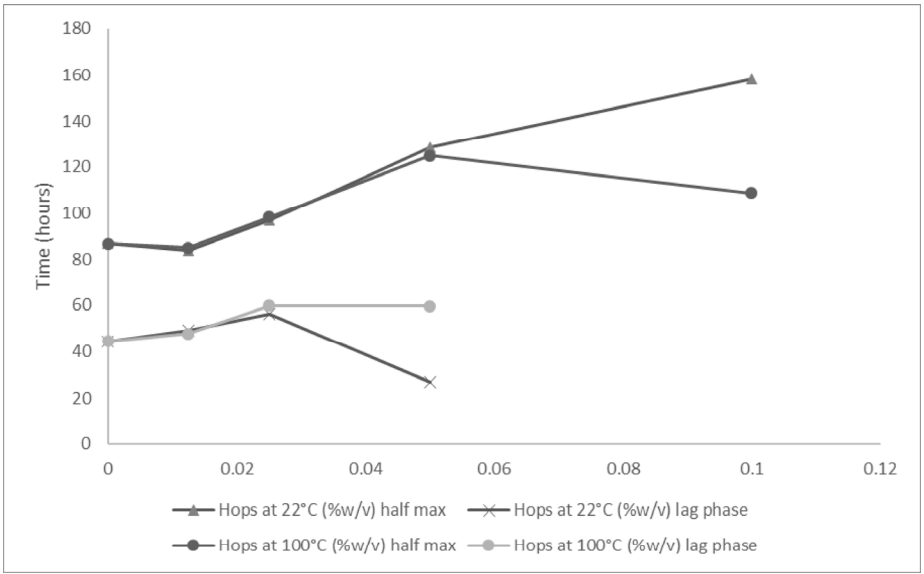

Figure 3.19 The time of each phase: half max time and lag phase (time to reach 5% of max) for the different concentrations of hops prepared at different temperatures.

The time to reach either phase was similar in concentrations 0.0125-0.025 % w/v. However, the lag phase was earlier in 0.1% w/v boiled hops than the hops prepared at room temperature and the half max could not be calculated for either preparation.

4 Discussion – In Vitro

The in vitro part of this study was done to identify whether hops had any effect on α-syn aggregation and thereby to identify whether hops was worth pursuing as a potential therapeutic agent for the treatment of the α-syn pathology associated with PD progression. The effects analysed in this part of the study were to look for any changes in maximum fluorescence, the time before onset of aggregation, changes in the rate of aggregation and the time to reach half of maximum fluorescence. Briefly, the principle findings of this study were that the addition of a raw homogenate solution of hops resulted in a dramatic, concentration dependent decrease in fluorescence over the course of a week compared to monomeric α-syn alone as determined using a ThT assay. Several methods of preparation of hops were investigated, two of which demonstrated a similar degree of inhibition of fluorescence. What this tells us about the potential effect of hops on the aggregation of α-syn will be examined here.

4.1 Technical considerations of ThT assay

The first step that was necessary to evaluate compounds that may affect α-syn aggregation was selecting a method in order to measure aggregation. The method chosen for this study was the ThT assay. ThT is a dye which becomes fluorescent when it binds to proteins with a β-sheet conformation (Voropai and Samtsov, 2003; Krebs et al., 2005). The dye is thought to intercalate between side chains of the amyloid fibril, parallel to the fibril axis (Krebs et al., 2005). The use of the ThT assay in order to monitor α-syn aggregation is well established and used in a number of studies (Krebs et al., 2005; Stsiapura et al., 2008; Wolfe et al., 2010; Alavez et al., 2011). As described in section 3.1.1, the change in fluorescence over time of α-syn in the presence of ThT when plotted, typically forms a sigmoidal curve consisting of an initial lag phase in which fluorescence dramatically increases and a final plateau phase in which no further increase in fluorescence is observed (see Figure 3.1).

When the aggregation of an amyloid protein is examined using the ThT assay, any treatment which reduces the amount of fluorescence is interpreted as a reduction in the amount of β-sheet

containing aggregates forming (Daturpalli et al., 2013). However, there are three possibilities that a given treatment may result in a decreased level of fluorescence. 1) There may be a decreased level of aggregation and thus β-sheet formation resulting in a decreased level of fluorescence, 2) the treatment may be competing with the ThT for the ThT binding sites on the β-sheets, thereby reducing the amount of ThT binding and the level of fluorescence observed but not necessarily reducing the amount of aggregation of α-syn, and 3) that the amyloid protein being examined may be broken down or altered by the treatment and thus not cable of forming β-sheets. Because of the chance of these three possible outcomes, the second step in this study was to measure the size of the protein after aggregation in thioflavin T, using size separation with polyacrylamide gel electrophoresis. These two techniques together were used to test treatments against aggregation in an in vitro model by measuring their effects on α-syn aggregation.

Another technical consideration of the ThT assays is the impracticability of using physiological concentrations, found to be 0.8 to 16.2 pg/µl ($8x10^{-7}$ to $1.6x10^{-5}$ mg/mL) (Mollenhauer et al., 2008). Using the minute concentrations found in the human body would cause aggregation to take months or years when proportionally compared to prior studies measuring aggregation (Kostka et al., 2008; Giehm et al., 2011; Daturpalli et al., 2013). Although physiological concentrations would be ideal in an assay to increase relevance to PD pathology, the small concentrations are impractical.

The average shape of the α-syn aggregation curve had a lag phase in the first 48 hours. The α-syn was most likely forming small oligomers in this phase, undetected by ThT fluorescence (Leung et al., 2015). After this phase, the curve increased exponentially, reaching a maximum rate after three days, where the aggregates were forming fibrillar β-sheets. In the final phase after the fluorescence rate peaked, the curve plateaued, which means the aggregates were mostly bound to each other with fewer small aggregates left unbound. In Figure 4.1 below, researchers observed a single fibril's growth using total internal reflection fluorescence microscopy stained with ThT.

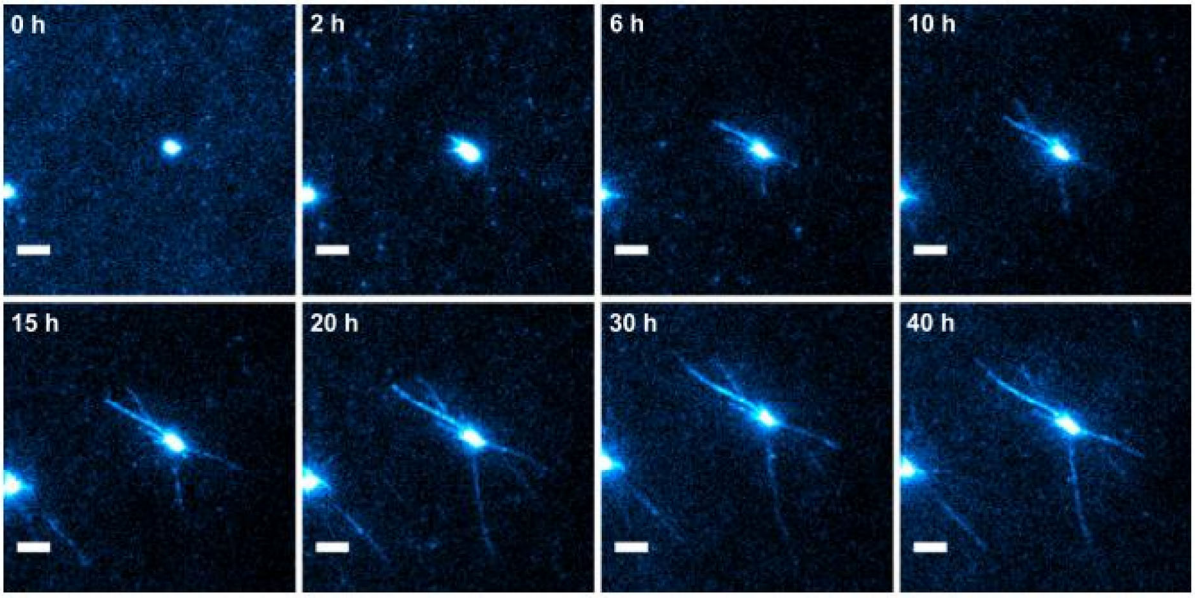

Figure 4.1 Direct observation of α-syn fibril growth by total internal reflection fluorescence microscopy (TIRFM). Time series of TIRFM images of a solution (160 µM) of monomeric α-syn in the presence of 15 µg/ml seeds and 7 µM ThT. Excitation of ThT fluorescence with a 405-nm laser, filtering of fluorescence emission through a 450/50 bandpass filter. The scale bar represents 2 µm (Wördehoff et al., 2015).

The figure above demonstrates the effectiveness of using ThT to track the aggregation process and helps visualise what is most likely occurring in the ThT assays (Wördehoff et al., 2015). The speed and simplicity of ThT assays allow multiple treatment candidates to be tested and to further validate findings another in vivo assay was performed.

The treatment tested in this study was hops, an ingredient used to brew beer. Hops was chosen because of its high flavonoid content and the evidence suggesting that flavonoids may affect α-syn aggregation (Liu et al., 2014). Moreover, hops was also found to reduce memory impairment in mouse Alzheimer model (Sasaoka et al., 2014). Thus, the flavonoid content and the potential therapeutic effect in another neurodegenerative disease makes hops an ideal first candidate for this study.

4.2 Alpha-synuclein ThT assay

The first ThT assay analysed was α-syn without additional treatments. The α-syn was analysed at 1 mg/mL because the maximum fluorescence was in the measurable range of the spectrophotometer and was also generated aggregation in vitro in a reasonable amount of time (Giehm et al., 2010). The hops-treated α-syn assays were compared to the average fluorescence rate of this first

untreated α-syn aggregation to detect any possible therapeutic effects by comparing maximum fluorescence, peak fluorescence rate, time to half max and the lag phase (time to reach 5% of max).

The different parts of the fluorescence curve will be examined in chronological order, starting with the lag phase. In another study, 50 µM or 0.7 mg/mL of α-syn with 50 µM ThT agitated with a 3-mm glass bead in a 96-well microplate showed a lag phase at 30-40 hours (seen in Figure 4.2 below) (Coelho-Cerqueira et al., 2014), which was close to the lag phase in this study, an average of 44.5 hours.

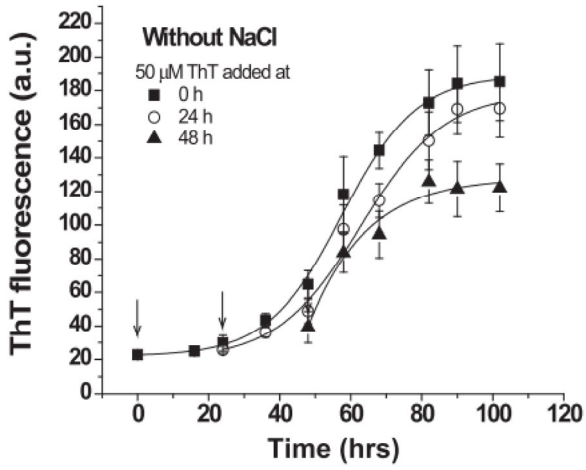

Figure 4.2 ThT (50 µM) was added at different stages (0, 24 or 48 h) to a solution of 50 µM α-syn monomer in 10 mM NaPB, pH 7.5. The α-syn aggregation was carried out in a 96-well plate at 37 °C and agitation in the presence of a 3-mm glass bead per well (Coelho-Cerqueira et al., 2014).

The experimental setups were quite similar in both studies with the key differences in a 70% concentration of protein and 20% increased concentration of ThT compared to this study, the fluorescence curves reflected these changes. Despite this, the results were quite similar, suggesting that the results reported for α-syn alone in a ThT assay in our study are keeping with what was reported previously in the literature.

Depending on the method of agitation, the fluorescence curve can increase at a faster rate. Small changes to pH or salt content can also increase the aggregation rate (Hoyer et al., 2002). In Figure 4.3 below, ultrasonication was used in another study to aggregate α-syn resulting in higher

peak rate. The peak fluorescence rate was greater and the maximum fluorescence occurred at 6-7 hours as opposed to 169 hours in this study.

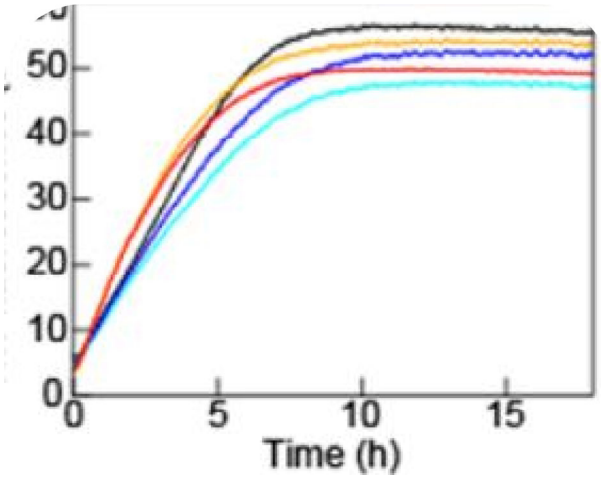

Figure 4.3 Time-dependent changes in ThT fluorescence under various conditions of ultrasonication: cycles of ultrasonication for 9 min with quiescence for 1 min with a high (red) or low (blue) ultrasonic amplitude or cycles of ultrasonication for 4 min with quiescence for 1 min with a high (orange) or low (cyan) amplitude (Noda et al., 2016).

The peak rate and maximum fluorescence in a study using agitation to aggregate 70 µM (~1 mg/mL) α-syn resulted in values closer to the one observed in this study. After α-syn was shaken in a plate reader for over 3 days at 37°C, the peak rate occurred between 40 and 50 hours and the maximum fluorescence after 110 hours seen in Figure 4.4 (Daturpalli et al., 2013). Daturpalli et al. (2013) also took transmission electron microscopy (TEM) images before and after the ThT assays and showed that α-syn was forming fibrils.

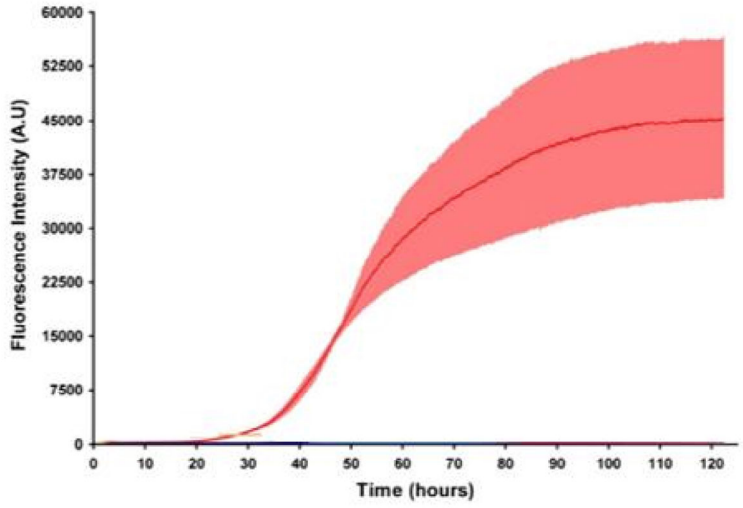

Figure 4.4 The red line represents fluorescence of 70 µM or ~1 mg/mL α-synuclein with 70 µM ThT shaken for 3 days (Daturpalli et al., 2013).

The ThT assays performed in this study were consistent with those found in the literature with minor differences caused by variations in methodology. It is noteworthy that there was less variation between replicates in the present study compared with the previously reported studies, suggesting good consistent execution of the assay. The untreated α-syn aggregation served as the control for the hops treatments. The effects of hops on the different phases of the fluorescence curve were compared to detect whether there was an effect on aggregation.

4.3 Hops effects on aggregation

Treating α-syn with hops resulted in a concentration dependent decrease in fluorescence compared with α-syn alone. The increase in fluorescence of α-syn in the presence of ThT is widely regarded as representing an increase in α-syn aggregation (Anderson and Webb, 2011; Giehm et al., 2011; Zhao et al., 2011; Ahmad and Lapidus, 2012). A decrease in fluorescence is likely to be either due to a reduction in aggregation, the prevention of the dye binding to the aggregated protein or the loss of the protein. As described in section 4.1, any decrease in fluorescence is most likely due to a decrease in aggregation similar to the changes shown in other studies looking at the effects of heat shock protein or immunoglobulin on aggregation using a ThT assay (Smith et al., 2012; Daturpalli et al., 2013). There is therefore a concentration dependant inhibition of aggregation observed when treating monomeric human α-syn with hops.

Hops decreased fluorescence with every increase in concentration. By including 0.0125% w/v of hops prepared at room temperature with 1 mg/mL of α-syn, the maximum fluorescence dropped by more than half. The shape of the curve remained the same, but the intensity was reduced, and the lag phase was longer. Increasing the concentration of hops to 0.025% w/v reduced the maximum fluorescence and delayed the lag phase compared to α-syn only. Finally, a concentration of 0.1% w/v hops caused a 53-fold reduction in maximum fluorescence with no calculable lag phase. Compared to heat shock protein (Hsp90), a protein involved in the folding, stabilization, activation and assembly of a specific set of proteins, a high enough concentration of hops delayed the lag phase similar to how Hsp90 delayed an increase in fluorescence seen in Figure 4.5 (Daturpalli et al., 2013).

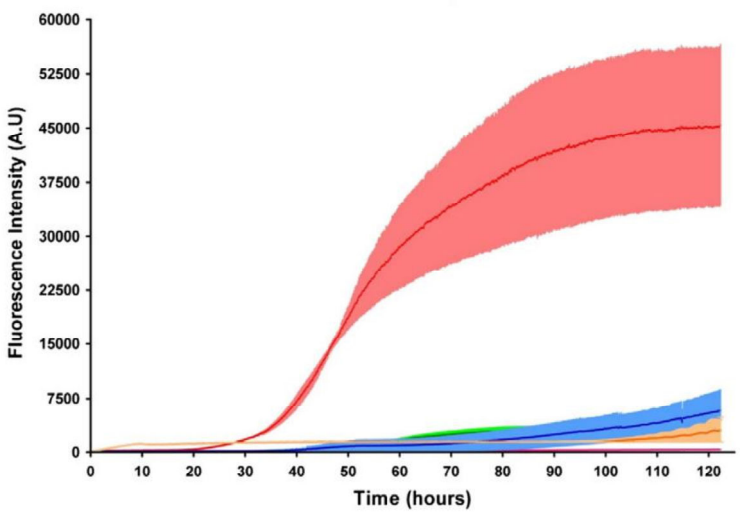

Figure 4.5 The red line represents fluorescence of 70 µM or ~1 mg/mL α-synuclein with 70 µM ThT shaken for 3 days, blue represents α-synuclein with C Hsp90 and orange represents α-synuclein with N Hsp90 (Daturpalli et al., 2013).

With a high enough concentration, Hsp90 may lead to a similar reduction in fluorescence. Whether hops is only affecting fluorescence and not aggregation was still unclear at this point. Hops could be interfering with α-syn aggregates from binding with each other or one of the few possibilities discussed previously in the technical considerations.

As mentioned in the technical considerations, ThT is not a viable means to understand the effects of a treatment on α-syn aggregation on its own (Hudson et al., 2009). The hops may not

affect α-syn aggregation, instead it could be acting on the mechanism of fluorescence. The hops may be affecting fluorescence by competitively binding to Thioflavin T, reducing the available Thioflavin T that could fluoresce in between the β-sheets. This could be true because of the dose dependent relationship between hops and fluorescence, but still does not eliminate the likelihood of hops binding to α-syn. To determine what hops was binding to, the assay samples were analysed on protein acrylamide gels.

4.4 Technical Considerations of gel electrophoresis

Gel electrophoresis was used because it can reveal molecular weights of the proteins present in the samples and can also give an approximate representation of protein content in each molecular weight. Gels were silver stained because of the high sensitivity to low protein content, which can reveal low concentrations of higher molecular weight oligomers present on the gel compared to Coomassie blue staining, which has a lower sensitivity (Oakley et al., 1980). The high sensitivity of silver staining was useful in detecting the low protein content of oligomers and other higher molecular weight forms of α-syn, but higher content of monomers caused smearing. In future studies, it may be worth staining gels with a silver stain to detect oligomers and Coomassie to visualise the higher content of monomers.

Additionally, the use of polyacrylamide gels is common place when analysing proteins because of the smaller size of proteins 1-200 kDa (Bhilocha et al., 2011). Agarose gels are usually used to analyse DNA with sizes going over 200 kDa. When analysing aggregated protein compounds larger than 200 kDa, using agarose gels to separate fibrillar species may be a viable technique (Cowman et al., 2011).

Another limitation to consider with gel electrophoresis in this study was manual pipetting of small volumes sampled from the ThT assays loaded into the gels. Manual pipetting of a volume as little as 10 µL is prone to error (Pandya et al., 2010). In this study, volumes of 1 µL were taken from ThT assay samples to for gel analysis and must be taken into consideration when interpreting results.

There are strategies that can be used to minimise variability with manual pipetting (Pandya et al., 2010).

Condensation was also a common occurrence after a week of incubation at 37°C. This may explain the increase in protein content in lanes 2 and 3 in Figure 3.14 compared to lanes 1 and 4. In the future, microplates should be spun in a centrifuge to recollect any condensation on the seal.

4.5 The effect of Hops on α-syn using gel analysis

A significant difference between protein aggregate sizes was not observed using gel analysis. The presence of putative trimers (42 kDa), quatrimers (~70 kDa) and 10-11 monomers (164 kDa) in samples with and without hops showed that hops was not preventing these aggregates from forming. A study using a substrate to cause α-syn aggregation observed bands in similar regions (Lee et al., 2001). In this study, the sum of total band intensity in each lane was not equal as seen in Figure 3.9. This is likely due to the small volumes pipetted, which may have impacted the amount of protein present in each well (Pandya et al., 2010). The lanes containing hops only without α-syn showed little smearing and bands that were barely visible, meaning any bands present in the hops and α-syn lane were a result of hops affecting α-syn rather than protein extracted directly from hops. The presence of higher molecular weight species in lanes containing hops and α-syn show that hops is not preventing the formation of aggregates, and when combined with the results of the ThT assays where fluorescence was reduced, the hops is likely changing the morphology of α-syn aggregates. This finding is similar to that of Singh et al., (2013), where curcumin, another polyphenolic compound was found to alter aggregate morphology of α-syn rather than preventing aggregation altogether. Pandey et al., (2008) also showed a similar effect of curcumin on α-syn aggregation and presented gel results similar to this study. The lanes containing curcumin and α-syn still had higher molecular weight species (Pandey et al., 2008) and the atomic force microscopy data of curcumin and α-syn resulted in more globular matter than fibrillar outlines (Singh et al., 2013). Gel analysis confirmed the presence of α-syn and the higher molecular weight species and although analysis did not conclusively determine the effects of hops on the size of α-syn aggregate species, it

did reveal that hops is not preventing aggregation. Hops is most likely changing the morphology of α-syn aggregates.

4.6 Effects of temperature on hops treatment

The hops extract was prepared in multiple ways to determine whether different methods of preparation may affect any anti-amyloidogenic activity of the extract. Hops was prepared by 1) infusion of homogenised hops in room temperature (22°C) water, 2) 0.2-µm filtration of infused hops, 3) by boiling hops for 10 minutes and 4) using a CO_2 extract of hops. The two treatments used in this thesis was the room temperature hops preparation and the hops steeped in boiling water. The 0.2-µm filtered preparation and the CO_2 hops extract both presented technical challenges which were not overcome in the time constraints of the present study.

Filtration was initially an issue because the hops particles blocked the filter pores during filtration. Multistep filtration is a solution to this issue but due to time constraints not enough data could be collected using filtered hops.

The CO_2 extract became cloudy in the ThT samples with and without protein, resulting in greater absorbance rather than fluorescence. There might be other methods to perform another colorimetric assay by changing pH and using different dyes (Giasson et al., 2014), however this was not pursued as one of the goals of this study is to reduce procedures to maintain efficiency and reproducibility.

The only difference between boiling hops and preparing it at room temperature was that boiling the hops during preparation resulted in noticeably lower variability between replicates making the distinction between treatment concentrations clearer. This tells us two things, firstly the active component of the hops homogenate that gives rise to the reduced fluorescence is not affected by boiling. Secondly, while the precise mechanism is of course unknown, perhaps boiling results in the addition or removal of some component of the raw homogenate which resulted in the reduced variability in the fluorescence readings observed when the preparation is boiled.

Other techniques such as shaking powdered hops with methanol for several hours and filtering the supernatant could be used to isolate different constituents in future ThT assays. This technique was used to prepare mulberry leaf extract for a ThT assay that measured the of the mulberry leaf on amyloid b-peptide aggregation (Niidome et al., 2007).

The gel analysis showed bands in four molecular weight regions similar to the hops prepared at room temperature. The boiled hops also did not affect the number of aggregate species. In future experiments, treatments that inhibit fluorescence in ThT assays could be analysed further by observing effects on fibrils using total internal reflection fluorescence microscopy (TIRFM) as shown in Figure 4.1 (Wördehoff et al., 2015). Any inhibition of α-syn fibril growth would make a treatment a contender for behavioural/clinical experiments.

A procedure that could potentially be used before or after ThT assays is a newly developed piece of equipment called BLItz that measures binding affinity. Alpha-syn could be biotinylated and then checked for direct binding of a treatment to α-syn using the label free BLItz. BLItz works by using a proprietary sensor that can detect optical changes when proteins bind to the sensor (King et al.). Any further binding to the protein can also be detected by further reduction of light reaching the sensor. Using BLItz to measure binding affinity to α-syn should be used as a preliminary experiment to behavioural experiments, if the procedure is reproducible and allows a high throughput of treatments to be tested.

After the completion of this study, a machine for carrying out dynamic light scattering (DLS) became available was used by the lab to analyse α-syn aggregate morphology post-ThT assay. DLS is the measure of light intensity with laser exposure and is a non-invasive technique contrast to SDS-PAGE (Bitan et al., 2001). DLS can determine the size of small particles and so measure the change in particle size over time by direct measurement of the particles themselves rather than relying on the binding of a dye to a molecule as in the case of ThT assay used in the present study. The drawback of this technique is that it can only measure the average size of molecules across the

whole solution and does not measure each individual particle (Bitan et al., 2001). However, DLS can still be used if an oligomer population is generally uniform.

Atomic force microscopy (AFM) used in the early stages of this project is another non-invasive technique worth revisiting, which involves light reflecting off a cantilever that makes contact with the surface being measured (McAllister et al., 2005). We had difficulty using AFM initially since we relied on purchasing commercially produced α-syn and could not get it in sufficient quantity to use this method. Since we now make α-syn our selves this technique would be possible and would be worth using in future studies. AFM can visualise individual molecules and so is useful in particular for not only reporting the size of the molecules but also showing the morphologies assumed by the molecules upon aggregation (McAllister et al., 2005).

Refinements to techniques using SDS-PAGE, may also be useful including chemically crosslinking the aggregates to make them more stable prior to running on a gel (Lee et al., 1998; Bitan et al., 2001; Bitan and Teplow, 2004). Some studies used N- (Ethoxycarbonyl)-2-Ethoxy-l,2-Dihydroquinoline (EEDQ) to cross-link α-syn before running SDS-PAGE; aggregated α-syn with EEDQ resulted in clear high molecular weight bands (Lee et al., 1998). Samples containing EEDQ could also be reanalysed using DLS and/or AFM to check for any possible morphological changes caused by EEDQ.

One final method worth noting used to analyse aggregation of α-syn was electrochemical analysis. Lopes et al. (2014) monitored α-syn aggregation by oxidizing tyrosine (Tyr) residues surface-exposed in monomeric α-syn and buried in fibrillated α-syn adsorbed onto graphite electrodes. The study performed cyclic voltammetry (CV) and differential pulse voltammetry (DPV) and observed increased peaks in voltage when fibrillation occurred, which was further verified by the ThT-based assays also conducted (Lopes et al., 2014). A few of the different techniques could be simultaneously completed to provide a more complete picture of the aggregation process occurring and verify whether a treatment is disrupting the aggregation process.

The in vitro portion of this study determined that using a ThT assay as a preliminary test of possible PD treatments is viable and that hops was able to dose dependently reduce the fluorescence of α-syn compared to un-treated α-syn. This reduction in α-syn fluorescence was likely due to a reduction in α-syn aggregation but as discussed other methods should be performed in the future in order to confirm this finding. With these observations in mind we sought to examine the effect of hops treatment on the behavioural effects noted in an animal model of α-syn induced behavioural disturbance. The model used in the present study was *C. elegans* due to their ease of production and rapid turnover. There was also an α-syn over-expressing strain available which had previously reported behavioural deficits. Since α-syn is increasingly implicated in the initiation and or progression of PD, any compound that could modify the pathological behavioural deficits that resulted would be of interest for the treatment of human PD.

5 Results – In Vivo

5.1 Developing in vivo PD model

To establish an in vivo model to test potential therapeutic agents for use against pathologies underlying PD, an invertebrate model using *C. elegans* was chosen. *C. elegans* were chosen because of their short life span and low maintenance requirements, some of the many qualities that make them ideal preliminary subjects (Duty and Jenner, 2011). The first method of instigating α-syn pathology presented below is the overexpression of α-syn in *C. elegans* muscle cells. The second method is the overexpression of α-syn in *C. elegans* food and the final method was the exogenous exposure to pre-aggregated α-syn.

5.1.1 The effect of α-syn in *C. elegans* that overexpressed α-syn

Two strains of *C. elegans* were used in order to study the effect of α-syn over expression in this species. The DDP1 strain of *C. elegans* overexpressed α-syn in muscle cells (unc-54 is the gene that codes for myosin-4) together with a fluorescent marker (CFP and YFP) (uonEx1 [unc-54::alpha-syn::CFP + unc-54::alpha-syn::YFP(Venus)]) and the DDP2 strain only has a fluorescent marker expressed via the unc-54 promoter fragment (uonEx2 [unc-54::CFP::YFP(Venus)]), serving as a control. The maximum speed, average speed and body bends/second (calculated by dividing the Length of the track by Perimeter/2 and the time) of the two strains were compared in these two strains. *C. elegans* were recorded at a single time point 48 hours after being plated, at early stage of adulthood. A life span assay was also run alongside the recordings and living worms were tallied every second day, however, scoring living worms was unreliable and required more time to optimise.

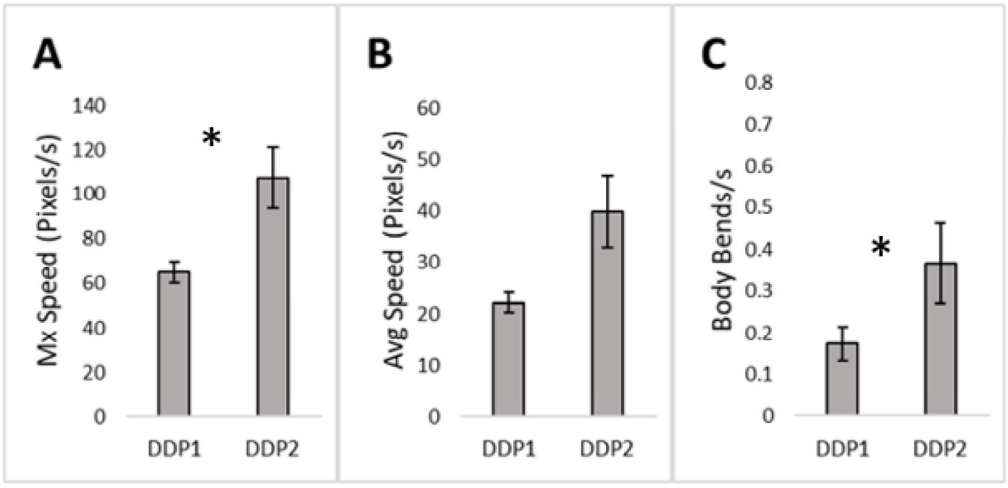

*Figure 5.1 The mean speeds (pixels travelled/second) of DDP1 C. elegans (overexpress α-syn) (n=108) were compared to DDP2 (control) (n=31) with SEM error bars. (A) shows the comparison of maximum speed. (B) shows the average speed. (C) shows the mean body bends per second. The nonparametric Mann-Whitney test was used to determine significance. * indicates p<0.05.*

Both strains were fed OP50-1, a normal strain of *E. coli* commonly used to feed *C. elegans* and exposed to buffer only (no other α-syn treatments). Over expression of α-syn in the muscles of *C. elegans* resulted in a significant decrease in both maximum speed (Figure 5.1, panel A) and mean bend speed (Figure 5.1, panel C). The mean maximum speed (A) of DDP2 *C. elegans* (Mdn=120.60 px/s) was 1.65-fold greater than DDP1 (Mdn=49.71 px/s), U=1286.64, p=0.011. The mean bend speed (C) of DDP2 *C. elegans* (Mdn=0.01 bb/s) was 2.1-fold greater than DDP1 (Mdn=0 bb/s), U=1345.45, p=0.015). There was no significant change in mean average speed as a result of over expression of α-syn in the skeletal muscles of *C. elegans* U=1286.64, p=0.25. It was also noted that there was no difference in the length of the worms between each strain. There was no significant difference between mean nematode strain length, U= 1286.64, p=0.16.

5.1.2 The effect of feeding *C. elegans E. coli* that overexpress α-syn

The second method of α-syn exposure was feeding normal, wild type *C. elegans* with a food source that over expresses normal human α-syn. The wild type strain of *C. elegans* (N2) was used in the following experiments. Control worms were fed OP50-1, a streptomycin resistant strain of *E. coli* which is often given to *C. elegans*. OP50-1 tends not to form mounds when grown on agar plates and so is ideal for feeding c elegans, but is otherwise normal. The experimental group of *C. elegans*

were fed a strain of e coli which over expressed full length, normal human α-syn in order to examine the effect of exogenous exposure to α-syn.

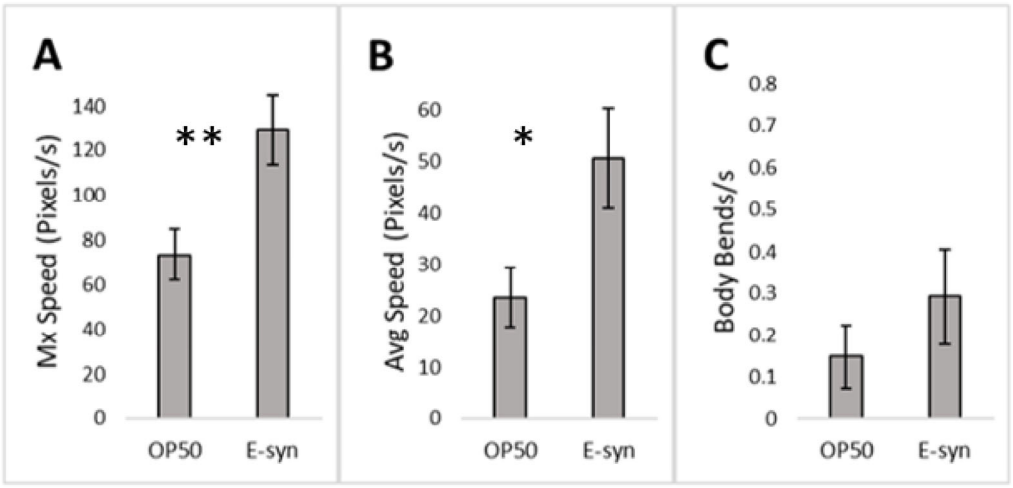

*Figure 5.2 Three behavioural parameters were compared in the N2 C. elegans fed OP50-1 (control) (n=21) and the experimental group that were fed e coli expressing human monomeric α-syn(E-syn) (n=11). (A) shows the comparison of maximum speed. (B) shows the average speed. (C) shows the mean body bends per second. The nonparametric Mann-Whitney test was used to determine significance. * indicates p<0.05, ** indicates p<0.01.*

The *C. elegans* that fed on *E. coli* overexpressing α-syn (E-syn) (Mdn=121.93 px/s) showed a 1.75-fold increase in maximum speed (A) compared to the elegans that fed on OP50-1 (Mdn=66.18 px/s), U=66.10, p=0.0074. The *C. elegans* that fed on E-syn (Mdn=48.10 px/s) were 2.14-fold faster in average speed (B) compared to the elegans that fed on OP50-1 (Mdn=17.32 px/s), U=66.10, p=0.015. There was no significant difference in bend speed (C), however, in *C. elegans* that fed on E-syn (Mdn=0.291 bb/s) compared to the elegans that fed on normal, OP50-1 *E. coli* (Mdn=0.008 bb/s), U=67.78, p=0.11. There was no significant difference in nematode length between food sources, U= 66.10, p=0.17.

In summary, wild type, N2 nematodes fed a strain of *E. coli* that overexpressed α-syn have a significantly greater max speed and average speed, but there was no difference in the number of body bends per second when compared to *C. elegans* that were fed non- α-syn expressing *E. coli*.

5.1.3 The effect of exposing *C. elegans* to extrinsic aggregated α-syn

The final method used to induce α-syn pathology in *C. elegans* in order to examine any potential behavioural deficits induced exogenous exposure to aggregated α-syn. Aggregated α-syn is

proposed to be the pathological form of α-syn generating the downstream pathologies associated with PD (Danzer et al., 2007; Goedert et al., 2013). The aggregated α-syn treatment was compared to vehicle buffer exposure (same buffer used to dissolve aggregated α-syn). The wild type N2 strain of *C. elegans* were also used for this experiment.

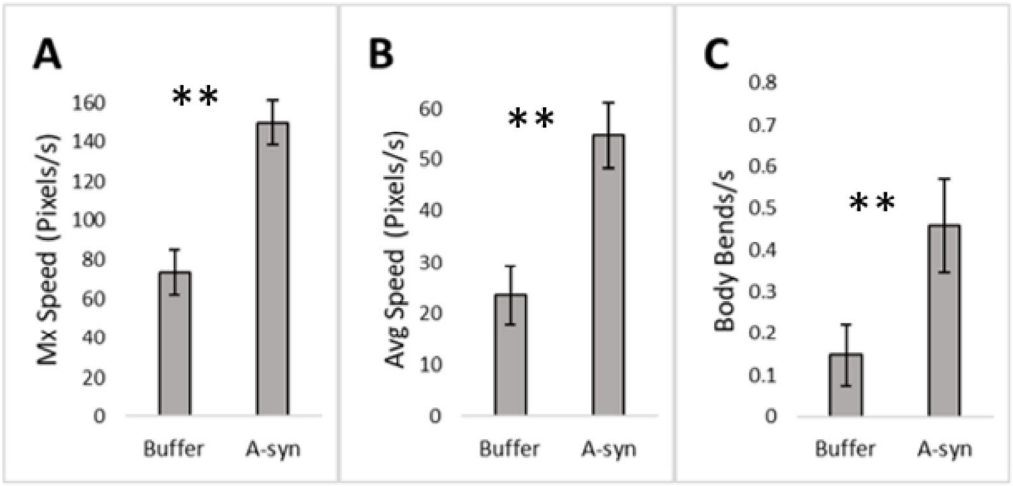

*Figure 5.3 Three behavioural parameters of wild type, N2 C. elegans exposed to 200 µg of aggregated α-syn (n=19) were compared with those that were exposed to vehicle only (n=21). (A) shows the comparison of maximum speed. (B) shows the average speed. (C) shows the mean body bends per second. The nonparametric Mann-Whitney test was used to determine significance. ** indicates p<0.01.*

The mean maximum speed (A) was 2.03-fold greater in N2 *C. elegans* treated with aggregated α-syn (Mdn=146.97 px/s) compared to those treated by vehicle alone (Mdn=66.18 px/s), U=127.13, p<0.001. The mean average speed (B) was 2.32-fold greater in N2 *C. elegans* in aggregated α-syn (Mdn=63.43 px/s) compared to those in vehicle (Mdn=17.32 px/s), U=127.13, p=0.0019. The mean number of bends per second (C) was 3.1-fold greater in N2 *C. elegans* in aggregated α-syn (Mdn=0.329 bb/s) compared to those in vehicle (Mdn=0.008 bb/s), U=128.39, p=0.0051. There was no significant difference in nematode length between treatments, U= 127.13, p=0.19. The N2 worms exposed to aggregated α-syn were on average faster over the three parameters examined than those exposed to vehicle alone.

5.2 Compounded effects of exposure to α-syn from multiple sources

The two methods of exposing *C. elegans* used previously were combined to measure the possible additive effects of the different methods on *C. elegans* movement. Wild type, N2 worms were fed

with E-syn and exposed to aggregated α-syn and were compared to those fed with OP50-1 and vehicle exposure.

5.2.1 The effects of overexpression of α-syn and exogenous α-syn exposure

The first combination of factors examined in the present study was to use the DDP1 strain of *C. elegans* overexpressing α-syn and combine that with exposure to exogenous aggregated α-syn.

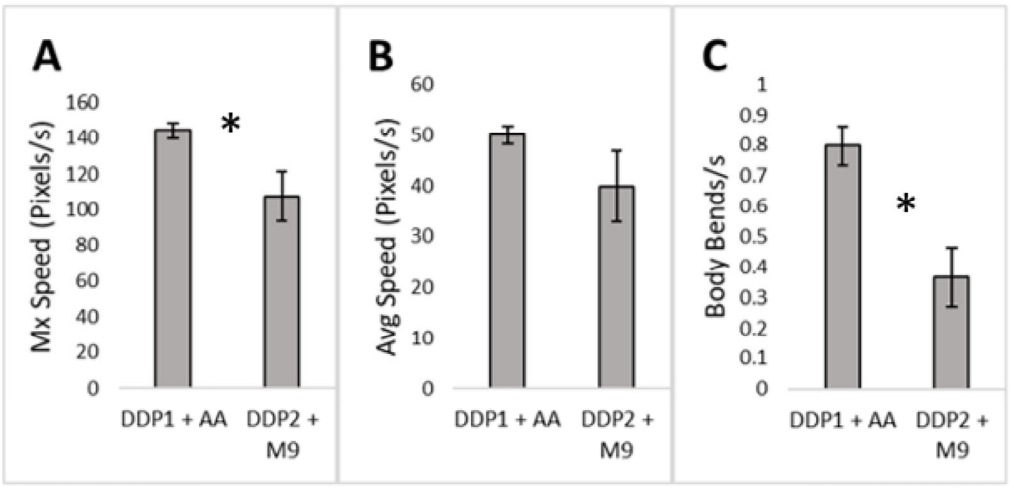

*Figure 5.4 Three behavioural parameters were examined between α-syn over expressing DDP1 C. elegans treated with 200 µg of aggregated α-syn (n=108) were compared to empty vector control c elegans, DDP2, exposed to vehicle alone (n=31). (A) maximum speed (B) average speed (C) body bends per second. The nonparametric Mann-Whitney test was used to determine significance. * indicates p<0.05.*

There was a significant difference in the mean maximum speed (A) of α-syn expressing c elegans, DDP1, treated with aggregated α-syn (Mdn=144.54 px/s) was 1.34-fold greater than vector control animals, DDP2 in vehicle alone (Mdn=120.60 px/s), U=1286.64, p=0.02. The mean bend speed (C) of DDP1 exposed to aggregated α-syn (Mdn=0.69 bb/s) was also significantly greater than the mean bend speed of non α-syn expressing vector control worms, DDP2 in vehicle alone. The treated worms demonstrated a 2.18-fold difference in bend speed compared to the untreated controls (Mdn=0.008 bb/s), U=1289.02, p<0.05.

There was no significant difference in mean average speed (B) of α-syn expressing DDP1 worms treated with aggregated α-syn (Mdn=52.06 px/s) when compared with non-α-syn expressing control animals in vehicle (Mdn=16.72 px/s) by 1.25-fold, U=1286.64, p=0.060.

Interestingly, the mean body length of treated animals (DDP1 exposed to aggregated α-syn) (Mdn=115.05 px) was longer than the non-treated (DDP2 in vehicle) (Mdn=68.78 px), U= 1286.64, p=0.0025 in this experiment. In summary, the combination of overexpression of α-syn and the environmental exposure to α-syn increased movement speed when compared with worms that were neither overexpressing α-syn and nor exposed to exogenous aggregated α-syn.

5.2.2 The effects of α -syn in food and environment

The final combination of factors examined was to expose N2 wildtype *C. elegans* fed E-syn to exogenous aggregated α-syn to see if any effects on mobility were compounded by exposure to α-syn through multiple administrative methods when compared to untreated wild type worms. The combination of exposure to α-syn exogenously while fed E-syn was expected to cause an increased reduction in movement speed and bend rate.

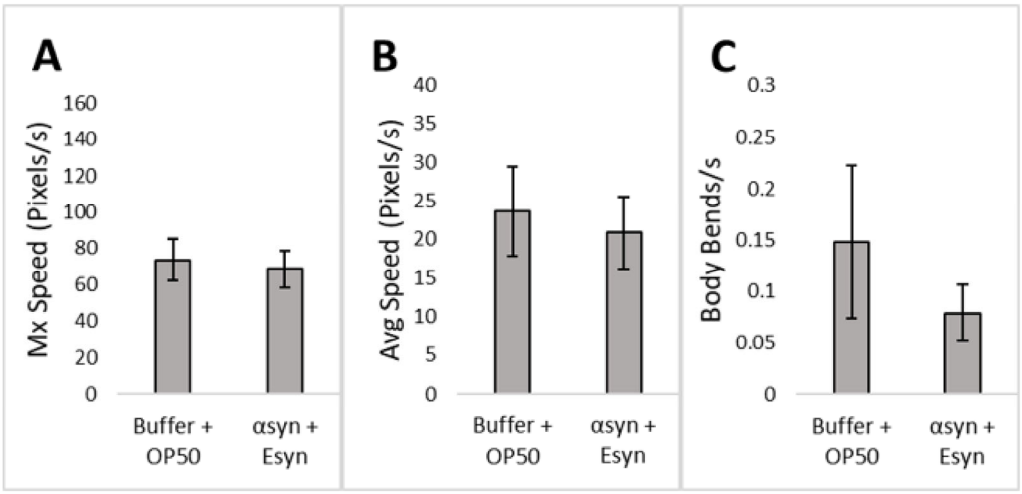

*Figure 5.5 Three behavioural parameters were examined in wild type, N2 C. elegans in vehicle fed with normal, OP50-1 (n=21) bacteria and were compared to the experimental treatment of wild type, N2 c elegans exposed to 200 µg of aggregated α-syn and fed with E. coli overexpressing α-synuclein (n=23). (A) maximum speed (B) average speed (C) body bends per second were examined. The nonparametric Mann-Whitney test was used to determine significance. * indicates p<0.05, ** indicates p<0.01.*

There was no difference in the maximum speed (A) between N2 *C. elegans* fed with OP50-1 in buffer (Mdn=66.18 px/s) compared to those fed E-syn and exposed to aggregated α-syn (Mdn=56.17 px/s), U=158.09, p=0.70. There was also no difference in the mean average speed (B) of N2 *C. elegans* fed with OP50-1 in buffer (Mdn=17.32 px/s) compared to those fed E-syn and in aggregated α-syn (Mdn=13.41 px/s), U=158.09, p=0.73; and there was no difference between these treatments in

mean bend speed (C), U=164.27, p=0.62. Lastly, there was no significant difference in nematode length between treatments, U= 158.09, p=0.79. The combined treatment of feeding E-syn and aggregated α-syn had no significant effect on *C. elegans* movement behaviour.

5.3 Anti-amyloidogenic effect of hops in vivo

In the in vitro part of this study, hops reduced fluorescence in the ThT assays which likely represented a decrease in α-syn aggregation, suggesting that this hops preparation may be worth investigating as a potential therapeutic against the α-syn pathology associated with PD. In the following experiments, the effect of hops extract on the α-syn induced behavioural changes observed in *C. elegans* were examined to see if the hops extract could reverse the observed behavioural effect of α-syn exposure. In addition, the effect of hops on *C. elegans* behaviour in the absence of α-syn was also examined to determine whether any effect of hops was due to interaction with α-syn or with the *C. elegans* alone.

5.3.1 Effects of hops on *C. elegans* overexpressing α-syn

The following results show the effect of hops on *C. elegans* overexpressing α-syn (DDP1). DDP1 was expected to reveal any possible effects hops may have on α-syn pathology because of the reduction in movement speed compared to DDP2 seen in Figure 5.1.

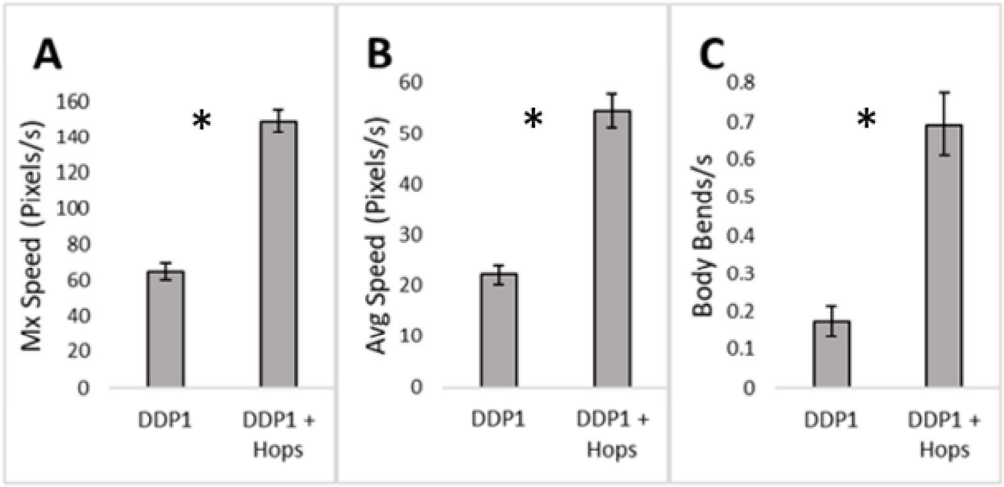

*Figure 5.6 Three behavioural parameters were examined between DDP1 C. elegans (n=108) and DDP1 exposed to hops (n=39). (A) maximum speed (B) average speed (C) body bends per second. The nonparametric Mann-Whitney test was used to determine significance. * indicates p<0.05.*

Each of the four parameters examined demonstrated a significant difference compared to the α-syn over expressing DDP1 *C. elegans* alone. The mean maximum speed (A) of DDP1 exposed to hops (Mdn=148.63 px/s) was 2.3-fold faster than DDP1 alone (Mdn=49.71 px/s), U=1659.28, p<0.05. Mean average speed (B) of worms exposed to hops (Mdn=55.21 px/s) was 2.5-fold faster than just DDP1 (Mdn=14.88 px/s), U=1659.28, p<0.05. Average number of body bends per second (C) of DDP1 exposed to hops (Mdn=0.581 bb/s) was 4-fold faster than DDP1 (Mdn=0 bb/s), U=1696.87, p<0.05. While the mean length of DDP1 exposed to hops (Mdn=111.78 px) was 2.7-fold longer than the DDP1 in buffer (Mdn=34.79 px), U= 1659.28, p<0.05. Exposure to hops increased worm movement speed in the DDP1 strain, but the worms exposed to hops were also longer.

5.3.2 Effects of hops on *C. elegans* fed E-syn

Even though there was no significant difference in bend between E-syn fed N2 and OP50-1 fed N2, the significant difference in movement speed was enough to justify the analysis of hops treatment on E-syn. The effect of hops on movement behaviour of N2 worms fed E-syn was examined next.

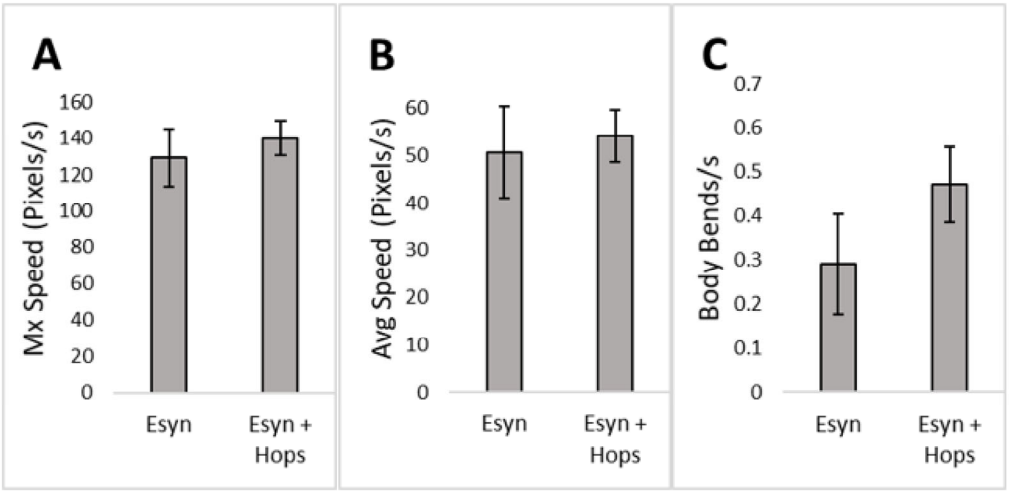

*Figure 5.7 Three behavioural parameters were examined between N2 C. elegans fed E-syn (n=11) and N2 fed E-syn exposed to hops (n=21). (A) maximum speed (B) average speed (C) body bends per second. The nonparametric Mann-Whitney test was used to determine significance. * indicates p<0.05, ** indicates p<0.01.*

There was no significant difference in any of the parameters examined in these experiments when worms fed α-syn expressing *E. coli* were treated with hops extract. The mean maximum speed (A) of worms fed E-syn and exposed to hops (Mdn=148.01 px/s) compared to those only fed E-syn (Mdn=121.93 px/s), U=66.10, p=0.54. Mean average speed (B) of N2 exposed to hops (Mdn=53.48

px/s) was also no different than those only fed E-syn (Mdn=48.85 px/s), U=66.10, p=0.71. Mean number of body bends per second (C) in N2 exposed to hops (Mdn=0.431 bb/s) was also no different than N2 fed E-syn (Mdn=0.29 bb/s), U=66.26, p=0.16. Lastly, there was also no significant difference in nematode length between treatments, U= 66.10, p=0.68.

In summary, there was no significant difference in speed between N2 fed with α-syn expressing *E. coli*, E-syn and exposed to hops and those that were not. It was also noted that the variability in the measures taken were greater the worms that were fed E-syn only.

5.3.3 Effects of hops on *C. elegans* expose to aggregated α-syn

The addition of hops may reduce the changes evident in N2 exposed to aggregated α-syn in Figure 5.3 similar to how changes were observed when DDP1 was exposed to hops. The results of this hops treatment are presented next.

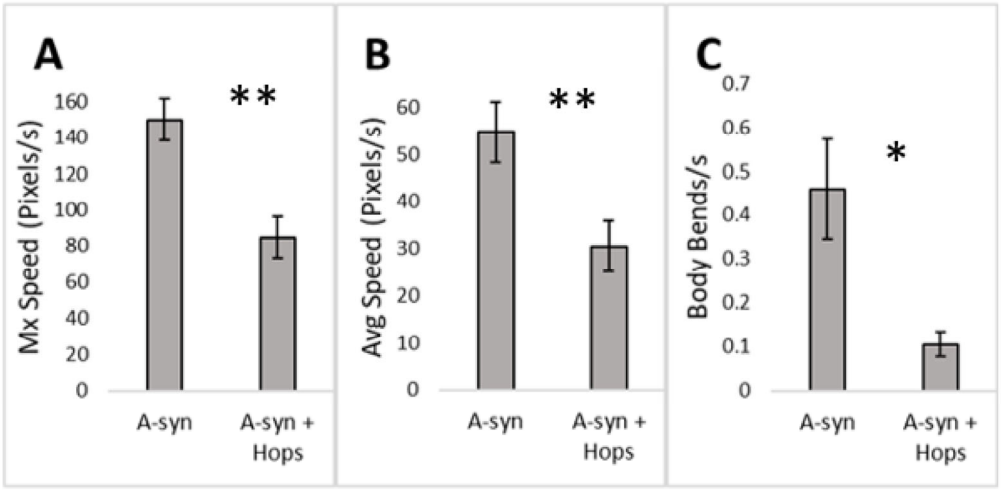

*Figure 5.8 Three behavioural parameters were examined between N2 C. elegans with 200 µg of aggregated α-syn (n=19) and N2 in aggregated α-syn exposed to hops (n=25). (A) maximum speed (B) average speed (C) body bends per second. The nonparametric Mann-Whitney test was used to determine significance. * indicates p<0.05, ** indicates p<0.01.*

Of the four parameters examined in this experiment each of the three behavioural parameters demonstrated a significant change as a result of hops treatment, while there was no effect of hops treatment on the length of the worms in these experiments. The mean maximum speed (A) of N2 *C. elegans* treated with aggregated α-syn (Mdn=146.97 px/s) was 76% greater than those also exposed to hops (Mdn=82.00), U=154.78, p=0.0010. Mean average speed (B) of nematodes exposed to aggregated α-syn (Mdn=63.43 px/s) was 80% greater than those also exposed to hops (Mdn=19.39

px/s), U=154.78, p=0.0095. Mean number of body bends per second (C) of worms exposed to aggregated α-syn (Mdn=0.33 bb/s) was 4.4-fold greater those also exposed to hops (Mdn=0.039 bb/s), U=155.62, p=0.0032. There was no significant difference in nematode length between treatments, U= 154.78, p=0.43. Adding hops to aggregated α-syn reduced movement speed.

5.3.4 The effects of hops on *C. elegans* without any exposure to α-syn

Lastly, in order to determine whether the hops extract its self was having any effect on the worms directly as opposed to any effect the hops may be having on any form of α-syn treatment, the effect of hops extract on wild type *C. elegans*, N2, without any other form of α-syn treatment was examined followed by the hops treatment of DDP2.

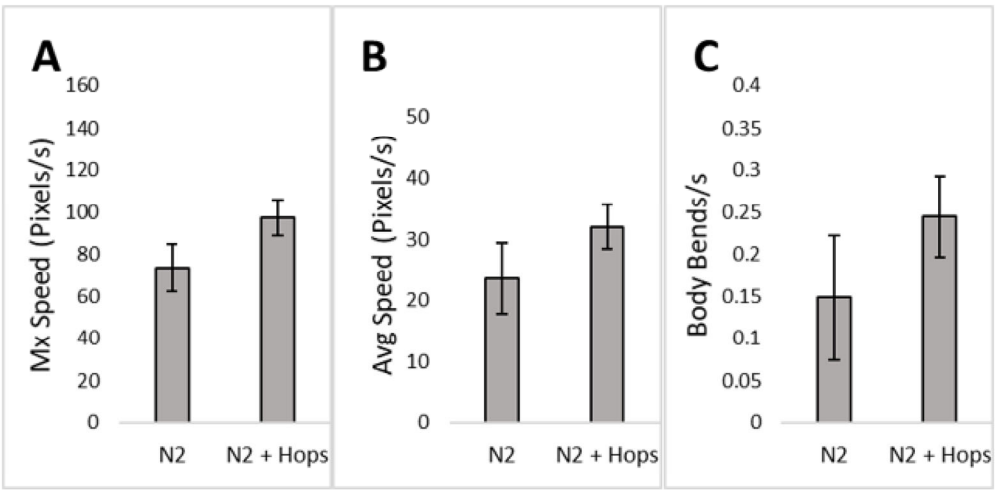

*Figure 5.9 Three behavioural parameters were examined between N2 C. elegans (n=21) and N2 exposed to hops (n=54). (A) maximum speed (B) average speed (C) body bends per second. The nonparametric Mann-Whitney test was used to determine significance. * indicates p<0.05, ** indicates p<0.01.*

There was no effect of hops on any of the four parameters examined in these experiments in wild type *C. elegans*. There was no significant change in the mean maximum (A) and average speeds (B) in N2 exposed to hops (Mdn=81.61, 21.34 px/s) compared to those that were not (Mdn=66.18, 17.32 px/s), U=400.90 for both, p=0.17, 0.18. N2 in hops (Mdn=0.059 bb/s) body bends per second (C) was also no different than N2 only (Mdn=0.008 bb/s), U=408.83, p=0.28. There was no significant difference in nematode length between treatments, U= 400.90, p=0.97. It was also noted that the variance in speeds of the N2 samples was high with larger error bars.

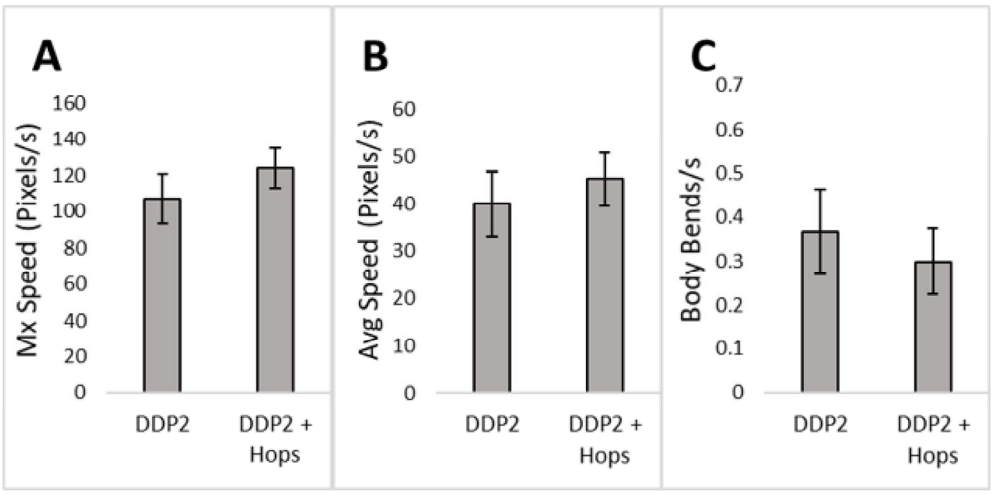

*Figure 5.10 Three behavioural parameters were examined between DDP2 C. elegans (n=31) and DDP2 exposed to hops (n=24). (A) maximum speed (B) average speed (C) body bends per second. The nonparametric Mann-Whitney test was used to determine significance. * indicates p<0.05, ** indicates p<0.01.*

When the vector control *C. elegans*, DDP2, were treated with hops none of the behavioural parameters demonstrated a significant change, but body length of the worms was significantly longer as a result of hops treatment. The mean maximum (A) and average speeds (B) were no different between DDP2 exposed to hops (Mdn=133.73, 39.80 px/s) compared to those that were not (Mdn=120.60, 16.72 px/s), U=256.51 for both, p=0.54, 0.41. DDP2 (Mdn=0.147 bb/s) body bends per second (C) showed no significant change compared to DDP2 exposed to hops (Mdn=0.008 bb/s), U=260.81, p=0.63. The mean length of DDP2 exposed to hops (Mdn=149.42 px) was longer than the DDP2 in buffer (Mdn=68.78 px), U= 256.51, p=0.017. The hops did not influence worm movement.

6 Discussion – In Vivo

The in vivo part of this study was completed to investigate a behavioural model of PD pathology by 1) measuring the effects of aggregated α-syn on *C. elegans* behaviour and 2) any effects of treatments on behaviour altered by α-syn pathology. One of the major considerations of this study was whether *C. elegans* may be useful as an in vivo model to examine pathological mechanisms proposed to underlie human PD. Thus, this possibility will be discussed next followed by an examination of the behavioural results obtained.

6.1 *C. elegans* as a model for PD

There are a number of animal models of PD which have been used to examine PD experimentally over the two hundred years since the first description of the disease in 1817 (Duty and Jenner, 2011; Blesa and Przedborski, 2014). Some major models include: 6-OHDA mouse and rat primate, MPTP mouse & primate, rotenone and paraquat mouse and rat – all of these only serve to examine the effect of dopamine cell loss as they specifically kill dopaminergic neurons via their specific mechanisms but do not induce other principle pathologies underlying PD (Blesa and Przedborski, 2014). Higher order animals such as rodents and primates are expensive and require a great deal of special care and a reasonably large amount of space for housing.

For financial and ethical reasons, the numbers of animals available for experimentation with these models is often quite limited and so complex experiments requiring large numbers of groups may not be possible, or mechanisms resulting in little change requiring the greater statistical power offered by larger numbers are not always available particularly for primate models. In addition, the death of dopaminergic neurons is but one characteristic of PD and one that does not occur for some years following the initiation of the disease, so particularly for studies that aim to examine the initiation of PD, rather than simply the cause of the motor deficits associated with the disease, models which examine other primary pathologies associated particularly with the earliest stages of the disease may be more useful. Genetic models are useful as they examine specific genetic deficits which have been associated with familial forms of Parkinsonism in humans, however since these forms of Parkinsonism represent only 5-10% of Parkinsonian cases the development of other models not necessarily examining the specific genetic deficits directly may be useful.

One of the other characteristic pathologies of PD, and one which appears to occur at the earliest stages of the disease (Dehay et al., 2015) is the formation of intra cellular protein aggregates referred to as Lewy bodies (LB). This LB formation and the proteins involved appear to be one of the important steps in the initiation of PD, but little research has been done into this earliest of mechanism. It has been noted that one of the most prevalent proteins involved in the formation of

LB is the pre-synaptic protein α-syn. Support for the importance of α-syn in the initiation or progression of PD lies in the observation that several mutations to the α-syn gene, SNCA result in several of the familial forms of Parkinsonism referred to above. Again, while these specific genetic deficits have not been associated with sporadic PD which constitutes greater than 90% of cases, the triggering of parkinsonism as a result of damage to the α-syn protein is taken as evidence that α-syn may play an important role even in the sporadic form in which there is no known genetic deficit.

Thus, an animal model in which α-syn is used to initiate some form of measurable disease pathology would be useful for the study of the initiation or progression of the human disease, as these processes seem to be highly implicated in the earliest stages of the disease. Mouse models have been developed in which α-syn is either over expressed or injected into selected parts of the brain (George et al., 2008), but as described above particularly for early stage investigations or the screening of large libraries of potential therapeutic compounds rodent models may be difficult or expensive to use, requiring resources or facilities not widely available. An invertebrate model may be useful in that pathological mechanisms may be investigated in a living organism without the same ethical constraints that can hinder experiments using higher order animals including vertebrates. *C. elegans* have been used to model many human diseases, they require little space and due to their ease of breeding can be expanded into numbers which provide more meaningful results for these sorts of experiments.

C. elegans were considered a viable model because of their unique characteristics. For this investigation, there were many reasons to prefer *C. elegans* over other organisms. *C. elegans* are about a millimetre long when fully grown and do not require a dedicated facility to maintain. The small size enables many nematodes to be maintained on a petri dish filled with agar (Dexter et al., 2012). Other invertebrates have been used to study PD such as drosophila melanogaster (Whitworth et al., 2006). However, behavioural analysis of drosophila can be difficult due to rapid

movements in three dimensions of this species, *C. elegans* on the other hand stay on a 2-dimensional surface agar plate (Dexter et al., 2012).

C. elegans were also chosen because of their short life span. Their lifespan depends on the temperature around them and they can live up to 20 days (Bodhicharla et al., 2012). Having a short life span means more experiments can be run in a shorter period and more treatments can be tested, allowing for high throughput screening of compounds or treatments of interest.

One of the goals of this study was to establish a preliminary animal model of PD pathology using *C. elegans*. According to the currently understood mechanism of cellular death in PD, oligomers were shown to be cytotoxic in vitro when they were taken up by neurons (Cremades et al., 2017). The fundamental elements to establish a model of PD pathology are neurons that are susceptible to cytotoxic species of α-syn.

The *C. elegans* used, however, overexpressed α-syn in muscle cells not in the neurons. Although overexpression was in the muscle cells, *C. elegans* had reduced lifespans. *C. elegans* overexpressing α-syn also showed reduced motility and pharyngeal pumping compared to N2 wild type C. elegans (Bodhicharla et al., 2012). In humans, PD not only causes motor control issues and tremors, but also cause oesophageal and pharyngeal dysfunction (Johnston et al., 1995). Reduced pharyngeal pumping observed in worms is reminiscent of human difficulty swallowing. In addition, human lifespan of individuals with PD is also reduced (Hobson et al., 2010; Apfeld and Fontana, 2017).

Bodhicharla et al., 2012 also showed localisation of α-syn in neurons in the strain overexpressing α-syn in muscle cells. Although the cellular complexity is not the same, this represents a likeness to the presence of α-syn deposits in the substantia nigra in human PD (Baba et al., 1998). Taken together the α-syn over-expressing strain of *C. elegans* used in this study demonstrate several characteristics which are similar to the human condition, potentially making it a useful model in an experimental setting.

6.2 PD pathology in *C. elegans*

The first goal of the in vivo part of this study was to induce α-syn PD pathology in *C. elegans* using different methods of administration and exposure to α-syn. 1) Alpha-syn production was overexpressed in a *C. elegans* strain, 2) *C. elegans* were also fed a strain of *E. coli* that overexpresses α-syn and 3) *C. elegans* were exposed to aggregated α-syn (oral administration). The effects of each method would be compared using movement speed, bend speed and worm size.

6.2.1 Overexpression of α-syn in *C. elegans* as a model of PD pathology

C. elegans overexpressing α-syn (DDP1 strain) were analysed in this study because they showed reduced pharyngeal pumping and shorter life spans in a previous study (Bodhicharla et al., 2012). This is comparable to dysphagia, the cardinal motor deficit of bradykinesia and the reduced lifespan seen in humans with PD (Mu et al., 2012). DDP1 overexpresses α-syn in muscle cells (unc-54 gene) with a fluorescent marker. DDP2 only expresses the fluorescent markers via the promoter fragment of the unc-54 gene. DDP1 worms were expected to be slower than their control counterpart DDP2 because of the other effects of α-syn observed on lifespan and pharyngeal pumping.

When treated with buffer and fed normal *E. coli*, OP50-1, the maximum and average speeds of DDP1 were less than DDP2. The difference between DDP2 and DDP1 was more than 1.5-fold in maximum speed and bend speed ($p<0.05$). There was no difference in body bends per second between DDP1 and DDP2 ($p=0.26$). Overexpression of α-syn was expected to have a direct effect on mobility with no evidence of reduced movement speed in prior research. Based on the behavioural results described here, the over expression of α-syn in muscle cells of the DDP1 strain of *C. elegans* does result in a significant reduction in average speed.

Comparing the results of this study to previous findings, a study examining DDP1 reported the effects of α-syn overexpression on egg to adult development time, brood size, life span, pharyngeal pumping and locomotion (bend) rate (Bodhicharla et al., 2012). Egg to adult development and brood size were the same between transgenic strains and N2. *C. elegans* overexpressing α-syn also had shorter life spans, reduced by about 5 days compared to the nearly

20-day life span of wild type *C. elegans*. Pharyngeal pumping and locomotion (bend) rate were slower in α-syn overexpressing *C. elegans* compared to wild type N2 (Bodhicharla et al., 2012). Compared to the findings in this study examining DDP1, the bend rate of DDP1 was also reduced compared to DDP2. There was also no difference in worm/brood size between the strains in both studies.

The overexpression of α-syn in *C. elegans* muscle cells is not commonly found in the literature. The findings of this study, however, can still be compared to other studies also looking at *C. elegans* affected by the expression of A53T mutation of α-syn, who found a reduction in bend speed relative to wild type *C. elegans* (Lakso et al., 2004). Another study also looking at A53T α-syn expression showed bend speeds reduced by up to 35% compared to wild type N2 *C. elegans* (Kuwahara et al., 2006); while, this study showed a 50% reduction. Although the expression of α-syn in this study was different to the studies mentioned now, the effect on bend rate is consistent with the literature.

A reduced bend rate in DDP1 compared to DDP2 is very likely an indication of α-syn oligomer cytotoxicity because the study mentioned above, Lakso et al. (2004), showed neuronal loss in worms affected by A53T α-syn expression. Kuwahara et al. (2006) also found worms affected by the A53T mutation to have fewer dopaminergic neurons. The reduced bend rate found in the DDP1 observed in this study is likely caused by α-syn pathology.

When considering movement speed that is the velocity of worms moving across the agar, greater movement speed does not always indicate healthier behaviour. The addition of a food source for example, according to one study can result in decreased velocity in order to increase exposure to food (Kuwahara et al., 2006), and so is not necessarily a measure of loss of function. The introduction of food in another study was shown to have no effect on worm speed (Angstman et al., 2016). To prevent worm speeds from being affected by food exposure in the present study, bacteria were added 2 days prior to recording to both DDP1 and DDP2. This does not fully discount

the possibility that the worms slowed down because they were passing through bacteria, but both strains were treated the same way and both strains were expected to slow for feeding, meaning changes in speed are likely due to α-syn expression.

While there is currently limited research on the effects of overexpression of α-syn on *C. elegans* movement speeds, the findings in this study can still be compared to those looking at *C. elegans* movement speed affected by amyloid β expression, the protein associated with Alzheimer's (Dosanjh et al., 2010). Dosanjh et al. (2010) categorised movement speed into two categories: 1) enhanced slowing response (ESR), a conserved response to starvation and 2) basal slowing response (BSR), an adaptive mechanism that increases the amount of time animals spend in a nutrient rich environment. The study found a reduced ESR in amyloid β expressing worms, although this signifies an increase in movement speed, what this result shows is a change in worm speeds under the effect of a cytotoxic protein. The significant reduction in movement speed in DDP1 compared to DDP2 was probably caused by α-syn cytotoxicity.

This study can confirm that looking at movement/bend speed of DDP1 to study α-syn pathology in *C. elegans* is possible and may even be a preferable method over the use of A53T mutation, which better models genetic PD because the A53T mutation is found in familial cases of human PD (Goedert et al., 2017), whereas DDP1 might better simulate sporadic PD. Bodhicharla et al. (2012) showed an increase in α-syn aggregation with age.

One recommendation for future analysis of *C. elegans* in this study is the recording of multiple time points to observe any attenuated changes in movement behaviour. This study did not look at the progression of movement changes over a period. *C. elegans* were only observed at a single time point. Multiple time recordings would provide further evidence of any effects of α-syn on *C. elegans*. Finally, the results from this investigation support the use of DDP1 *C. elegans* strain to model PD pathology exhibited by changes in movement speeds (Angstman et al., 2016).

6.2.2 Overexpression of α-syn in *C. elegans* food as a model of PD pathology

The next method of α-syn exposure examined was feeding the N2 wildtype strain of *C. elegans* with *E. coli* that overexpresses α-syn (E-syn; the same strain used to produce α-syn). This method was based on evidence that different *E. coli* can influence *C. elegans* physiology. One study showed the transfer of silver nanoparticles from *E. coli* to the gut lumen, subcutaneous tissue and gonad of *C. elegans* (Luo et al., 2016). The silver nanoparticles reduced reproduction and life span in affected worms. The results of E-syn ingestion are presented next.

The N2 worms fed E-syn demonstrated a significant increase in maximum speed, and average speed and though there was a trend towards an increase in the number of body bends per second, this did not reach significance (See Figure 5.2). The change in maximum and average speed was between 1.75 and 2-fold. There was also no difference in length of worms as a result of each treatment.

There are no previous studies looking at the effects of *C. elegans*' ingestion of *E. coli* overexpressing α-syn, the results in this study were instead compared to studies looking at the effects of movement behaviours of *C. elegans* being fed *E. coli* stimulated to express OxyS, a noncoding RNA that protects the bacterial cells from oxidative damage. A study found that the OxyS changed foraging behaviour in N2 wild type worms causing them to move away from OxyS expressing bacteria (Liu et al., 2012). In this study, the wild type worms exposed to E-syn could also be moving away from the E-syn and foraging for non-α-syn-expressing *E. coli*, which may explain the increased movement speed.

The lack of any change in body bends/second may be because the form of the protein in E-syn is mostly monomeric as seen in the early stages of Figure 3.1. The protein produced by the *E. coli* is still monomeric, which has not been shown to be neuro toxic. It has been shown that oligomeric species are the pathological forms of α-syn, demonstrating both increased levels of cytotoxicity and increasing levels of aggregation (Danzer et al., 2007). The insignificant difference

between bend rates might also be because the amount of α-syn in the E-syn present on each plate was too low to have an effect.

If the content of α-syn was too low to have any significant effect on younger worms, another time point is recommended for future studies. As Bodhicharla et al. (2012) showed an increase in effects on pharyngeal pumping and bend rate as worms aged, an indication of progressive changes that could be detected in a second recording.

The increased movement speed was unexpected, but is likely because the N2 worms eating E-syn had more food available. The OP50 strain of *E. coli* is specifically used due to its limited growth on NGM plates because it is unable to synthesize uracil (Hahm et al., 2011; Porta-de-la-Riva et al., 2012). E-syn is only modified to overexpress α-syn and not to limit growth on NGM, meaning the rate of bacterial growth for the E-syn group would be larger and therefore results in more food availability on the plate after 48 hours of incubation. The increased movement speed was not caused by an increase in worm size because there was no difference between N2 with normal food and E-syn. The N2 worms with E-syn might be faster because of the prior exposure to increased food content (Angstman et al., 2016).

One way to avoid increased E-syn in future experiments would be to perhaps, use an OP50 strain modified to overexpress α-syn so that the growth rate of the food given in both experiments is equivalent. Another way to ensure worms exposed to E-syn do not have more food in the period of observation is to kill the bacteria before storage. In this study, the bacteria were stored live at 4°C after the final concentration was prepared. In the future, all *E. coli* used to feed the *C. elegans* could be heated to 70°C for 2 minutes to kill bacteria before feeding thus eliminating the growth rate of the food source as being a variable in these experiments (Stringer et al., 2000). Heating may have a two-fold effect useful for this study, the first would be to kill the bacteria and the second to possibly cause the α-syn to aggregate (Ferreon and Deniz, 2007), which might increase the presence of oligomers.

Another possible explanation for the reduced bend rate and increased movement speed in using E-syn was that the strain of *E. coli* used may be more nutritious than OP50. Xu et al., (2017) showed that feeding *E. coli* expressing a polypeptide found in scorpion venom increased lifespan and reproduction. This may be the case with the E-syn used in this study, where E-syn expressing monomeric α-syn, a protein that does not exhibit α-syn toxicity, but rather may exhibit increased levels of nutrition. The results of this study, nonetheless, show that feeding *C. elegans* E-syn may have affected movement speeds, but the changes in movement speed may not be due to α-syn toxicity because the cause of the effect is not entirely clear with less literature on behavioural effects of *E. coli* expressing α-syn.

Analysing *C. elegans* fed E-syn using an immunohistochemistry assay in addition to behavioural analysis would add evidence to a possible effect of α-syn (Lakso et al., 2004; Kuwahara et al., 2006). Methods on antibody staining in *C. elegans* can be found in the literature using "freeze cracking" (Crittenden and Kimble, 1999; Duerr, 2013). This method is used because of the inability to take slices as is usually done with larger tissue samples. Freeze cracking is the freezing of *C. elegans* between to slides and then splitting the frozen slides, resulting in a percentage of worms being split onto each slide allowing staining to reach the interior parts of the worm (Crittenden and Kimble, 1999). Several different monoclonal antibodies can be used to detect human α-syn. Some of which include mouse monoclonal antibodies LB509, SYN211, or a rabbit poly- clonal antibody number 259 (Kuwahara et al., 2006). Any increase in fluorescence in stained worms affected by E-syn would substantiate any behavioural changes observed in the in vivo assays performed in this study.

6.2.3 Effects of exogenous exposure to aggregated α-syn on *C. elegans*

The final means of treating *C. elegans* with α-syn was the external administration of pre-aggregated α-syn. This method relies on the way that *C. elegans* feed. *C. elegans* feed via rhythmic contractions and relaxations of their pharynx (Trojanowski et al., 2016). By mixing aggregated α-syn with OP50-1, the worms were expected to incidentally ingest the aggregated form of the protein during normal

foraging behaviour and should not be able to filter out the aggregates (Fang-Yen et al., 2009). The expected result was that there would be a difference between vehicle treated and the α-syn treated animals. Since α-syn and in particular aggregated α-syn has been associated with increased levels of cell death and increased levels of mitochondrial dysfunction, it was expected that there would be reduced mobility in worms exposed to aggregated α-syn (Li et al., 2007; Cole et al., 2008).

The worms exposed to aggregated α-syn, however, showed greater movement and bend speeds than worms exposed to buffer and no difference in worm size between treatments ($p<0.05$). This result was similar to the worms treated with *E. coli* which expressed monomeric α-syn. In both cases the oral intake of either monomeric α-syn or aggregated α-syn both resulted in an increase in mobility in this species. The reason for this is unknown but will be examined here.

Exposing *C. elegans* to exogenous aggregated α-syn is a novel part of this investigation. *C. elegans* overexpressing α-syn are usually used to model PD because of evidence of neuronal loss in transgenic *C. elegans* (van Ham et al., 2008). Hence, the results cannot be directly compared to the literature, but the results can be compared to a study observing delivering proteins using lipid vesicles (Perni et al., 2017). The study incubated an antibody that inhibits α-syn aggregation with lipid vesicles to encapsulate the antibodies and then incubated transgenic *C. elegans* expressing α-syn with encapsulated proteins. Perni et al. (2017) first showed that the antibody was indeed taken into the worm bodies and then analysed using different fitness parameters such as body bends/minute, speed, bend amplitude, displacement per bend, and moving fraction. The study showed an increase in movement parameters when treated with antibodies.

In this study, α-syn may be affecting the *C. elegans* because no other factors were different between the two subjects. A recommendation for future experiments is to incubate α-syn aggregates in lipids to encapsulate the α-syn and make them more readily absorbable by the *C. elegans* (Perni et al., 2017) along with immunostaining and confocal examination to carefully monitor the uptake of α-syn. A fusion protein of α-syn and Venus, a fluorescent protein that can be

used to tag proteins, could be aggregated and administered to the *C. elegans* (Levin et al., 2016). Venus is a version of yellow fluorescent protein (YFP) and more acid tolerant than YFP (Emission at 530 nm with excitation at 515 nm) (Nagai et al., 1989). Fluorescence in *C. elegans* would indicate the presence of aggregated α-syn, but not monomers (Levin et al., 2016), however, this could be advantageous when observing the cytotoxic effects of α-syn aggregates.

6.3 The combined effects of α-syn exposure using multiple methods

In this experiment, exogenous exposure to aggregated α-syn was combined with one of the first two methods of exposure to α-syn (1) DDP1 and 2) N2 worms fed E-syn) to see if any effects would be amplified. Aggregated α-syn was expected to seed further aggregation of α-syn as shown in previous research and to increase any cytotoxic effects (Danzer et al., 2007; Kim et al., 2007; Ono et al., 2012). The results of the combined treatments were analysed next.

6.3.1 The effects of overexpression of α-syn and exogenous α-syn exposure

DDP1 exposed to aggregated α-syn showed greater maximum speed and body bends/second than DDP2 exposed to buffer ($p<0.05$), but DDP1 worms were 70% longer than DDP2 ($p<0.05$). A difference in worm size is usually indicative of an unsuccessful synchronisation (Bodhicharla et al., 2012; Chew et al., 2013). Since all DDP1 worms were synchronised together and no other treatments showed a significant difference in worm lengths, the cause of the difference in length may be another factor (Nagashima et al., 2017).

Nagashima et al. (2016) showed dopamine negatively regulates *C. elegans* body size by binding to a dopamine receptor that is similar between species. The study confirmed that the change in body size was not due to faster development and the *C. elegans* with increased dopamine levels were in fact smaller than those with reduced dopamine levels by (Nagashima et al., 2016). The findings of Nagashima et al. (2016) provide a few clues and possible recommendations for future experimental attempts.

Firstly, an increase in body size in DDP1 in this study could mean that there may be a reduction in dopamine levels. Secondly, unlike the Nagashima et al. (2016) study, this study did not

monitor other developmental stages of the worms to check if some worms developed faster after synchronisation. It is unclear whether the DDP1 exposed to hops developed more quickly or were in fact larger than the DDP2 in vehicle control. In future studies, a second or third recording after the initial recording as suggested earlier would not only provide evidence of increased changes in movement behaviour, but also determine whether the worms are still growing. In this study, it is possible that the aggregated α-syn seeded aggregation in the DDP1 already overexpressing α-syn (Danzer et al., 2007), which may have reduced dopamine levels via cytotoxicity in neurons.

Even though there was an increase in maximum movement and bend speed of DDP1 with aggregated α-syn compared to DDP2 in vehicle, there was no significant difference between average speeds and the increase in size was not proportional to the increase in maximum speed and bend speed. This result might be caused by the increase in worm length, but is difficult to comment on these findings without further confocal examination of these worms.

6.3.2 The effects of α -syn in food and environment

When the N2 were exposed to both E-syn and α-syn, there was no significant difference when compared to the N2 exposed to only α-syn ($p>0.05$), in other words the combined exposure of α-syn from the food and the aggregated α-syn had no additive effect. According to prior analysis, both monomeric α-syn (from the E-syn) and aggregated α-syn applied exogenously enhanced worm movement speed therefore an additive effect was expected when exposed to both E-syn and α-syn. However, this did not occur, suggesting that the observed increase in locomotion occurred by the same mechanism regardless of the form of α-syn delivered. This finding may not be consistent with the literature.

Chen et al. (2016) conducted an experiment like the experiment here in section 6.3.2. Their study examined the effects of an *E. coli* strain that produces the extracellular amyloid protein curli on an α-syn expressing *C. elegans* strain (Chen et al., 2016). The study found an increase in α-syn aggregates in the head region and as the worms aged, an increase in α-syn deposits in the tail. The study also saw a 15-20% reduction in thrashing (similar to body bends/second). This experiment

looking at the effects of E-syn and α-syn exposure did not find any changes in body bends/second, but the results from the experiments looking at the effects of E-syn also pointed to the possibility of E-syn not being toxic to *C. elegans*.

6.4 Treating PD pathology in *C. elegans*

Hops was used to treat *C. elegans* with one of the 3 methods of α-syn exposure/overexpression. The results of each are discussed below. This is followed by a discussion on the effects of hops on *C. elegans* without exposure/overexpression of α-syn to see the general effect of hops on worms.

6.4.1 Hops treating DDP1

According to the inhibitory effect of hops on α-syn aggregation observed in the ThT assays, hops could potentially affect any α-syn cytotoxicity found in one of the exposure methods used. DDP1 originally had reduced maximum speeds and bend speeds when compared to DDP2. When DDP1 *C. elegans* were exposed to hops, the worms showed a significant increase in mobility. DDP1 exposed to hops were over two times faster than just DDP1 ($p<0.05$). However, the DDP1 strain exposed to hops were also more than double the length of the untreated DDP1 strain which may have caused the observed increase in speed equivalent to the increase in size. It is possible that the hops may have increased the size of the worms but further investigation is needed to confirm this.

Treating *C. elegans* with hops is another novel part of this study, the findings of treating DDP1 with hops were compared to a study looking at the effects of betulin (an active compound found in the bark of birch trees) in transgenic *C. elegans* expressing α-syn. The study tested different concentrations of betulin to determine the optimal concentration to use to study the any neuroprotective effects of betulin (Tsai et al., 2017). The study found that increased concentrations of betulin caused a reduction in body sizes. Tsai et al. (2017) also went on to find increases in life span and food sensing behaviour (the reduction in bend speed near a food source) in worms when treated with betulin. Considering the effect of betulin on worm size, the concentration of hops used may have increased worm size. The increase in size may also be the cause of the proportional increase in movement/bend speed.

Due to the limited literature on the treatment of *C. elegans* affected by α-syn with hops, which contains polyphenols, the findings of this study were also compared to studies treating *C. elegans* affected by amyloid beta with polyphenols such as quercetin (Jagota and Rajadas, 2012; Regitz et al., 2014). One study found that the quercetin reduced paralysis in worms affected by amyloid beta (Regitz et al., 2014). Another study found that ferulic acid showed greater protection against amyloid toxicity than polyphenols: morin, quercetin, and gossypol (Jagota and Rajadas, 2012). These findings show the potential effect of different polyphenols on the physical phenotype of movement and the level of efficacy of each.

Since the hops treated DDP1 were larger than the untreated DDP1, the changes in movement/bend speed are difficult to assess. Nonetheless, this studied showed that hops did affect worm growth and increased the reduced speeds observed in untreated DDP1. The speed effects of hops on DDP1 most likely involved α-syn because hops treatment of DDP2 in section 6.4.4 resulted in DDP2 increased body growth, but no significant change in speeds. Recording worms at a second time point to measure any changes in worm growth of the untreated DDP1 would help determine if the hops affected development rate or final body size. Observing all the *C. elegans* at another time point may also reveal in progressive decline in mobility due to longer exposure to α-syn, perhaps recording again 1-2 weeks after the first recording. The effects on aged worm populations is another advantage of recording at another time point because van Ham et al., (2008) showed aged *C. elegans* contained aggregated α-syn. This study did not attempt secondary recordings due to time constraints. In future experimentation, testing saturated concentrations of hops to evaluate optimal concentrations to use on worms is also recommended.

6.4.2 Hops treating E-syn fed *C. elegans*

Feeding N2 with E-syn resulted in increased maximum and average speeds. E-syn fed *C. elegans* with hops did not result in any significant change between speeds or worm length. Considering the possibility that E-syn did not negatively influence the movement behaviour of N2 wildtype worms

with no significant difference in bend speeds, it is possible that there was no α-syn toxicity for hops to inhibit.

Even though treatments are found to increase life span or enhance worm movement (Cañuelo et al., 2012), some studies seem to suggest a targeted mechanism of action, where the treatment may be inhibiting aggregation and toxic species (Jagota and Rajadas, 2012). In this experiment, the hops may not have an effect on exposure to E-syn because of the lack of toxic protein aggregates. The experiments observing the effects of hops on *C. elegans* untreated with α-syn in section 6.4.4 present more evidence to this possibility.

6.4.3 Hops treating aggregated α-syn exposure

N2 exposed to aggregated α-syn treated with hops, on the other hand, showed decreased movement speeds compared to N2 with α-syn. Hops binding to α-syn and preventing any enhancing effect on worm movement speed is a possible explanation, but further evidence is required. There was no significant difference in length between N2 exposed to aggregated α-syn.

The results of this experiment seem to indicate that hops is reversing the increased movement and bend speeds caused by the exogenous exposure to aggregated α-syn. Although the α-syn caused increased speeds and hops reduced these speeds, the increased movement speeds maybe a phenotype indicative of an effect of α-syn. This is similar to how worms are unable to slow down to forage for food when exposed to 6-OHDA and then when treated with betulin, were able to slow their bending frequency near food (Tsai et al., 2017). The experiment discussed next helped determine if hops was generally enhancing worms or if hops was targeting α-syn.

6.4.4 Effect of hops on *C. elegans* without α-syn exposure

Hops exposure was compared in DDP2 and wild type N2. When DDP2 were exposed to hops, there was no significant difference in movement speeds. The same was true of the N2 exposed to hops and fed OP50-1 meaning that hops did not affect movement speeds. There was no change in N2 body size when treated with hops, but there was a significant increase in body size of DDP2 treated with hops. Since the DDP2 showed an increase in body size, but no difference in speeds, the effect

of hops on DDP1 speeds was more likely due to an interaction of hops with the overexpression of α-syn.

Summarising the effects of hops, this study found that hops reversed any possible effects caused by α-syn exposure in DDP1 and N2 exposed to aggregated α-syn, and did not affect DDP2 or N2 without α-syn exposure. This study presents evidence that hops may be affecting α-syn toxicity produced in *C. elegans*.

There is limited research on the effect of hops on *C. elegans*, but considering the safety of hops in humans, hops is safe for consumption (Sasaoka et al., 2014). The potential effects of hops on α-syn exposure should be validated using immunostaining and confocal microscopy before moving onto clinical trials as this study provides evidence of the potential effects of hops on worm behaviour. The final experiment discussed is a high throughput life span assay.

6.5 High throughput life span assay

A high throughput life span assay was attempted using previous methodologies, but this study found data collection to be unreliable. Using a 96 well plate and magnification strong enough to count living worms is not feasible in large numbers when depending on human eyes; tracking moving worms leads to double counting and miscounting. Worms did not always move even after a stimulus of light (from the microscope) and gentle tapping on the plate. These worms were counted as dead because animals that did not move and were determined dead in the preceding count might move later on. Solis and Petrascheck (2011) suggested the use of strong light, specifically blue light to induce movement and to shake the 96-well plate on a microtiter plate shaker for 2 min before counting. A recurring issue was that worms sometimes swarmed together, making the life and death count less reliable because the dead worms appeared to move when adjacent living worms moved.

This life span assay was repeated 4 times and the same issue of observing worm count came up every single time. The size of the well and the field of view of the microscope are very important

to the success of counting living worms. Taking small video snippets of the field of view and using video analysis is the ideal method of counting living worms whilst minimising potential human error.

Analysing worm movement behaviour was found to be more time efficient compared to measuring life span and may detect more minute changes in treatment effects (Angstman et al., 2016).

6.6 Recommendations for developing a PD model in *C. elegans*

Some recommendations for future optimisations were already mentioned such as secondary recordings, confocal analysis of worms and testing saturated concentrations of treatments before analysing the effects on α-syn exposure. More recommendations are discussed below.

Another limitation considered was the use of 5.5 cm plates. This plate was larger than the field of view that the microscope used. Multiple fields of view were filmed on a single plate and while the fields were distant from each other and did not overlap, it remains possible that fast worms could have moved to other fields of view and therefore been double counted. The use of a different microscope allowing a larger field of view, or only measuring one field of view per plate would prevent this from happening in future experiments.

Treated worms could be observed in 12-well plates instead of 5.5 cm plates. This would eliminate the need to record worm plates in quadrants and reduce the likelihood of multiple recordings of the same worms. This would also reduce the amount of space necessary to store numerous treatments and more treatments could be tested in less time.

One final optimisation would be to double blind researchers to the treatments used from recording to analysis. This would reduce any bias to any treatments that pass each stage of testing, making them likely to be candidates for PD therapy.

6.7 Conclusions

This study considered the issue of current PD treatments that current treatments do not target disease progression. The aims of this study were to develop an in vitro and an in vivo assay targeting

the earliest pathology known in PD. The target was the aggregation of α-syn. In the in vitro assay, ThT, a dye widely used in research to measure aggregation rate, was used to measure α-syn aggregation and then to test a potential PD treatment, hops. In the in vivo assay, transgenic and wild type *C. elegans* were exposed to α-syn or hops and movement/bend speeds were analysed.

The aim to develop an in vitro assay that can measure the effects α-syn aggregation and to test a treatment was considered successful because the study found the use of ThT to be consistent with the literature where the fluorescence curves were similar to prior research. The fluorescence curves using 1 mg/mL of α-syn showed similar maximal fluorescence, peak rate and lag phases when compared to similar methodologies. Using the ThT assay to measure the effects of a particular treatment on α-syn aggregation showed a dose relationship between hops treatment and maximal fluorescence, peak rate and the lag phase. Hops did not show any change in higher molecular weight species of α-syn using gel analysis. The effect of hops on the aggregation of α-syn suggested that hops may potentially affect aggregation in vivo. The use of electron microscopy to analyse the development of aggregation when treated with hops is recommended to further validate these findings, but these findings were also confirmed using the in vivo assay.

C. elegans were used in this study because of their low maintenance, cost and high reproduction rate. The study found significant behavioural changes in line with prior research in transgenic *C. elegans* expressing α-syn. DDP1, the α-syn expressing strain, had reduced maximum movement speeds and body bends/second. The exposure of E-syn and aggregated α-syn, however, had an inverse effect, increasing N2 wildtype worm movement and bend speeds. Nonetheless, the α-syn exposures affected the *C. elegans* behaviour and as observed in the literature, increased speeds can also indicate poor foraging behaviour. These findings demonstrated the practicality of *C. elegans* as a PD model with α-syn pathology, which was the other aim of this investigation.

When treating *C. elegans* exposed to α-syn with hops, hops reversed or subdued any behavioural changes possibly caused by α-syn. In the case of DDP1, the worms treated with hops

were twice the size of untreated DDP1 and the movement speeds about twice as fast. This study recommends secondary recordings to monitor development, which may reveal the cause of any changes in body size, be it increased development rate or final growth size. No changes were observed in the hops treated N2 fed with E-syn suggesting that E-syn may not have an impact on *C. elegans* via α-syn toxicity. Finally, hops reversed the increased speeds in N2 exposed to aggregated α-syn, signifying a possible reaction between α-syn and hops. The final aim of this study was to explore the effects of hops in an in vitro and in vivo model, both of which revealed a possible relationship between α-syn and hops, however, confocal study of the treated worms is recommended to supplement these findings.

In the screening process, multi-validation is required to provide evidence of treatment effects on a disease target. This study showed that the use of ThT assays and *C. elegans* behavioural assays are useful in detecting potential PD treatments. By adding a few additional steps such as multiple recordings over time and using electron microscopy/immunostaining, any changes detected in the assays may be used as evidence for larger animal studies or clinical trials.

7 References

Ahmad, B., and Lapidus, L.J. (2012). Curcumin prevents aggregation in α-synuclein by increasing reconfiguration rate. J. Biol. Chem. 287: 9193–9.

Alavez, S., Vantipalli, M.C., Zucker, D.J.S., Klang, I.M., and Lithgow, G.J. (2011). Amyloid-binding compounds maintain protein homeostasis during ageing and extend lifespan. Nature 472: 226–9.

Anders, H.J.J., and Vielhauer, V. (2007). Identifying and validating novel targets with in vivo disease models: Guidelines for study design. Drug Discov. Today 12: 446–451.

Anderson, V.L., and Webb, W.W. (2011). Transmission electron microscopy characterization of fluorescently labelled amyloid beta 1-40 and alpha-synuclein aggregates. BMC Biotechnol 11: 125.

Angstman, N.B., Frank, H.-G., and Schmitz, C. (2016). Advanced Behavioral Analyses Show that the Presence of Food Causes Subtle Changes in *C. elegans* Movement. Front. Behav. Neurosci. 10: 1–10.

Apfeld, J., and Fontana, W. (2017). Age-Dependence and Aging-Dependence: Neuronal Loss and Lifespan in a *C. elegans* Model of Parkinson's Disease. Biology (Basel). 7: 1.

Armstrong, S.E., Mariano, J.A., and Lundin, D.J. (2010). The scope of mycoplasma contamination within the biopharmaceutical industry. Biologicals 38: 211–213.

Bereznicki, L. (2010). Dopamine agonists in Parkinson's disease. Aust. Pharm. 29: 1056–1062.

Beyer, K., Domingo-Sàbat, M., and Ariza, A. (2009). Molecular pathology of lewy body diseases. Int. J. Mol. Sci. 10: 724–745.

Bhilocha, S., Ripal, A., Pandya, M., Yuan, H., Tank, M., LoBello, J., et al. (2011). Agarose and polyacrylamide gel electrophoresis methods for molecular mass analysis of 5- to 500-kDa hyaluronan. Anal. Biochem. 417: 41–49.

Blesa, J., and Przedborski, S. (2014). Parkinson's disease: animal models and dopaminergic cell vulnerability. Front. Neuroanat. 8: 1–12.

Bodhicharla, R., Nagarajan, A., Winter, J., Adenle, A., Nazir, A., Brady, D., et al. (2012). Effects of α-synuclein overexpression in transgenic *Caenorhabditis elegans* strains. CNS Neurol. Disord. Drug Targets 11: 965–75.

Breydo, L., Wu, J.W., and Uversky, V.N. (2012). α-Synuclein misfolding and Parkinson's disease. Biochim. Biophys. Acta (BBA)-Molecular Basis Dis. 1822: 261–285.

Brundin, P., and Melki, R. (2017). Prying into the Prion Hypothesis for Parkinson's Disease. J. Neurosci. 37: 9808–9818.

Cannon, J.R., Tapias, V., Na, H.M., Honick, A.S., Drolet, R.E., and Greenamyre, J.T. (2009). A highly reproducible rotenone model of Parkinson's disease. Neurobiol. Dis. 34: 279–290.

Cañuelo, A., Gilbert-López, B., Pacheco-Liñán, P., Martínez-Lara, E., Siles, E., and Miranda-Vizuete, A. (2012). Tyrosol, a main phenol present in extra virgin olive oil, increases lifespan and stress resistance in *Caenorhabditis elegans*. Mech. Ageing Dev. 133: 563–574.

Chen, S.G., Stribinskis, V., Rane, M.J., Demuth, D.R., Gozal, E., Roberts, A.M., et al. (2016). Exposure to the Functional Bacterial Amyloid Protein Curli Enhances Alpha-Synuclein Aggregation in Aged Fischer 344 Rats and *Caenorhabditis elegans*. Sci. Rep. 6: 1–11.

Chen, S.W., Drakulic, S., Deas, E., Ouberai, M., Aprile, F.A., Arranz, R., et al. (2015). Structural characterization of toxic oligomers that are kinetically trapped during α-synuclein fibril formation. Proc. Natl. Acad. Sci. 112: E1994–E2003.

Cheng, F., Vivacqua, G., and Yu, S. (2011). The role of α-synuclein in neurotransmission and synaptic plasticity. J. Chem. Neuroanat. 42: 242–8.

Chew, Y.L., Fan, X., Götz, J., and Nicholas, H.R. (2013). PTL-1 regulates neuronal integrity and lifespan in *C. elegans*. J. Cell Sci. 126: 2079–91.

Coelho-Cerqueira, E., Pinheiro, A.S., and Follmer, C. (2014). Pitfalls associated with the use of Thioflavin-T to monitor anti-fibrillogenic activity. Bioorganic Med. Chem. Lett. 24: 3194–3198.

Cole, N.B., DiEuliis, D., Leo, P., Mitchell, D.C., and Nussbaum, R.L. (2008). Mitochondrial translocation of α-synuclein is promoted by intracellular acidification. Exp. Cell Res. 314: 2076–2089.

Cowman, M.K., Chen, C.C., Pandya, M., Yuan, H., Ramkishun, D., LoBello, J., et al. (2011). Improved agarose gel electrophoresis method and molecular mass calculation for high molecular mass hyaluronan. Anal. Biochem. 417: 50–6.

Crabtree, D.M., and Zhang, J. (2012). Genetically engineered mouse models of Parkinson's disease. Brain Res. Bull. 88: 13–32.

Cremades, N., Chen, S.W., and Dobson, C.M. (2017). Structural Characteristics of α-Synuclein Oligomers (Elsevier Inc.).

Crittenden, S.L., and Kimble, J. (1999). Confocal methods for *Caenorhabditis elegans*. Methods Mol. Biol. 122: 141–51.

D'Amelio, M., Cavallucci, V., and Cecconi, F. (2010). Neuronal caspase-3 signaling: Not only cell

death. Cell Death Differ. 17: 1104–1114.

Danzer, K.M., Haasen, D., Karow, A.R., Moussaud, S., Habeck, M., Giese, A., et al. (2007). Different species of α-synuclein oligomers induce calcium influx and seeding. J Neurosci 27: 9220–9232.

Danzer, K.M., Kranich, L.R., Ruf, W.P., Cagsal-Getkin, O., Winslow, A.R., Zhu, L., et al. (2012). Exosomal cell-to-cell transmission of alpha synuclein oligomers. Mol. Neurodegener. 7: 42.

Danzer, K.M., Krebs, S.K., Wolff, M., Birk, G., and Hengerer, B. (2009). Seeding induced by α-synuclein oligomers provides evidence for spreading of α-synuclein pathology. J Neurochem 111: 192–203.

Daturpalli, S., Waudby, C.A., Meehan, S., and Jackson, S.E. (2013). Hsp90 inhibits α-synuclein aggregation by interacting with soluble oligomers. J. Mol. Biol. 425: 4614–4628.

Daviaud, N., Garbayo, E., Lautram, N., Franconi, F., Lemaire, L., Perez-Pinzon, M., et al. (2014). Modeling nigrostriatal degeneration in organotypic cultures, a new ex vivo model of Parkinson's disease. Neuroscience 256: 10–22.

Dehay, B., Bourdenx, M., Gorry, P., Przedborski, S., Vila, M., Hunot, S., et al. (2015). Targeting α-synuclein for treatment of Parkinson's disease: Mechanistic and therapeutic considerations. Lancet Neurol. 14: 855–866.

Dexter, P.M., Caldwell, K.A., and Caldwell, G.A. (2012). A Predictable Worm: Application of *Caenorhabditis elegans* for Mechanistic Investigation of Movement Disorders. Neurotherapeutics 9: 393–404.

Dosanjh, L.E., Brown, M.K., Rao, G., Link, C.D., and Luo, Y. (2010). Behavioral phenotyping of a transgenic *Caenorhabditis elegans* expressing neuronal amyloid-β. J. Alzheimer's Dis. 19: 681–690.

Duerr, J.S. (2013). Antibody staining in *C. elegans* using 'freeze-cracking'. J. Vis. Exp. 1–9.

Duty, S., and Jenner, P. (2011). Animal models of Parkinson's disease: a source of novel treatments and clues to the cause of the disease. Br. J. Pharmacol. 164: 1357–1391.

Fang-Yen, C., Avery, L., and Samuel, A.D.T. (2009). Two size-selective mechanisms specifically trap bacteria-sized food particles in *Caenorhabditis elegans*. Proc. Natl. Acad. Sci. 106: 20093–20096.

Feng, D.Q.Q., Liu, G., Zheng, W., Liu, J., Chen, T., and Li, D. (2011). A highly selective and sensitive on-off sensor for silver ions and cysteine by light scattering technique of DNA-functionalized gold nanoparticles. Chem. Commun. 47: 8557–8559.

Ferreon, A.C.M., and Deniz, A.A. (2007). α-Synuclein Multistate Folding Thermodynamics: Implications for Protein Misfolding and Aggregation. Biochemistry 46: 4499–4509.

Freitas, M.E., Ruiz-Lopez, M., and Fox, S.H. (2016). Novel Levodopa Formulations for Parkinson's Disease. CNS Drugs 30: 1079–1095.

Freundt, E.C., Maynard, N., Clancy, E.K., Roy, S., Bousset, L., Sourigues, Y., et al. (2012). Neuron-to-neuron transmission of α-synuclein fibrils through axonal transport. Ann. Neurol. 72: 517–524.

Gelb, D., Oliver, E., and Gilman, S. (2008). Diagnostic criteria for Parkinson disease. J Neurol Neurosurg Psychiatry 79: 368–376.

George, S., Buuse, M. van den, San Mok, S., Masters, C.L., Li, Q.X., and Culvenor, J.G. (2008). α-Synuclein transgenic mice exhibit reduced anxiety-like behaviour. Exp. Neurol. 210: 788–792.

Ghosh, D., Mehra, S., Sahay, S., Singh, P.K., and Maji, S.K. (2017). A-Synuclein Aggregation and Its Modulation. Int. J. Biol. Macromol. 100: 37–54.

Giasson, M.A., Averill, C., and Finzi, A.C. (2014). Correction factors for dissolved organic carbon extracted from soil, measured using the Mn(III)-pyrophosphate colorimetric method adapted for a microplate reader. Soil Biol. Biochem. 78: 284–287.

Giehm, L., Lorenzen, N., and Otzen, D.E. (2011). Assays for α-synuclein aggregation. Methods 53: 295–305.

Giehm, L., Oliveira, C.L., Christiansen, G., Pedersen, J.S., and Otzen, D.E. (2010). SDS-induced fibrillation of α-synuclein: an alternative fibrillation pathway. J Mol Biol 401: 115–133.

Goedert, M., Jakes, R., and Spillantini, M.G. (2017). The Synucleinopathies: Twenty Years on. J. Parkinsons. Dis. 7: S53–S71.

Goedert, M., Spillantini, M.G., Tredici, K. Del, and Braak, H. (2013). 100 years of Lewy pathology. Nat. Rev. Neurol. 9: 13–24.

Haddad, F., Sawalha, M., Khawaja, Y., Najjar, A., and Karaman, R. (2018). Dopamine and levodopa prodrugs for the treatment of Parkinson's disease. Molecules 23:.

Hahm, J.H., Kim, S., and Paik, Y.K. (2011). GPA-9 is a novel regulator of innate immunity against *Escherichia coli* foods in adult *Caenorhabditis elegans*. Aging Cell 10: 208–219.

Ham, T.J. van, Thijssen, K.L., Breitling, R., Hofstra, R.M.W., Plasterk, R.H. a, and Nollen, E. a a (2008). *C. elegans* model identifies genetic modifiers of alpha-synuclein inclusion formation during aging. PLoS Genet. 4: e1000027.

Harrington, A.J., Hamamichi, S., Caldwell, G.A., and Caldwell, K.A. (2010). *C. elegans* as a model

organism to investigate molecular pathways involved with Parkinson's disease. Dev. Dyn. 239: 1282–1295.

Harvey, A.L. (2008). Natural products in drug discovery. Drug Discov. Today 13: 894–901.

Hobson, P., Meara, J., and Ishihara-Paul, L. (2010). The estimated life expectancy in a community cohort of Parkinson's disease patients with and without dementia, compared with the UK population. J. Neurol. Neurosurg. Psychiatry 81: 1093–8.

Hoyer, W., Antony, T., Cherny, D., Heim, G., Jovin, T.M., and Subramaniam, V. (2002). Dependence of α-synuclein aggregate morphology on solution conditions. J. Mol. Biol. 322: 383–393.

Hudson, S. a, Ecroyd, H., Kee, T.W., and Carver, J. a (2009). The thioflavin T fluorescence assay for amyloid fibril detection can be biased by the presence of exogenous compounds. FEBS J. 276: 5960–72.

Hughes, J.P., Rees, S.S., Kalindjian, S.B., and Philpott, K.L. (2011). Principles of early drug discovery. Br. J. Pharmacol. 162: 1239–1249.

Jagota, S., and Rajadas, J. (2012). Effect of phenolic compounds against Aβ aggregation and Aβ-induced toxicity in transgenic *C. elegans*. Neurochem. Res. 37: 40–48.

Johnston, B.T., Li, Q., Castell, J.A., and Castell, D.O. (1995). Swallowing and Esophageal Function in Parkinson's Disease. Am. J. Gastroenterol. 90: 1741–1746.

Ke, Z., Zhang, X., Cao, Z., Ding, Y., Li, N., Cao, L., et al. (2016). Drug discovery of neurodegenerative disease through network pharmacology approach in herbs. Biomed. Pharmacother. 78: 272–279.

Kim, H., Chatani, E., Goto, Y., and Paik, S. (2007). Seed-dependent accelerated fibrillation of α-synuclein induced by periodic ultrasonication treatment. J. Microbiol. 17: 2027–2032.

Kim, W.S., Kågedal, K., and Halliday, G.M. (2014). Alpha-synuclein biology in Lewy body diseases. Alzheimers. Res. Ther. 6: 73.

King, D., Ma, W., Yao, D., and Tobias, R. Instant Determination of Protein Presence Using the BLItz System.

Koch, M. a. (2006). Experimental modeling and research methodology (Elsevier Inc.).

Krauss, S., and Vorberg, I. (2013). Prions ex vivo: What cell culture models tell us about infectious proteins. Int. J. Cell Biol. 2013:.

Krebs, M.R.H., Bromley, E.H.C., and Donald, A.M. (2005). The binding of thioflavin-T to amyloid fibrils: Localisation and implications. J. Struct. Biol. 149: 30–37.

Kulisevsky, J., and Pagonabarraga, J. (2010). Tolerability and safety of ropinirole versus other dopamine agonists and levodopa in the treatment of Parkinson's disease: meta-analysis of randomized controlled trials. Drug Saf. 33: 147–161.

Kuwahara, T., Koyama, A., Gengyo-Ando, K., Masuda, M., Kowa, H., Tsunoda, M., et al. (2006). Familial Parkinson mutant α-synuclein causes dopamine neuron dysfunction in transgenic *Caenorhabditis elegans*. J. Biol. Chem. 281: 334–340.

Lakso, M., Vartiainen, S., Moilanen, A.-M., Sirviö, J., Thomas, J.H., Nass, R., et al. (2004). Dopaminergic neuronal loss and motor deficits in *Caenorhabditis elegans* overexpressing human α-synuclein. J. Neurochem. 86: 165–172.

Leão, A.H.F.F., Sarmento-Silva, A.J., Santos, J.R., Ribeiro, A.M., and Silva, R.H. (2015). Molecular, Neurochemical, and Behavioral Hallmarks of Reserpine as a Model for Parkinson's Disease: New Perspectives to a Long-Standing Model. Brain Pathol. 25: 377–390.

Lee, D., Lee, E.K., Lee, J.H., Chang, C.S., and Paik, S.R. (2001). Self-oligomerization and protein aggregation of alpha-synuclein in the presence of Coomassie Brilliant Blue. Eur. J. Biochem. 268: 295–301.

Lees, A.J., Hardy, J., and Revesz, T. (2009). Parkinson's disease. Lancet 373: 2055–2066.

Lees, A.J., Tolosa, E., and Olanow, C.W. (2015). Four pioneers of L-dopa treatment: Arvid Carlsson, Oleh Hornykiewicz, George Cotzias, and Melvin Yahr. Mov. Disord. 30: 19–36.

Leung, C.W.T., Guo, F., Hong, Y., Zhao, E., Kwok, R.T.K., Leung, N.L.C., et al. (2015). Detection of oligomers and fibrils of α-synuclein by AIEgen with strong fluorescence. Chem. Commun. 51: 1866–1869.

Li, W.-W., Yang, R., Guo, J.-C., Ren, H.-M., Zha, X.-L., Cheng, J.-S., et al. (2007). Localization of α-synuclein to mitochondria within midbrain of mice. Neuroreport 18: 1543–1546.

Lim, K.-L. (2010). Non-mammalian animal models of Parkinson's disease for drug discovery. Expert Opin. Drug Discov. 5: 165–176.

Liu, H., Wang, X., Wang, H.D., Wu, J., Ren, J., Meng, L., et al. (2012). *Escherichia coli* noncoding RNAs can affect gene expression and physiology of *Caenorhabditis elegans*. Nat. Commun. 3: 1011–1073.

Liu, M., Yin, H., Liu, G., Dong, J., Qian, Z., and Miao, J. (2014). Xanthohumol, a prenylated chalcone from beer hops, acts as an α-glucosidase inhibitor in vitro. J. Agric. Food Chem. 62: 5548–5554.

Lohmiller, J.J., and Swing, S.P. (2006). Reproduction and Breeding (Elsevier Inc.).

Luo, X., Xu, S., Yang, Y., Li, L., Chen, S., Xu, A., et al. (2016). Insights into the Ecotoxicity of Silver Nanoparticles Transferred from *Escherichia coli* to *Caenorhabditis elegans*. Sci. Rep. 6: 1–13.

Macchi, F., Deleersnijder, A., Haute, C. Van den, Munck, S., Pottel, H., Michiels, A., et al. (2016). High-content analysis of α-synuclein aggregation and cell death in a cellular model of Parkinson's disease. J. Neurosci. Methods 261: 117–127.

Magalingam, K.B., Radhakrishnan, A.K., and Haleagrahara, N. (2015). Protective Mechanisms of Flavonoids in Parkinson ' s Disease. Hindawi Publ. Corp. 2015:.

Maturana, M.G.V., Pinheiro, A.S., Souza, T.L.F. de, and Follmer, C. (2015). Unveiling the role of the pesticides paraquat and rotenone on α-synuclein fibrillation in vitro. Neurotoxicology 46: 35–43.

Mu, L., Sobotka, S., Chen, J., Su, H., Sanders, I., Adler, C.H., et al. (2012). Altered pharyngeal muscles in Parkinson disease. J. Neuropathol. Exp. Neurol. 71: 520–30.

Müller, M.L.T.M., and Bohnen, N.I. (2013). Cholinergic dysfunction in Parkinson's disease. Curr. Neurol. Neurosci. Rep. 13: 377.

Muñoz-Manchado, A.B., Villadiego, J., Romo-Madero, S., Suárez-Luna, N., Bermejo-Navas, A., Rodríguez-Gõmez, J.A., et al. (2016). Chronic and progressive Parkinson's disease MPTP model in adult and aged mice. J. Neurochem. 136: 373–387.

Nagashima, T., Ishiura, S., and Suo, S. (2017). Regulation of body size in *Caenorhabditis elegans*: effects of environmental factors and the nervous system. Int. J. Dev. Biol. 61: 367–374.

Nagashima, T., Oami, E., Kutsuna, N., Ishiura, S., and Suo, S. (2016). Dopamine regulates body size in *Caenorhabditis elegans*. Dev. Biol. 412: 128–138.

Niidome, T., Takahashi, K., Goto, Y., Goh, S., Tanaka, N., Kamei, K., et al. (2007). Mulberry leaf extract prevents amyloid beta-peptide fibril formation and neurotoxicity. Neuroreport 18: 813–816.

Nikfarjam, L., and Farzaneh, P. (2012). Prevention and Detection of Mycoplasma Contamination in Cell Culture. Cell J. 13: 203–212.

Noda, S., So, M., Adachi, M., Kardos, J., Akazawa-Ogawa, Y., Hagihara, Y., et al. (2016). Thioflavin T-silent denaturation intermediates support the main-chain-dominated architecture of amyloid fibrils. Biochemistry 55: 3937–3948.

Noelker, C., Morel, L., Lescot, T., Osterloh, A., Alvarez-Fischer, D., Breloer, M., et al. (2013). Toll like receptor 4 mediates cell death in a mouse MPTP model of Parkinson disease. Sci. Rep. 3: 1–6.

Oakley, B.R., Kirsch, D.R., and Morris, N.R. (1980). A simplified ultrasensitive silver stain for detecting

proteins in polyacrylamide gels. Anal. Biochem. 105: 361–363.

Olanow, C.W., Perl, D.P., DeMartino, G.N., and McNaught, K.S.P. (2004). Lewy-body formation is an aggresome-related process: A hypothesis. Lancet Neurol. 3: 496–503.

Ono, K., Takahashi, R., Ikeda, T., and Yamada, M. (2012). Cross-seeding effects of amyloid β-protein and α-synuclein. J. Neurochem. 122: 883–90.

Ottolini, D., Calí, T., Szabò, I., and Brini, M. (2017). Alpha-synuclein at the intracellular and the extracellular side: Functional and dysfunctional implications. Biol. Chem. 398: 77–100.

Pandya, K., Ray, C.A., Brunner, L., Wang, J., Lee, J.W., and DeSilva, B. (2010). Strategies to minimize variability and bias associated with manual pipetting in ligand binding assays to assure data quality of protein therapeutic quantification. J. Pharm. Biomed. Anal. 53: 623–630.

Panov, A., Dikalov, S., Shalbuyeva, N., Taylor, G., Sherer, T., and Greenamyre, J.T. (2005). Rotenone model of Parkinson disease: Multiple brain mitochondria dysfunctions after short term systemic rotenone intoxication. J. Biol. Chem. 280: 42026–42035.

Perni, M., Aprile, F.A., Casford, S., Mannini, B., Sormanni, P., Dobson, C.M., et al. (2017). Delivery of Native Proteins into *C. elegans* Using a Transduction Protocol Based on Lipid Vesicles. Sci. Rep. 7: 1–9.

Pollanen, M.S., Dickson, D.W., and Bergeron, C. (1993). Pathology and biology of the Lewy body. J. Neuropathol. Exp. Neurol. 52: 183–91.

Postuma, R.B., Berg, D., Stern, M., Poewe, W., Olanow, C.W., Oertel, W., et al. (2015). MDS clinical diagnostic criteria for Parkinson's disease. Mov. Disord. 30: 1591–1601.

Rascol, O., Perez-Lloret, S., and Ferreira, J.J. (2015). New treatments for levodopa-induced motor complications. Mov. Disord. 30: 1451–1460.

Raslan, A.A., and Kee, Y. (2013). Tackling neurodegenerative diseases: animal models of Alzheimer's disease and Parkinson's disease. Genes Genomics 35: 425–440.

Ratelade, J., Miot, M.C., Johnson, E., Betton, J.M., Mazodier, P., and Benaroudj, N. (2009). Production of recombinant proteins in the lon-deficient BL21(DE3) strain of *Escherichia coli* in the absence of the DnaK chaperone. Appl. Environ. Microbiol. 75: 3803–3807.

Regitz, C., Dußling, L.M., and Wenzel, U. (2014). Amyloid-beta (Aβ1-42)-induced paralysis in *Caenorhabditis elegans* is inhibited by the polyphenol quercetin through activation of protein degradation pathways. Mol. Nutr. Food Res. 58: 1931–1940.

Ribeiro, F.M., Ribeiro, E., Souza, L.C. De, and Teixeira, A.L. (2013). Animal models of

neurodegenerative diseases. 82–92.

Risley, M.G., Kelly, S.P., Jia, K., Grill, B., and Dawson-Scully, K. (2016). Modulating behavior in *C. elegans* using electroshock and antiepileptic drugs. PLoS One 11: 1–14.

Sachs, C., and Jonsson, G. (1975). Mechanisms of action of 6-OHDA. Biochem. Pharmacol. 24: 1–8.

Sasaoka, N., Sakamoto, M., Kanemori, S., Kan, M., Tsukano, C., Takemoto, Y., et al. (2014). Long-term oral administration of hop flower extracts mitigates alzheimer phenotypes in mice. PLoS One 9:.

Schapira, A.H. V (2009). Neurobiology and treatment of Parkinson's disease. Trends Pharmacol. Sci. 30: 41–47.

Schlachetzki, J.C.M., Saliba, S.W., and Oliveira, A.C.P. de (2013). Studying neurodegenerative diseases in culture models. Rev. Bras. Psiquiatr. 35:.

Sliwoski, G., Kothiwale, S., Meiler, J., and Lowe Jr, E.W. (2014). Computational Methods in Drug Discovery. Pharmacol. Rev. 66: 334–395.

Smith, L.M., Klaver, A.C., Coffey, M.P., Dang, L., and Loeffler, D.A. (2012). Effects of intravenous immunoglobulin on alpha synuclein aggregation and neurotoxicity. Int. Immunopharmacol. 14: 550–557.

Solis, G.M., and Petrascheck, M. (2011). Measuring *Caenorhabditis elegans* life span in 96 well microtiter plates. J. Vis. Exp. 4–9.

Stott, S.R.W., and Barker, R.A. (2014). Time course of dopamine neuron loss and glial response in the 6-OHDA striatal mouse model of Parkinson's disease. Eur. J. Neurosci. 39: 1042–1056.

Stringer, S.C., George, S.M., and Peck, M.W. (2000). Thermal inactivation of *Escherichia coli* 0157 : H7. Joumal Appl. Microbiol. Symp. Suppl. 88: 79S–89S.

Stsiapura, V.I., Maskevich, A. a, Kuzmitsky, V. a, Uversky, V.N., Kuznetsova, I.M., and Turoverov, K.K. (2008). Thioflavin T as a molecular rotor: fluorescent properties of thioflavin T in solvents with different viscosity. J. Phys. Chem. B 112: 15893–902.

Tanner, C.M., Kamel, F., Ross, G.W., Hoppin, J.A., Goldman, S.M., Korell, M., et al. (2011). Rotenone, Paraquat, and Parkinson's Disease. Environ. Health Perspect. 119: 866–872.

Trojanowski, N.F., Raizen, D.M., and Fang-Yen, C. (2016). Pharyngeal pumping in *Caenorhabditis elegans* depends on tonic and phasic signaling from the nervous system. Sci. Rep. 6: 1–11.

Tsai, C.W., Tsai, R.T., Liu, S.P., Chen, C.S., Tsai, M.C., Chien, S.H., et al. (2017). Neuroprotective Effects of Betulin in Pharmacological and Transgenic *Caenorhabditis elegans* Models of Parkinson's

Disease. Cell Transplant. 26: 1903–1918.

Vaquer, G., Rivière, F., Mavris, M., Bignami, F., Llinares-Garcia, J., Westermark, K., et al. (2013). Animal models for metabolic, neuromuscular and ophthalmological rare diseases. Nat. Rev. Drug Discov. 12: 287–305.

Voropai, E., and Samtsov, M. (2003). Spectral properties of thioflavin T and its complexes with amyloid fibrils. J. Appl. … 70: 767–773.

Waring, M.J. (2010). Lipophilicity in drug discovery. Expert Opin. Drug Discov. 5: 235–248.

Whitworth, A.J., Wes, P.D., Pallanck, L.J., Sciences, B., and Sheffield, S. (2006). Drosophila models pioneer a new approach to drug discovery for Parkinson ' s disease REVIEWS. 11:.

Wolfe, L.S., Calabrese, M.F., Nath, A., Blaho, D. V, Miranker, A.D., and Xiong, Y. (2010). Protein-induced photophysical changes to the amyloid indicator dye thioflavin T. PNAS 107: 16863–16868.

Wördehoff, M.M., Bannach, O., Shaykhalishahi, H., Kulawik, A., Schiefer, S., Willbold, D., et al. (2015). Single fibril growth kinetics of α-synuclein. J. Mol. Biol. 427: 1428–1435.

Xu, J., Jiang, Y., Wan, L., Wang, Q., Huang, Z., Liu, Y., et al. (2017). Feeding recombinant *E. coli* with GST-mBmKTX fusion protein increases the fecundity and lifespan of *Caenorhabditis elegans*. Peptides 89: 1–8.

Zbarsky, V., Datla, K.P., Parkar, S., Rai, D.K., Aruoma, O.I., and Dexter, D.T. (2005). Neuroprotective properties of the natural phenolic antioxidants curcumin and naringenin but not quercetin and fisetin in a 6-OHDA model of Parkinson's disease. Free Radic. Res. 39: 1119–1125.

Zesiewicz, T.A., Sullivan, K.L., and Hauser, R.A. (2006). Nonmotor symptoms of Parkinson's disease. Expert Rev. Neurother. 6: 1811–1822.

Zhao, M., Cascio, D., Sawaya, M.R., and Eisenberg, D. (2011). Structures of segments of α-synuclein fused to maltose-binding protein suggest intermediate states during amyloid formation. Protein Sci. 20: 996–1004.

8 Emended Bibliography

Agosta, F., Canu, E., Stojković, T., Pievani, M., Tomić, A., Sarro, L., et al. (2013). The topography of brain damage at different stages of Parkinson's disease. Hum. Brain Mapp. *34*: 2798–807.

Baba, M., Nakajo, S., Tu, P.-H., Tomita, T., Nakaya, K., Lee, V.M.Y., et al. (1998). Aggregation of α-synuclein in lewy bodies of sporadic Parkinson's disease and dementia with lewy bodies. Am J Pathol

152: 879–884.

Braak, H., Tredici, K. Del, Rüb, U., Vos, R.A.I. de, Jansen Steur, E.N.H., and Braak, E. (2003). Staging of brain pathology related to sporadic Parkinson's disease. Neurobiol. Aging *24*: 197–211.

Breydo, L., Wu, J.W., and Uversky, V.N. (2012). α-Synuclein misfolding and Parkinson's disease. Biochim. Biophys. Acta (BBA)-Molecular Basis Dis. *1822*: 261–285.

Cappai, R., Leck, S.-L., Tew, D.J., Williamson, N. a, Smith, D.P., Galatis, D., et al. (2005). Dopamine promotes alpha-synuclein aggregation into SDS-resistant soluble oligomers via a distinct folding pathway. FASEB J. *19*: 1377–9.

Chen, S.G., Stribinskis, V., Rane, M.J., Demuth, D.R., Gozal, E., Roberts, A.M., et al. (2016). Exposure to the Functional Bacterial Amyloid Protein Curli Enhances Alpha-Synuclein Aggregation in Aged Fischer 344 Rats and Caenorhabditis elegans. Sci. Rep. *6*: 1–11.

Cheng, F., Vivacqua, G., and Yu, S. (2011). The role of α-synuclein in neurotransmission and synaptic plasticity. J. Chem. Neuroanat. *42*: 242–8.

Conrad, M.S., Sutton, B.P., Dilger, R.N., and Johnson, R.W. (2014). An in vivo three-dimensional magnetic resonance imaging-based averaged brain collection of the neonatal piglet (Sus scrofa). PLoS One *9*: 1–6.

Danzer, K.M., Haasen, D., Karow, A.R., Moussaud, S., Habeck, M., Giese, A., et al. (2007). Different species of α-synuclein oligomers induce calcium influx and seeding. J Neurosci *27*: 9220–9232.

Danzer, K.M., Krebs, S.K., Wolff, M., Birk, G., and Hengerer, B. (2009). Seeding induced by α-synuclein oligomers provides evidence for spreading of α-synuclein pathology. J Neurochem *111*: 192–203.

Daturpalli, S., Waudby, C.A., Meehan, S., and Jackson, S.E. (2013). Hsp90 inhibits α-synuclein aggregation by interacting with soluble oligomers. J. Mol. Biol. *425*: 4614–4628.

Daubner, S.C., Le, T., and Wang, S. (2011). Tyrosine hydroxylase and regulation of dopamine synthesis. Arch. Biochem. Biophys. *508*: 1–12.

Daviaud, N., Garbayo, E., Lautram, N., Franconi, F., Lemaire, L., Perez-Pinzon, M., et al. (2014). Modeling nigrostriatal degeneration in organotypic cultures, a new ex vivo model of Parkinson's disease. Neuroscience *256*: 10–22.

Deleidi, M., and Gasser, T. (2013). The role of inflammation in sporadic and familial Parkinson's disease. Cell. Mol. Life Sci. *70*: 4259–4273.

Duty, S., and Jenner, P. (2011). Animal models of Parkinson's disease: a source of novel treatments

and clues to the cause of the disease. Br. J. Pharmacol. *164*: 1357–1391.

Elder, A.M., Henderson, D.M., Nalls, A. V., Hoover, E.A., Kincaid, A.E., Bartz, J.C., et al. (2015). Immediate and Ongoing Detection of Prions in the Blood of Hamsters and Deer following Oral, Nasal, or Blood Inoculations. J. Virol. *89*: 7421–7424.

Franco, L., Bravo, R., Galan, C., Sanchez, C., Rodriguez, A.B., Barrigs, C., et al. (2013). Effects of beer, Hops (Humulus lupulus) on total antioxidant capacity in plasma of stressed subjects. Cell Membr. Free Radic. Res. *5*: 232–235.

Freundt, E.C., Maynard, N., Clancy, E.K., Roy, S., Bousset, L., Sourigues, Y., et al. (2012). Neuron-to-neuron transmission of α-synuclein fibrils through axonal transport. Ann. Neurol. *72*: 517–524.

Frimpong, A.K., Abzalimov, R.R., Uversky, V.N., and Kaltashov, I.A. (2010). Characterization of intrinsically disordered proteins with electrospray ionization mass spectrometry: Conformational heterogeneity of α-synuclein. Proteins Struct. Funct. Bioinforma. *78*: 714–722.

Ghosh, D., Mehra, S., Sahay, S., Singh, P.K., and Maji, S.K. (2017). A-Synuclein Aggregation and Its Modulation. Int. J. Biol. Macromol. *100*: 37–54.

Giehm, L., Lorenzen, N., and Otzen, D.E. (2011). Assays for α-synuclein aggregation. Methods *53*: 295–305.

Greten-Harrison, B., Polydoro, M., Morimoto-Tomita, M., Diao, L., Williams, A.M., Nie, E.H., et al. (2010). Alpha-Synuclein triple knockout mice reveal age-dependent neuronal dysfunction. Proc. Natl. Acad. Sci. *107*: 19573–19578.

Gureviciene, I., Gurevicius, K., and Tanila, H. (2007). Role of alpha-synuclein in synaptic glutamate release. Neurobiol. Dis. *28*: 83–9.

Hahm, J.H., Kim, S., and Paik, Y.K. (2011). GPA-9 is a novel regulator of innate immunity against Escherichia coli foods in adult Caenorhabditis elegans. Aging Cell *10*: 208–219.

Ham, T.J. van, Thijssen, K.L., Breitling, R., Hofstra, R.M.W., Plasterk, R.H. a, and Nollen, E. a a (2008). C. elegans model identifies genetic modifiers of alpha-synuclein inclusion formation during aging. PLoS Genet. *4*: e1000027.

Hashimoto, M., Yoshimoto, M., Sisk, A., Hsu, L.J., Sundsmo, M., Kittel, A., et al. (1997). NACP, a Synaptic Protein Involved in Alzheimer's Disease, Is Differentially Regulated during Megakaryocyte Differentiation. Biochem. Biophys. Res. Commun. *237*: 611–616.

Hill, W.D., and Tompkins, M.M. (1997). Contribution of somal Lewy bodies to neuronal death. Brain Res. *775*: 24–29.

Holmqvist, S., Chutna, O., Bousset, L., Aldrin-Kirk, P., Li, W., Björklund, T., et al. (2014). Direct evidence of Parkinson pathology spread from the gastrointestinal tract to the brain in rats. Acta Neuropathol. *128*: 805–820.

Huang, C., Ren, G., Zhou, H., and Wang, C. (2005). A new method for purification of recombinant human alpha-synuclein in Escherichia coli. Protein Expr. Purif. *42*: 173–7.

Irizarry, M.C., Whitfield, G., Gomez-Isla, T., Newell, K., George, J.M., Clayton, D.F., et al. (1998). Nigral and cortical Lewy bodies and dystrophic nigral neurites in Parkinson's disease and cortical Lewy body disease contain α-synuclein immunoreactivity. J. Neuropathol. Exp. Neurol. *57*: 334–337.

Iwai, A., Masliah, E., Yoshimoto, M., Ge, N., Flanagan, L., Rohan de Silva, H.A., et al. (1995). The precursor protein of non-Aβ component of Alzheimer's disease amyloid is a presynaptic protein of the central nervous system. Neuron *14*: 467–475.

Kokel, D., Li, Y., Qin, J., and Xue, D. (2006). The nongenotoxic carcinogens naphthalene and para-dichlorobenzene suppress apoptosis in Caenorhabditis elegans. Nat. Chem. Biol. *2*: 338–345.

Kormish, J.D., Gaudet, J., and McGhee James D., J.D. (2010). Development of the C. elegans digestive tract. Curr. Opin. Genet. Dev. *20*: 346–354.

Kostka, M., Hogen, T., Danzer, K.M., Levin, J., Habeck, M., Wirth, A., et al. (2008). Single particle characterization of iron-induced pore-forming α-synuclein oligomers. J. Biol. Chem. *283*: 10992–11003.

Lee, H.J., and Lee, S.J. (2002). Characterization of cytoplasmic α-synuclein aggregates. Fibril formation is tightly linked to the inclusion-forming process in cells. J Biol Chem *277*: 48976–48983.

Levin, J., Hillmer, A.S., Högen, T., McLean, P.J., and Giese, A. (2016). Intracellular formation of α-synuclein oligomers and the effect of heat shock protein 70 characterized by confocal single particle spectroscopy. Biochem. Biophys. Res. Commun. *477*: 76–82.

Li, W., Lee, M.K., Stirling, W., Price, D.L., and Hoffman, P.N. (2010). Axonal transport of human α-synuclein slows with aging but is not affected by familial Parkinson's disease-linked mutations. J. Neurochem. *88*: 401–410.

Liu, M., Yin, H., Liu, G., Dong, J., Qian, Z., and Miao, J. (2014). Xanthohumol, a prenylated chalcone from beer hops, acts as an α-glucosidase inhibitor in vitro. J. Agric. Food Chem. *62*: 5548–5554.

Luk, K.C., Kehm, V., Carroll, J., Zhang, B., Brien, P.O., Trojanowski, J.Q., et al. (2012). Pathological a-Synuclein Transmission in Nontransgenic Mice. Science (80-.). *949*: 949–953.

Luk, K.C., Song, C., O'Brien, P., Stieber, A., Branch, J.R., Brunden, K.R., et al. (2009). Exogenous alpha-synuclein fibrils seed the formation of Lewy body-like intracellular inclusions in cultured cells. Proc.

Natl. Acad. Sci. U. S. A. *106*: 20051–6.

Magalingam, K.B., Radhakrishnan, A.K., and Haleagrahara, N. (2015). Protective Mechanisms of Flavonoids in Parkinson ' s Disease. Hindawi Publ. Corp. *2015*:.

Magdeldin, S., Enany, S., Yoshida, Y., Xu, B., Zhang, Y., Zureena, Z., et al. (2014). Basics and recent advances of two dimensional- polyacrylamide gel electrophoresis. Clin. Proteomics *11*: 16.

Manne, S., Kondru, N., Hepker, M., Jin, H., Anantharam, V., Lewis, M., et al. (2019). Ultrasensitive Detection of Aggregated α-Synuclein in Glial Cells, Human Cerebrospinal Fluid, and Brain Tissue Using the RT-QuIC Assay: New High-Throughput Neuroimmune Biomarker Assay for Parkinsonian Disorders. J. Neuroimmune Pharmacol.

Maroteaux, L., Campanelli, J., and Scheller, R. (2018). Synuclein: a neuron-specific protein localized to the nucleus and presynaptic nerve terminal. J. Neurosci. *8*: 2804–2815.

McNaught, K.S.P., Shashidharan, P., Perl, D.P., Jenner, P., and Olanow, C.W. (2002). Aggresome-related biogenesis of Lewy bodies. Eur. J. Neurosci. *16*: 2136–2148.

Mollenhauer, B., Cullen, V., Kahn, I., Krastins, B., Outeiro, T.F., Pepivani, I., et al. (2008). Direct quantification of CSF α-synuclein by ELISA and first cross-sectional study in patients with neurodegeneration. Exp. Neurol. *213*: 315–325.

Nagai, T., Ibata, K., Park, E., Kubota, M., and Mikoshiba, K. (1989). A variant of yellow fluorescent protein with fast and efficient maturation for cell-biological …. Genetics *20*: 1585–1588.

Niidome, T., Takahashi, K., Goto, Y., Goh, S., Tanaka, N., Kamei, K., et al. (2007). Mulberry leaf extract prevents amyloid beta-peptide fibril formation and neurotoxicity. Neuroreport *18*: 813–816.

Oakley, B.R., Kirsch, D.R., and Morris, N.R. (1980). A simplified ultrasensitive silver stain for detecting proteins in polyacrylamide gels. Anal. Biochem. *105*: 361–363.

Olanow, C.W., Perl, D.P., DeMartino, G.N., and McNaught, K.S.P. (2004). Lewy-body formation is an aggresome-related process: A hypothesis. Lancet Neurol. *3*: 496–503.

Ono, K., Takahashi, R., Ikeda, T., and Yamada, M. (2012). Cross-seeding effects of amyloid β-protein and α-synuclein. J. Neurochem. *122*: 883–90.

Ottolini, D., Calí, T., Szabò, I., and Brini, M. (2017). Alpha-synuclein at the intracellular and the extracellular side: Functional and dysfunctional implications. Biol. Chem. *398*: 77–100.

Paleologou, K.E., Kragh, C.L., Mann, D.M.A., Salem, S.A., Al-Shami, R., Allsop, D., et al. (2009). Detection of elevated levels of soluble ??-synuclein oligomers in post-mortem brain extracts from patients with dementia with Lewy bodies. Brain *132*: 1093–1101.

Pandey, N., Strider, J., Nolan, W.C., Yan, S.X., and Galvin, J.E. (2008). Curcumin inhibits aggregation of α-synuclein. Acta Neuropathol *115*: 479–489.

Pandya, K., Ray, C.A., Brunner, L., Wang, J., Lee, J.W., and DeSilva, B. (2010). Strategies to minimize variability and bias associated with manual pipetting in ligand binding assays to assure data quality of protein therapeutic quantification. J. Pharm. Biomed. Anal. *53*: 623–630.

Parkinson, J. (1817). On the Shaking Palsy. Sherwood, Heely and Jones 223–236.

Peña-Oliver, Y., Buchman, V.L., Dalley, J.W., Robbins, T.W., Schumann, G., Ripley, T.L., et al. (2012). Deletion of alpha-synuclein decreases impulsivity in mice. Genes, Brain Behav. *11*: 137–146.

Pham, C.L.L., Kirby, N., Wood, K., Ryan, T., Roberts, B., Sokolova, A., et al. (2014). Guanidine hydrochloride denaturation of dopamine-induced α-synuclein oligomers: A small-angle X-ray scattering study. Proteins Struct. Funct. Bioinforma. *82*: 10–21.

Porat, Y., Abramowitz, A., and Gazit, E. (2006). Inhibition of amyloid fibril formation by polyphenols: structural similarity and aromatic interactions as a common inhibition mechanism. Chem. Biol. Drug Des. *67*: 27–37.

Porta-de-la-Riva, M., Fontrodona, L., Villanueva, A., and Cerón, J. (2012). Basic Caenorhabditis elegans Methods: Synchronization and Observation. J. Vis. Exp. 1–9.

Rekas, A., Knott, R.B., Sokolova, A., Barnham, K.J., Perez, K. a, Masters, C.L., et al. (2010). The structure of dopamine induced alpha-synuclein oligomers. Eur. Biophys. J. *39*: 1407–19.

Rieker, C., Dev, K.K., Lehnhoff, K., Barbieri, S., Ksiazek, I., Kauffmann, S., et al. (2011). Neuropathology in mice expressing mouse alpha-synuclein. PLoS One *6*: e24834.

Rocca, W.A., McDonnell, S.K., Strain, K.J., Bower, J.H., Ahlskog, J.E., Elbaz, A., et al. (2004). Familial aggregation of Parkinson's disease: The mayo clinic family study. Ann. Neurol. *56*: 495–502.

Ryan, M.C., Sherman, P., Rowland, L.M., Wijtenburg, S.A., Acheson, A., Fieremans, E., et al. (2018). Miniature pig model of human adolescent brain white matter development. J. Neurosci. Methods *296*: 99–108.

Saito, Y., Shioya, A., Sano, T., Sumikura, H., Murata, M., and Murayama, S. (2016). Lewy body pathology involves the olfactory cells in Parkinson's disease and related disorders. Mov. Disord. *31*: 135–138.

Singh, P.K., Kotia, V., Ghosh, D., Mohite, G.M., Kumar, A., and Maji, S.K. (2013). Curcumin Modulates α-Synuclein Aggregation and Toxicity. ACS Chem. Neurosci. *4*: 393–407.

Stessl, M., Noe, C.R., and Lachmann, B. (2009). Influence of image-analysis software on quantitation

of two-dimensional gel electrophoresis data. Electrophoresis *30*: 325–328.

Stevens, J.F., and Page, J.E. (2004). Xanthohumol and related prenylflavonoids from hops and beer: To your good health! Phytochemistry *65*: 1317–1330.

Stott, S.R.W., and Barker, R.A. (2014). Time course of dopamine neuron loss and glial response in the 6-OHDA striatal mouse model of Parkinson's disease. Eur. J. Neurosci. *39*: 1042–1056.

Tanaka, M., Kim, Y.M., Lee, G., Junn, E., Iwatsubo, T., and Mouradian, M.M. (2004). Aggresomes Formed by α-Synuclein and Synphilin-1 Are Cytoprotective. J. Biol. Chem. *279*: 4625–4631.

Tang, Y., Das, U., Scott, D.A., and Roy, S. (2012). The slow axonal transport of alpha-synuclein-mechanistic commonalities amongst diverse cytosolic cargoes. Cytoskeleton *69*: 506–513.

Taylor, J.P., Tanaka, F., Robitschek, J., Sandoval, C.M., Taye, A., Markovic-Plese, S., et al. (2003). Aggresomes protect cells by enhancing the degradation of toxic polyglutamine-containing protein. Hum. Mol. Genet. *12*: 749–757.

Tretiakoff, C. (1919). Contribution a l'etude de l'Anatomie pathologique du Locus Niger de Soemmering avec quelques deduction relatives a la pathogenie des troubles du tonus musculaire et de la maladie de Parkinson.

Ulusoy, A., Phillips, R.J., Helwig, M., Klinkenberg, M., Powley, T.L., and Monte, D.A. Di (2017). Brain-to-stomach transfer of α-synuclein via vagal preganglionic projections. Acta Neuropathol. *133*: 381–393.

Voropai, E., and Samtsov, M. (2003). Spectral properties of thioflavin T and its complexes with amyloid fibrils. J. Appl. … *70*: 767–773.

Wördehoff, M.M., Bannach, O., Shaykhalishahi, H., Kulawik, A., Schiefer, S., Willbold, D., et al. (2015). Single fibril growth kinetics of α-synuclein. J. Mol. Biol. *427*: 1428–1435.

Wu, Z.C., Gao, J.H., Du, T.F., Tang, D.H., Chen, N.H., Yuan, Y.H., et al. (2019). Alpha-synuclein is highly prone to distribution in the hippocampus and midbrain in tree shrews, and its fibrils seed Lewy body-like pathology in primary neurons. Exp. Gerontol. *116*: 37–45.

Xu, J., Jiang, Y., Wan, L., Wang, Q., Huang, Z., Liu, Y., et al. (2017). Feeding recombinant E. coli with GST-mBmKTX fusion protein increases the fecundity and lifespan of Caenorhabditis elegans. Peptides *89*: 1–8.

Yanamandra, K., Gruden, M.A., Casaite, V., Meskys, R., Forsgren, L., and Morozova-Roche, L.A. (2011). a-Synuclein Reactive Antibodies as Diagnostic Biomarkers in Blood Sera of Parkinson ' s Disease Patients. PLoS One *6*: 1–13.

Yavich, L., Tanila, H., Vepsäläinen, S., and Jäkälä, P. (2004). Role of alpha-synuclein in presynaptic dopamine recruitment. J. Neurosci. *24*: 11165–70.

(2017). Protein purity (%) deetermination.

9 Appendix

9.1 Full gel image with lane descriptions

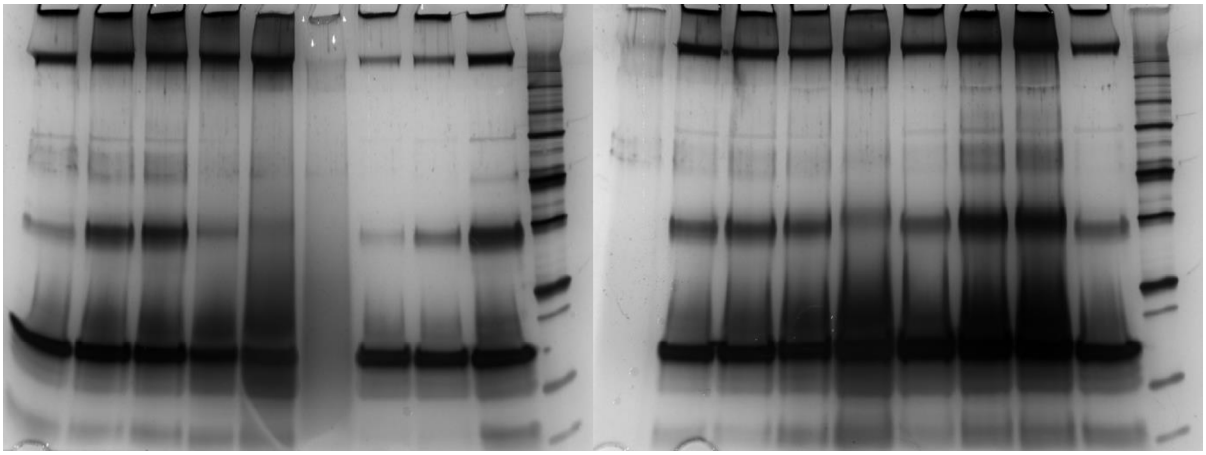

Figure 9.1 The gels (BioRad Mini-PROTEAN TGX Stain-Free Gels #456-8123) above were run at 200 V for 30 min, stained using Bio-Rad Silver Stain Plus #161-0449 and were imaged using Bio-Rad ChemiDoc MP System with Image Lab. Samples were taken after a microplate run, prepared using 4X sample buffer to sample and were diluted using running buffer (See Methods for buffer contents/concentrations). All samples contain 1 mg/mL a-syn dissolved in ThT buffer with a glass bead.

1) a-syn and buffer only,
2) 2.5% cold hops with a-syn
3) 5% cold hops with a-syn
4) 10% cold hops with a-syn
5) 20% cold hops with a-syn
6) 10% cold hops without a-syn
7) 2.5% CO2 hops with a-syn
8) 5% CO2 hops with a-syn
9) 10% CO2 hops with a-syn
10) Bio-Rad Precision Plus Protein Unstained Standards #161-0363
11) 10% cold filtered hops without a-syn
12) 2.5% cold filtered hops with a-syn
13) 5% cold filtered hops with a-syn
14) 10% cold filtered hops with a-syn
15) 20% cold filtered hops with a-syn
16) 2.5% hot hops with a-syn
17) 5% hot hops with a-syn
18) 10% hot hops with a-syn
19) a-syn and buffer only
20) Bio-Rad Precision Plus Protein Unstained Standards #161-0363.